AFRL-RH-WP-TR-2019-0040

AIRCREW RESTRAINT BIODYNAMICS (ARB) DURING VERTICAL DECELERATION

Mr. John Buhrman
Mr. Chris Perry
Dr. Casey Pirnstill
Mr. Ben Steinhauer
Warfighter Interface Division

Ms. Elyse V. Patrick
Infoscitex

July 2019
Interim Report

AIR FORCE RESEARCH LABORATORY
711th HUMAN PERFORMANCE WING,
AIRMAN SYSTEMS DIRECTORATE,
WRIGHT-PATTERSON AIR FORCE BASE, OH 45433
AIR FORCE MATERIEL COMMAND
UNITED STATES AIR FORCE

NOTICE AND SIGNATURE PAGE

Using Government drawings, specifications, or other data included in this document for any purpose other than Government procurement does not in any way obligate the U.S. Government. The fact that the Government formulated or supplied the drawings, specifications, or other data does not license the holder or any other person or corporation; or convey any rights or permission to manufacture, use, or sell any patented invention that may relate to them.

This report was cleared for public release by 88th Air Base Wing Public Affairs Office and is available to the general public, including foreign nationals. Copies may be obtained from the Defense Technical Information Center (DTIC) (http://www.dtic.mil).

AFRL-RH-WP-TR-2019-0040 HAS BEEN REVIEWED AND IS APPROVED FOR PUBLICATION.

//SIGNED//
DONALD L. HARVILLE
Work Unit Manager
Applied Neuroscience Branch

//SIGNED//
CLIFFORD N. OTTE
Chief, Applied Neuroscience Branch
Warfighter Interface Division

//SIGNED//
LOUISE A. CARTER
Chief, Warfighter Interface Division
Airman Systems Directorate
711 Human Performance Wing
Air Force Research Laboratory

This report is published in the interest of scientific and technical information exchange, and its publication does not constitute the Government's approval or disapproval of its ideas or findings.

REPORT DOCUMENTATION PAGE

Form Approved
OMB No. 0704-0188

1. REPORT DATE *(DD-MM-YY)*	2. REPORT TYPE	3. DATES COVERED *(From - To)*
05-07-19	Interim	January 2014 to August 2019

4. TITLE AND SUBTITLE

Aircrew Restraint Biodynamics (ARB) During Vertical Deceleration

5a. CONTRACT NUMBER
FA8650-14-D-6500-0001

5b. GRANT NUMBER

5c. PROGRAM ELEMENT NUMBER
62202F

6. AUTHOR(S)
John Buhrman, Chris Perry, Casey Pirnstill, Ben Steinhauer*,
Elyse V. Patrick**

5d. PROJECT NUMBER
5329

5e. TASK NUMBER
08

5f. WORK UNIT NUMBER
H0GW (53290812)

7. PERFORMING ORGANIZATION NAME(S) AND ADDRESS(ES)
Infoscitex Corporation**
Colonel Glenn Hwy, Suite 210
Dayton , OH 45431-4027

8. PERFORMING ORGANIZATION REPORT NUMBER

9. SPONSORING/MONITORING AGENCY NAME(S) AND ADDRESS(ES)
Air Force Materiel Command*
Air Force Research Laboratory
711th Human Performance Wing
Airman Systems Directorate
Warfighter Interface Division
Applied Neuroscience Branch
Wright-Patterson AFB, OH 45433

10. SPONSORING/MONITORING AGENCY ACRONYM(S)
711 HPW/RHCP

11. SPONSORING/MONITORING AGENCY REPORT NUMBER(S)
AFRL-RH-WP-TR-2019-0040

12. DISTRIBUTION/AVAILABILITY STATEMENT DISTRIBUTION STATEMENT A. Approved for public release.

13. SUPPLEMENTARY NOTES 88ABW-2019-0040, cleared on 12 September 2019

14. ABSTRACT A comparative research program was conducted to evaluate the effects of the restraint, seat geometry, and helmet system of the US16E ejection seat during the catapult phase of ejection. The study involved a series of vertical decelerations with both human subjects and ATDs on a Vertical Deceleration Tower (VDT). Biodynamic responses of the subjects were measured and analyzed to ascertain whether the parameters of the US16E seat would alter the risk of neck or spinal injury during upward ejection as compared to legacy seat systems. The results indicated that the forward position of the JSF head box increases horizontal and angular acceleration and neck loading during vertical impact acceleration, with very little effect on compressive acceleration or loading. The JSF restraint system mitigated head and chest accelerations but allowed for increased lumbar loading with improved lower torso restraint for the large occupant. The Gen II helmet system generated greater head accelerations and neck loads than the standard flight helmet due to the added weight and forward cg of the helmet. Although testing and analyses of the NPD was limited, no increased risk of neck injury was predicted during tests with NPD pressurization. This analysis did not address potential injury risk due to the effects of windblast, drogue and parachute opening phases, and/or other off-axis accelerations due to head and spinal misalignment during an actual ejection.

15. SUBJECT TERMS MK16E seat, Gen II helmet, SCH restraint system, forward headrest, Vertical Deceleration Tower (VDT), biodynamic response, ATD, Neck Protection Device (NPD)

16. SECURITY CLASSIFICATION OF:			17. LIMITATION OF ABSTRACT:	18. NUMBER OF PAGES	19a. NAME OF RESPONSIBLE PERSON (Monitor)
a. REPORT	b. ABSTRACT	c. THIS PAGE			Donald Harville
U	U	U	SAR	109	19b. TELEPHONE NUMBER (937) 255-3121

TABLE OF CONTENTS

LIST OF FIGURES

LIST OF TABLES

PREFACE

The impact tests and data analysis described in this report were accomplished by the Aircrew Biodynamics and Protection (ABP) Team of the Applied Neuroscience Branch (711 HPW/RHCPT) of the Warfighter Interface Division, and internally funded by the Human Effectiveness Directorate, 711 Human Performance Wing of the Air Force Research Laboratory at Wright-Patterson Air Force Base, Ohio. The test facility for this study was the Vertical Deceleration Tower (VDT) located in Building 824, Area B, at Wright-Patterson AFB. Engineering support was provided by Infoscitex Corp. under contract FA8650-14-D-6500.

ACKNOWLEDGEMENTS

The authors wish to thank the entire Aircrew Biodynamics and Protection (ABP) test support team including 711 HPW/RHBNB Aircrew Flight Equipment (AFEs) and Medical Technicians, Physicians and Physician Assistants (PAs) supplied by the USAF School of Medicine (USAFSAM), technical support personnel from Infoscitex Corp., and Martin-Baker Aircraft Co. LTD for supplying the US16E seat and technical support advisory personnel.

1.0 BACKGROUND

The new Joint Strike Fighter (JSF) aircraft is being fielded with the Martin-Baker Mk-US16E ejection seat, which is required to accommodate the full range of aircrew (103-245 lbs). However, there are significant differences in the seat geometry and restraint system of the US16E compared to the USAF's legacy Advanced Concept Ejection Seat (ACES II) ejection seat, which has been in the Air Force inventory since the 1980's. Early rocket sled qualification tests of the US16E seat have shown that under some conditions, the neck forces and head rotations, as measured in instrumented Articulated Test Devices (ATDs), were exceeding the JSF Neck Injury Criteria (NIC) limits for small occupants. In addition, recent scientific and technical publications have reported a higher than expected ejection injury rate for all size occupants in Royal Air Force (RAF) aircraft using legacy Mk series seats, as documented by a review of 232 mishaps through 2002 with most spinal injuries occurring in the region of T4-L1 (Lewis, 2006). This injury rate was not predicted accurately by the USAF Dynamic Response Index (DRI) spinal injury risk model, and there was concern in both the operational and research communities regarding this underestimation of spinal injury. While newer seat technologies in the US16E seat are expected to reduce the risk of spinal injury compared to legacy Mk versions, any causal factors that could potentially have an effect on aircrew safety need to be identified, along with recommendations for risk mitigation of spinal injuries during upward aircraft ejection.

It has been postulated that the reason for the ejection spinal injury rate of legacy Mk seats being greater than predicted by the DRI could be due to increased upper torso motion generated by the combination of the Mk seat's seat-mounted harness, forward-mounted headrest, and the implementation of helmet-mounted systems (Tulloch, 2011). The DRI limits were originally developed and validated based on seats using a standard torso-mounted harness, in-line headrest, seatback angle relative to the catapult thrust line of 5° or less, and standard flight helmet (Brinkley & Shaffer, 1971). Therefore, the seat configuration parameters of the Mk seat series may introduce error when calculating the DRI if the seating/restraint system allows increased upper-torso motion during ejection (Buhrman, Perry, & Wright, 2012). This research effort was conducted to address this dichotomy in ejection injury prediction, with the primary focus being to analyze the differences in the accelerations and displacements due to varying ejection seat and restraint parameters, and determine their influence on risk of injury during ejection from both new and legacy high performance aircraft. Human and ATD impact tests were conducted on the Vertical Deceleration Tower (VDT) to investigate the effects of these seat and restraint parameters under conditions similar to those experienced during the catapult phase of ejection using the Lightest Occupant in Service (LOIS), Large Anthropometric Research Device (LARD), and Hybrid III 50th Aerospace instrumented ATDs. The results will be used to ascertain whether a lowering of the DRI should be adopted for seats not conforming to the original DRI seat specifications and/or whether mitigation strategies should be considered, in order to maintain the 5% injury threshold which is normally required by the USAF for ejection injury risk.

2.0 OBJECTIVE

The objective of this research study was to investigate effects of the JSF ejection seat geometry, restraint system, and helmet system on the response of human volunteer subjects and ATDs during the catapult phase of ejection. The data collected during this program will be used to evaluate whether there is potential for injury risk to crewmembers due to the JSF specific seat parameters and/or helmet system, and to identify the underlying causes and recommend appropriate mitigation strategies. A secondary objective was to employ the human and ATD response data for development and validation of biodynamic models, including Finite Element (FE) and neck and spinal injury models.

3.0 TEST FACILITY AND EQUIPMENT

3.1 Vertical Deceleration Tower

The AFRL Vertical Deceleration Tower (VDT) was employed to conduct +Gz impact tests to evaluate acceleration response, neck and spine loading, and restraint system loading during the simulated catapult phase of an ejection (Figure 1). The composite parts of the VDT are: a) Instrumentation System, b) Video System, c) Safety and Control System, d) Data Collection System, e) VDT tower with guide rails and hydraulic decelerator (water cylinder), and f) primary VDT carriage weighing approximately 2,000 lbs (Strzelecki, 2004). To conduct a test, the carriage and an attached seat are lifted by an electronic hoist to a programmed drop height, and then released allowing the carriage to freefall while being guided by the rails. A contoured impact plunger mounted on the back of the carriage is guided into a cylindrical reservoir, and a +Gz acceleration pulse (actually a deceleration pulse) is produced when water is displaced through the open space between the plunger and an orifice plate attached to the top of the water-filled reservoir.

The pulse shape is controlled by varying the drop height, which also determines the peak G-level, and by varying the shape of the plunger, which determines the rise time of the pulse. The drop height of the carriage is determined by measuring the relative distance between the bottom of the plunger and the top of the water deceleration cylinder as the carriage is being raised to its final drop height prior to the initiation of free-fall. Various plungers are available which allow the VDT hydraulic decelerator to generate pulses up to 80 G peak acceleration, with maximum velocity changes up to 56 ft/s, and pulse durations of 40-180 ms. The plunger used during this effort was plunger # 102, which generated pulses from 4-15 G (Perry et al., 2017).

Figure 1. Vertical Deceleration Tower with Seated Human Volunteer Subject

3.2 Seat Fixture

An ACES II (F-16) and a Martin-Baker US16E -4 (JSF) seat were both employed for this program, and were rigidly mounted to the front face of the VDT carriage such that the seatbacks for both seats were approximately in-line with the front face of the VDT carriage and the vertical rails. The seat pans for both seats were inclined approximately 5° downward from the horizontal (Figure 2). Human and ATD subjects were positioned and restrained in the seats in an upright, seated position. Side handles were mounted on the ACES II seat for some tests. The primary modification to the seat fixtures for this series of tests was positioning the contoured headrest either at 0" in front of the plane of the seat back (normal position for ACES II), or at 2.5" in front of the plane of the seat back (normal position for US16E). Both seats were tested with the 0" and 2.5" headrest positions.

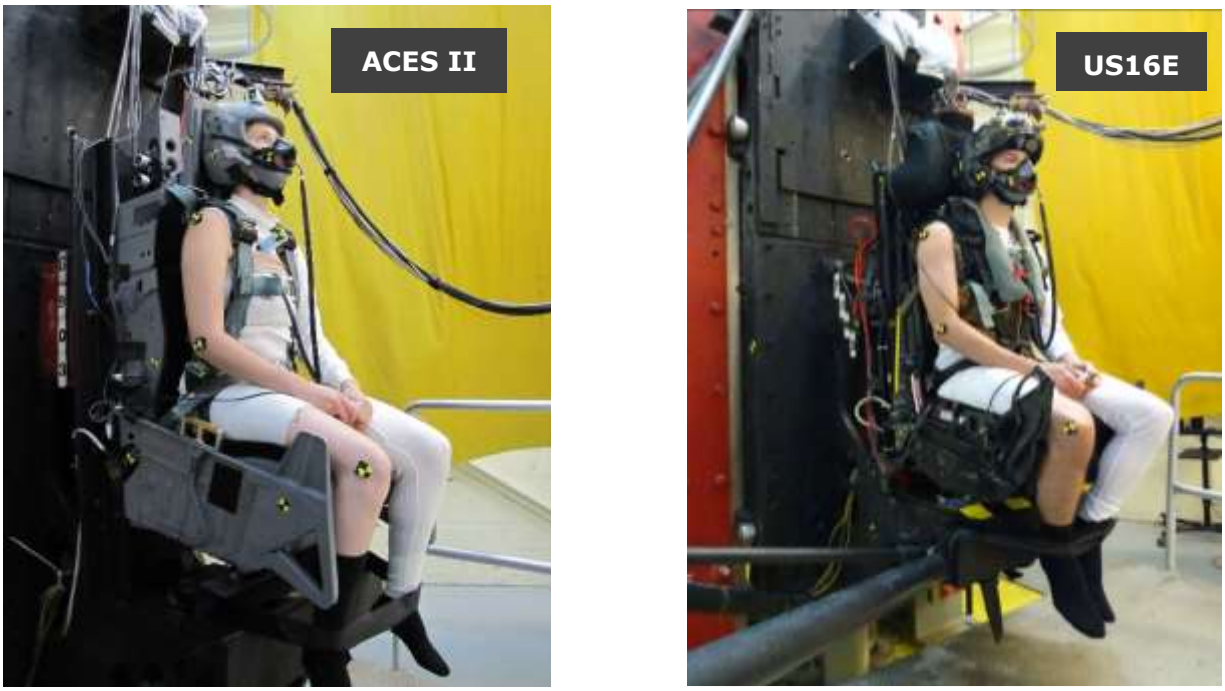

Figure 2. ACES II and US16E Seats with Human Subjects

The carriage and seat pan were instrumented with accelerometers to measure acceleration during impact. Load cells were also mounted at the lap belt termination points for both the ACES II and the US16E ejection seats. A crotch strap attachment point was affixed to the US16E seat pan for tests with the Simplified Combined Harness (SCH) configuration. The Neck Protection Device (NPD) was mounted on the head box for some tests with the US16E seat (Figure 3), and was inflated manually to approximately 20 psi prior to each test where it is deployed. The NPD is similar to a deployed air bag and is used with the US16E ejection seat to provide additional head and neck protection. It inflates as the seat accelerates up the rails and causes the head to be extended forward and inclined downward at an angle of approximately 30° from vertical. A cushion was provided to the subjects for chin/head support during tests with the NPD to prevent neck fatigue while seated and awaiting the impact. The cushion was removed by the subject just prior to impact.

Figure 3. Human Subject in US16E Seat with Inflated NPD

3.3 Restraint System

The subjects were restrained with either the standard USAF harness configuration (PCU-15/P or 16/P) or the SCH with flight vest and Life Preserver Unit (LPU) as shown in Figure 4. The USAF harness configuration was composed of parachute riser straps and lap belts that interfaced with the PCU-15/P or PCU-16/P torso harness (selected based on the subject size). The parachute riser straps were interfaced to the harness with Koch fittings, and then routed over each shoulder and secured to the inertia reel which was mounted just behind the seat back. The parachute riser straps and inertia reel straps were tightened securely and the inertia reel locked prior to the start of the impact. The lap belts were attached to load cells mounted on each side of the seat pan and tightened securely with pre-tension levels of 20 ± 5 lbs at each attachment point.

The SCH interfaces directly with the US16E seat, and also has its parachute riser straps routed over each shoulder and secured to the inertia reel. The harness was adjusted using set-up procedures based on on-site instruction from a Martin-Baker representative and the US16E Ejection Seat Aircrew Manual (Martin-Baker Aircraft Co. LTD, 2013), within the limitations of using human subjects and laboratory test facilities. The seat pan was raised or lowered such that the inertia reel straps were parallel to the horizontal and the subject's helmet approximately centered in the headrest. The subject was instructed to pull up on both crotch straps to remove excess slack. With the inertial reel in the unlocked position, the test operator instructed the subject on the proper procedure to route the shoulder straps and lap belts through the belt loops, and lock the ends into the Quick Release Box (QRB). The subject was instructed to place his or her fingers between the two lap belt straps and then pull to remove excess slack. The test operator then tightened the lap belts securely with pre-tension levels of 40 ± 5 lbs as measured at

each attachment point. With the inertia reel still unlocked, the subject was instructed to grab the shoulder buckles and lean forward to remove slack from behind the harness, and then lean back into the seat while pulling down on both shoulder strap adjusters. The test operator pushed with his thumbs to remove any excess slack in the rear of harness and checked to make sure that the upper rear cross strap was firmly in place up against the LPU. The test operator then locked the inertia reel and pushed the subject's shoulders and restraint adjusters back into seat until the inertia reel clicked a minimum of 2-3 times. The test operator then pulled the straps to obtain 20 ± 5 lbs of tension as measured on each shoulder strap using in-line strap load cells. For tests with the US16E seat, an additional safety strap was loosely connected around the subject's torso to prevent the subject from separating entirely from the seat in the unlikely event of a premature release of the SCH harness at the rotary connector.

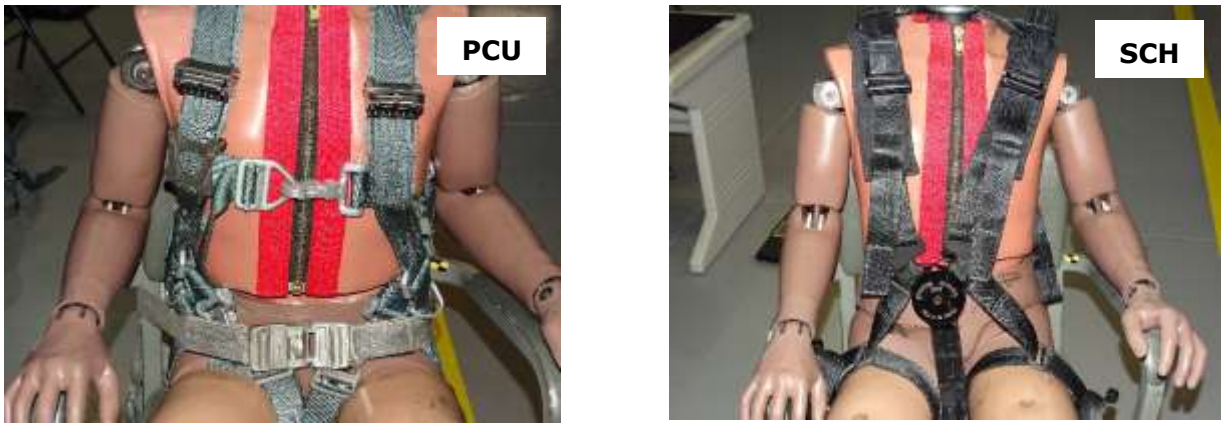

Figure 4. PCU-15/P and SCH Harness Systems

3.4 Helmet System

The subjects were fitted with either an HGU-55/P helmet system (M, L, XL) weighing approximately 2.4 lbs, or a JSF Gen 2 helmet mock-up (S, M, L), both shown in Figure 5. The JSF Gen 2 mock-up consisted of a Gen I helmet with weight and center-of-gravity (CG) modified to simulate a fully equipped Gen 2 helmet system weighing approximately 4.6 lbs (including visor and oxygen mask) with forward CG. The mass properties of the helmet were measured prior to impact testing to ensure it closely matched the Gen 2 helmet, and did not exceed safe guidelines. Three sizes for both helmets were necessary to accommodate the range of subjects. The HGU-55/P helmet used an integrated chin-nape strap, Zeta helmet liner, standard ear cups, and MBU-20/P oxygen mask with front section cut out to allow for instrumentation as described in Section 5.1. The Gen 2 had a built-in chin-nape strap, helmet liner, and ear cups, and also used the cut-out MBU-20/P oxygen mask. All helmet equipment (except the outer shell) were sprayed and/or wiped off with disinfectant after each human subject test. No visor was used with either helmet.

Figure 5. HGU-55/P and JSF Gen II Helmets

4.0 TEST SUBJECTS

4.1 Human Volunteers

Human test subjects were all active duty military volunteers who were screened to ensure they met medical criteria as determined by the Wright-Site Institutional Review Board's Medical Consultant and following the guidelines in Wright-Site Human Research Protocol FWR2014-0076H. Females that were pregnant or expected to be pregnant were not allowed to participate. The subjects were tested no more than once every 48 hours. The subjects wore cutoff long underwear to allow for mounting of accelerometers and motion targets, were fitted with either standard or weighted helmet with oxygen mask, and were restrained with either the PCU or SCH harness as previously described. For test cells employing the SCH, the subjects were also fitted with a flight vest and LPU. All human subjects were examined by a Medical Technician prior to and after each test, and a Medical Observer (Physician or PA) was on-call and within a 10 minute response time during the testing. Anthropometric data consisting of approximately 65 measurements was obtained for the human subjects by trained personnel employed by in-house support contractor, Infoscitex Corp. using traditional measurement techniques.

4.2 ATDs

Test ATDs that were used as part of this effort included the LOIS (instrumented weight approximately 110 lbs), LARD (instrumented weight approximately 245 lbs), Hybrid III 50th Aerospace (instrumented weight approximately 170 lbs), and Hybrid III 50th Automotive (instrumented weight approximately 182 lbs). Each ATD was dressed in an appropriately sized flight suit, and fitted with one of the two helmet systems. ATD test weights varied slightly for each test cell depending on the flight gear and instrumentation.

5.0 INSTRUMENTATION AND DATA ACQUISITION

5.1 Instrumentation

Electronic data channels collected during this effort are listed in Appendix A. Three single-axis accelerometers were mounted on the VDT carriage and seat pan to measure the impact accelerations. Carriage velocity was computed by integration of the carriage z-axis acceleration. Lap belt termination points on the test fixture were instrumented with three-axis load cells to measure restraint forces and pre-loads. An RQM (ride quality meter) acceleration pack was placed on top of the seat cushion to measure acceleration directly at the buttocks. Tri-axial linear accelerometers and angular rate sensors were mounted to a dental bite-block which was individually made for each subject and provided electrical isolation. Prior to each test, the Medical Technician ensured that the condition of the bite-block was satisfactory. Tri-axial accelerometer arrays were mounted to the subject's chest (and for some tests lower back) with adhesive tape and secured with a flexible wrap encircling the chest or lower back. Head, chest, and lumbar accelerometers, and 6-axis (3 orthogonal linear forces, 3 orthogonal moments) load cells in the upper neck and the lumbar spine/pelvis junction were mounted internally in the ATD to measure the respective accelerations, forces, and moments.

On-site personnel from Infoscitex, Inc. were responsible for conducting pre- and post-calibrations on all accelerometers, rate sensors, and load cells used on the carriage, seat fixture, and test subjects. The calibration records of individual transducers as well as the Standard Practice Instructions are maintained in the Impact Information Center and can be accessed by individual study. Entries are made identifying the data channel, transducer manufacturer, model number, serial number, date and sensitivity of pre-calibration, date and sensitivity of post-calibration, and percentage change. This information is listed in the Electronic Instrumentation Data Sheets and is available on-line through the Biodynamics Data Bank (Cheng, Mosher, & Buhrman, 2004).

The instrumentation coordinate system is shown in Figure 6 and uses the right-hand rule, with the z-axis parallel to the VDT guide rails, and positive (+z) being upward towards the top of the VDT facility. The x-axis is perpendicular to the z-axis with negative (-x) pointing outward away from the VDT impact carriage. The y-axis is perpendicular to the x- and z-axes according to the right-hand rule. The linear accelerometers were wired to provide a positive output voltage when the acceleration experienced by the accelerometer was applied in the +x, +y and +z directions.

The ATD coordinate system used for the loads and torques was a modified Society of Automotive Engineers or SAE J211 system with the following specifications: Positive Fx is generated with the head moving forward relative to the chest, and Positive Mx is generated with rotating the right ear to the right shoulder. Flexion (head rotation forward) was measured as positive, and extension (head rotation rearward) was measured as negative. Compression on the neck and lumbar load cells was negative, and tension was positive. Note that for simplicity, all tables and plots are shown as magnitude only (positive).

Figure 6. Impact Coordinate System

5.2 Data Collection

Dynamic response data were collected at 1,000 samples per second by a TDAS Pro 64-channel on-board data acquisition system manufactured by Diversified Technical Systems, Inc. The TDAS Pro was mounted on-board the VDT at the top of the impact carriage and provided digitization and anti-aliasing filtering at 120 Hz using a low-pass 8-pole Butterworth filter. Transducer signals are amplified, filtered, digitized and recorded on-board the TDAS using solid-state memory. The data acquisition system is controlled through an Ethernet interface using the Ethernet instruction language. A desktop PC with an Ethernet board configures the TDAS Pro before testing and retrieves the data after each test.

The Master Instrumentation Control Unit in the Instrumentation Room controls the data acquisition. A test was initiated when the countdown clock reached zero using a comparator, which was set to start data collection at a pre-selected time based on a positive reading of multiple safety inter-lock sensors used by the facility to protect the facility operators and human test subjects. Data were recorded to establish a zero reference for all transducers prior to restraining the subject to the seat fixture. The reference data were stored separately from the test data and were used in the processing of the test data. A reference mark pulse was generated to mark the electronic data at a pre-selected time after test initiation to place the reference mark close to the impact point. The reference mark time was used as the start time for data processing of the electronic data.

5.3 Video and Photographic Coverage

Two Phantom Miro-3 ruggedized high-speed video cameras were mounted on-board the VDT to provide documentation and immediate playback capability for each test. The cameras were mounted on the carriage at perpendicular and oblique angles relative to the subject. The video data was collected at 500 frames per second starting just prior to the release of the carriage as well as during the impact event. The raw video data was converted to MP4 format at the completion of testing. All photographic and MP4 video data were stored on a network drive and in the AFRL Biodynamics Data Bank (Cheng, Mosher, & Buhrman, 2004) for analysis and future use.

The test set up and pre-impact position of the subjects was documented by still photographs before each test. The photographs included a placard listing the test facility, test number, test cell, test date, and the subject's ID number. "Candid" shots of test preparations were also taken. Any structural failures or other items of interest as determined by the PI were also photographed following each test.

5.4 Quick Look Data Plots

After each test, the filtered data were graphically plotted in a portrait format of 4-6 plots per page, and grouped with similar channels. The spreadsheet of plots also contained pertinent maxima, minima, and respective times of each occurrence. For all data, start of impact is defined as the time at which carriage acceleration exceeds 0.5G for 5 ms (at 1000 samples/sec). The plots arranged in this fashion included: displacement versus time, force (load) versus time, and acceleration versus time. The plots were viewed to ensure there were no bad data channels and that the accelerations and forces are not excessively high.

6.0 EXPERIMENTAL DESIGN

6.1 Test Matrix

Human volunteer subjects were tested once at each of the 6-10 G conditions shown in Table 1. LOIS, LARD, and HB3-50 Aero instrumented ATDs were also tested once for each condition at 6-10 G, and also tested three times for 10 G test cells to assess repeatability. The ATDs were also tested at 12 and 15 G levels, although the LARD tests with the JSF seat were inadvertently omitted at the 15 G level. In addition, an HB3-50 Auto ATD was tested three times at 10 G conditions only. The acceleration waveform for the VDT was an approximate half-sine waveform with a time to peak of approximately 75 ms and a velocity change of approximately 27 ft/sec at 10 G (rise time and velocity change varied depending on G-level). The cell designation consisted of the cell letter and the peak G-level required for the test. All subjects were first tested in training cell TV6 prior to ACES II tests, and cell TV6m prior to US16E tests. These cells were low-level training runs and the data was not used in the analysis. The order of the remaining test cell sequences was counter-balanced as much as feasible using a Latin Squares Matrix. All tests progressed from lowest to highest acceleration levels within each cell. In cases where the human subject did not adequately brace (< 2% for humans) or if the seat pulse was outside the expected range (<7% for human and ATDs), the subject was re-run in the same cell if authorized by the Principal Investigator (PI) in conjunction with the Medical Observer. Post-test analysis of the acceleration levels and high-speed videos was conducted by the Test Conductor and Medical Observer prior to proceeding to the next level.

Table 1. VDT Impact Test Matrix

Test Cell/G Level	Seat	Restraint Harness	Headrest Position	Helmet Type
TV6	ACES II	PCU-15/P	0”	HGU-55/P
A6, A8, A10, A12, A15	ACES II	PCU-15/P	0”	HGU-55/P
AN10[1]	ACES II	PCU-15/P	0”	NONE
AC10[2]	ACES II	PCU-15/P	0”	HGU-55/P
AS6, AS10[3]	ACES II	PCU-15/P	0”	HGU-55/P
B6, B8, B10, B12, B15	ACES II	PCU-15/P	2.5”	HGU-55/P
C6, C8, C10, C12, C15	ACES II	PCU-15/P	0”	Gen 2
TV6m	US16E	SCH	2.5”	HGU-55/P
D6, D8, D10, D12, D15	US16E	SCH	0”	HGU-55/P
E6, E8, E10, E12, E15	US16E	SCH	2.5”	Gen 2
F4, F6, F8, F10, F12, F15	US16E	SCH	2.5” and NPD	Gen 2
FL6	US16E	SCH	2.5” and NPD	HGU-55/P
G6, G8, G10, G12, G15	US16E	SCH	2.5”	HGU-55/P

[1] No helmet
[2] No seat pan cushion (seat back cushion only)
[3] Side handles

6.2 Pre-Test Procedures

a. Medical checks are performed for human subjects including pregnancy tests for females.
b. The seat is adjusted vertically such that the back of the subject’s head is approximately centered in the headrest (US16E tests only).
c. Zeros are taken for channel calibration.
d. Subjects are fitted with the torso harness prior to being seated, or fitted with the seat-mounted harness and safety strap after being seated (see Section 3.3).
d. Accelerometer arrays are positioned on the human subjects’ bite block, chest, and lumbar regions (see Section 5.1).
e. Subjects are fitted with a flight helmet and oxygen mask. Velcro leg restraints are adjusted to loosely fit the around the ankles. The lap belt and shoulder harness are attached and preloaded.
f. ATD’s hands are placed in the lap near the ejection handle and secured with Velcro straps. Human subjects are instructed to grasp the ejection handle.
f. Still photographs are taken from the side view and/or frontal view.

g. An abort switch is placed in the human subjects' hand which he/she may use to abort the test at any time by releasing the switch. The Medical Observer and Safety Officer also have abort switches and can stop the test at any time prior to test initiation (release of the carriage).
h. The cylinder is filled with water, the Safety Officer performs all required safety checks, and the carriage is hoisted to the predetermined level.
i. The area inside the yellow line around the perimeter of the VDT is evacuated and the Safety Officer checks all safety systems and assures that the test area is safe and secured.
j. When the human subject is in proper test position and all safety checks have been completed, the subject is informed that he or she should prepare for impact and depress and hold the abort switch.
k. If all systems continue to be OK and the Medical Observer and Safety Officer consent, the Test Conductor instructs the facility operator to activate the instrumentation and data collection systems, and release the carriage.

6.3 Post-Test Procedures

a. After the carriage is at rest, the Medical Technician determines if the subject is injured. If the subject shows signs of injury, the Medical Technician contacts the Medical Observer and takes charge of the test subject and, if necessary, assures appropriate medical care is delivered. If warranted (i.e., if the injury is deemed serious), the Medical Technician or Medical Observer commences emergency procedures.
b. The Medical Technician or Medical Observer conducts a brief post-test assessment of the subject after which the subject completes a short questionnaire describing their response to the test.
c. Upon completion of a post-test questionnaire, the subject is instructed to contact the Medical Technician or Medical Observer if any symptoms develop that might be related to the test.
d. For ATD tests, the ATD and test equipment are inspected by Infoscitex personnel and the Safety Officer. Any damage is reported to the Principal Investigator and still photographs are taken for documentation.

6.4 Data Analysis

Head and chest accelerations (linear and angular) were collected and analyzed for both human and ATD subjects (LOIS and LARD only) to ascertain differences between the various seat parameters. Due to anomalies in the human angular acceleration data, those are not included in this report. Neck and lumbar forces and torques were also collected and analyzed for the ATDs. The ATD data was also evaluated for comparison with human tests and to ascertain responses at the higher acceleration levels. Data tables and plots showing the responses of the instrumented humans and ATDs as a function of impact level for specific measured variables were developed and assessed. Note that Carriage Acceleration is referred to as "Sled Acceleration" in some plots and Results narratives due to limitations in the graphing software.

All data plots were reviewed and any short-duration data spikes were removed from the analysis. These could occur due to the subject's head striking the headrest, chin striking the chest, bite-bar striking the oxygen mask, or chest pack striking the harness buckle. Typically

any spikes outside the range of 50-150 ms in the acceleration response were removed for these reasons. In some cases, the subjects repeated a test cell due to improper bracing or carriage acceleration level that was outside the required ± 2%, in which case only the most recent test was used. Statistical comparisons were accomplished using Matched-Pair T-tests. Results were considered significant if $\alpha \leq 0.05$. In cases where a subject did not complete all the cells being compared, his/her data would not be used for that comparison. The statistics were not accomplished for the ATD tests since only 1-3 ATD tests were conducted for each condition.

7.0 RESULTS

7.1 VDT Parametric Assessment: Headrest Position

A comparative assessment of data from impact acceleration tests with varying headrest configurations was conducted to determine the effects on human and ATD response of repositioning the headrests. Data from tests in the ACES II seat with the headrest in-line with the seat back (Cell A) were compared to tests with the headrest moved 2.5" forward of the seat back (Cell B). The comparisons were conducted with both test cells using a standard torso-mounted PCU-15/P harness and HGU-55/P helmet. Data from tests with a US16E (JSF) seat were also evaluated with the headrest in the standard 2.5" forward position (Cell G) being compared to tests with the headrest repositioned in-line with the seat back (Cell D). These comparisons were conducted with both test cells using the seat-mounted SCH harness and the HGU-55/P helmet.

The measured accelerations and loads generally increased linearly for both humans and ATDs (except for some non-linearity in the ATD neck torque) for all conditions as a function of impact acceleration, as shown in Figures 7-15. The LARD acceleration responses were larger than LOIS at all levels.

Head Z Acceleration. The human head z acceleration responses were generally in-between LOIS and LARD as shown in Figure 7. As shown in Table 2, the head z acceleration responses for both humans and ATDs tended to be slightly lower with the forward headrests (cells B and G) compared to the in-line headrests (cells A and D) for both ACES II and JSF seats, although the differences were not statistically significant except for the 10 G human tests with JSF seat. Notable exceptions were the LARD tests in the JSF seat at 8 G, and LARD tests in the ACES II seat at 12 G which both demonstrated higher head z accelerations for the forward headrest.

Table 2. Headrest Comparison (A vs B and D vs G) – Head Z Accel (G)

G Level	Test Subject	ACES II			JSF		
		In-line (A)	Forward (B)	% Diff	In-line (D)	Forward (G)	% Diff
6	Human	8.19 ± 0.6	8.08 ± 1.0	-1.34	6.94 ± 0.4	6.84 ± 0.6	-1.44
	LOIS	6.45	6.66	3.26	6.68	6.36	-4.79
	LARD	7.94	7.54	-5.04	6.90	7.24	4.93
8	Human	11.76 ± 1.0	11.35 ± 1.3	-3.49	9.82 ± 1.6	9.48 ± 1.1	-3.46
	LOIS	8.93	9.01	0.90	8.64	8.39	-2.89
	LARD	11.90	11.28	-5.21	10.45	11.79	12.82
10	Human	15.03 ± 1.5	14.10 ± 1.9	-6.19	12.81 ± 1.4	11.67 ± 1.4	-8.90*
	LOIS	12.13	11.70	-3.54	11.06	10.54	-4.70
	LARD	16.15	15.74	-2.54	15.66	14.58	-6.90
12	LOIS	14.88	14.11	-5.17	13.35	13.15	-1.50
	LARD	18.98	21.22	11.80	19.63		N/A
15	LOIS	19.60	18.94	-3.37	17.58	17.13	-2.56
	LARD	27.44	26.99	-1.64	28.75		N/A

* denotes statistical significance

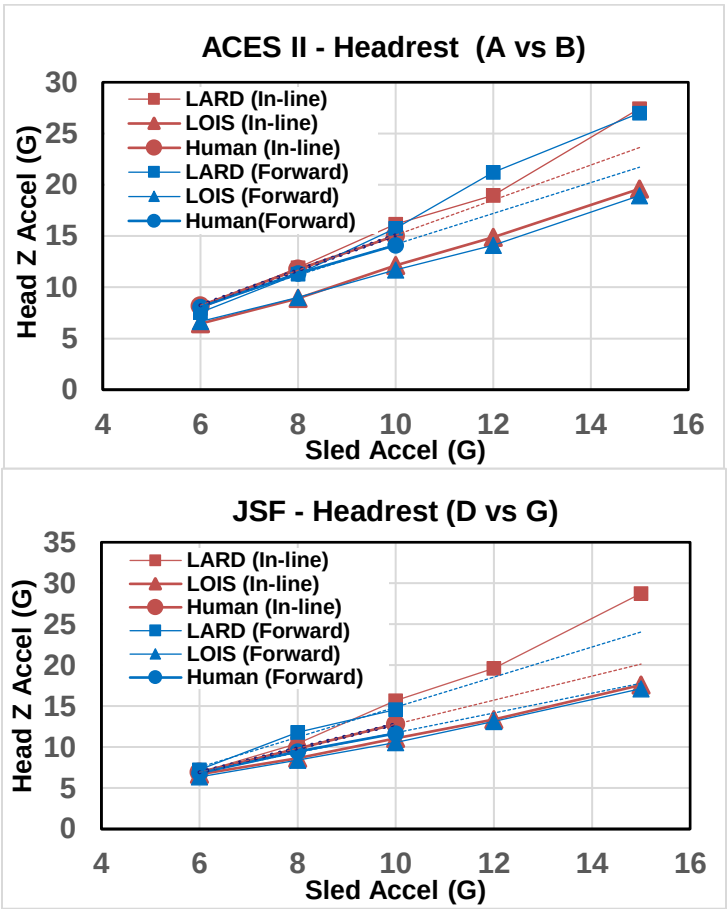

Figure 7. Headrest Comparison – Head Z Acceleration

Head X Acceleration. As shown in Figure 8, the magnitude of the human head x accelerations (forward direction away from the headrest) were toward the lower end of the ATD responses for all conditions. As shown in Table 3, the human subjects produced substantially greater head x accelerations (25-80%) in the forward headrest configurations for both the ACES II seat (Cell B) and JSF seat (Cell G) compared to the accelerations with the in-line headrest (cells A and D), and the results were significant at 10 G for both seats. The ATD subjects also produced greater head x accelerations in the forward headrest configuration with both seats at nearly all carriage acceleration levels, with the effects being more pronounced at higher acceleration levels.

Table 3. Headrest Comparison (A vsB and D vs G) – Head X Accel (G)

G Level	Test Subject	ACES II In-line (A)	ACES II Forward (B)	ACES II % Diff	JSF In-line (D)	JSF Forward (G)	JSF % Diff
6	Human	1.47 ± 0.8	2.50 ± 1.1	70.07*	1.09 ± 1.1	1.47 ± 1.0	34.86
	LOIS	2.77	2.86	3.25	0.77	1.82	136.4
	LARD	4.45	3.88	-12.81	1.90	2.26	18.95
8	Human	2.06 ± 1.1	3.23 ± 2.2	56.80	1.94 ± 0.8	2.45 ± 1.3	26.29
	LOIS	3.46	4.10	18.50	1.42	2.85	100.7
	LARD	6.10	6.20	1.64	3.72	3.96	6.45
10	Human	2.54 ± 1.2	4.57 ± 1.5	79.92*	1.99 ± 1.5	3.16 ± 1.6	58.79*
	LOIS	4.77	5.16	8.18	2.26	3.68	62.83
	LARD	7.30	7.84	7.40	4.69	4.74	1.07
12	LOIS	5.29	6.24	17.96	2.88	4.30	49.31
	LARD	7.41	8.98	21.19	5.18		N/A
15	LOIS	6.00	7.25	20.83	3.53	5.10	44.48
	LARD	9.83	10.57	7.53	5.39		N/A

* denotes statistical significance

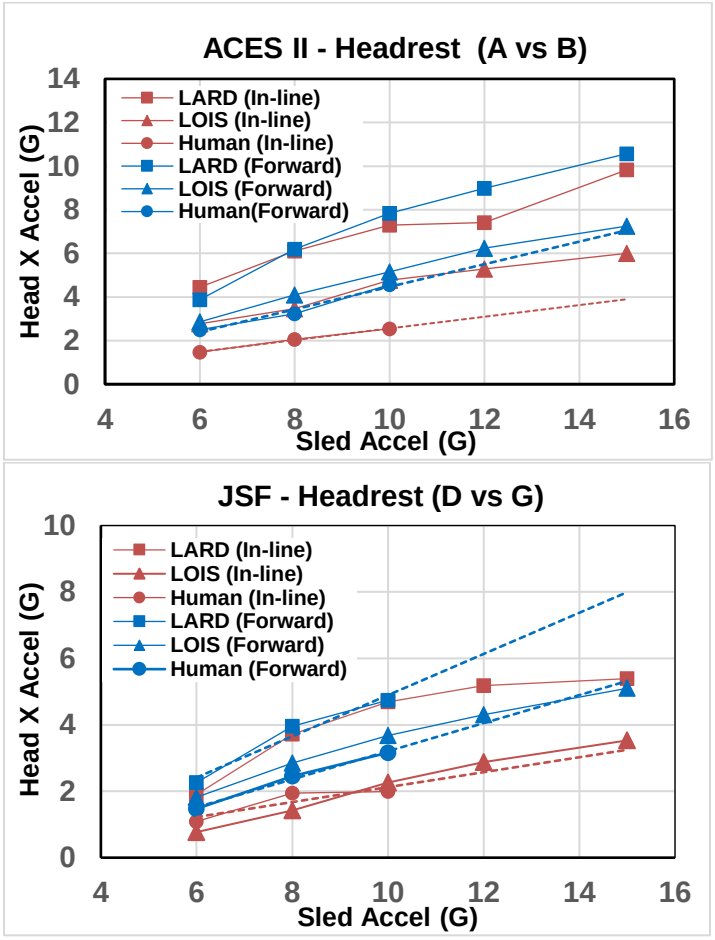

Figure 8. Headrest Comparison – Head X Acceleration (G)

Resultant Chest Acceleration. As shown in Figure 9, the magnitude of the human acceleration responses tended to be toward the higher end of the ATD responses in both seats. As shown in Table 4, the resultant chest accelerations for the human subjects were slightly lower (<5%) in the forward headrest configurations than with the in-line configuration for both seats. There were no meaningful correlations between the in-line and forward headrest configurations with either of the ATDs.

Table 4. Headrest Comparison (A vs B and D vsG) – Res Chest Accel (G)

G Level	Test Subject	ACES II In-line (A)	ACES II Forward (B)	ACES II % Diff	JSF In-line (D)	JSF Forward (G)	JSF % Diff
6	Human	8.51 ± 0.7	8.43 ± 0.6	-0.94	7.42 ± 0.3	7.14 ± 0.4	-3.77
	LOIS	6.65	6.95	4.51	6.67	6.57	-1.50
	LARD	8.70	8.01	-7.93	6.99	7.40	5.87
8	Human	12.30 ± 1.6	12.19 ± 1.1	-0.89	10.51 ± 0.7	10.36 ± 0.5	-1.43
	LOIS	9.36	9.65	3.10	8.58	8.72	1.63
	LARD	13.31	12.66	-4.88	10.85	12.47	14.93
10	Human	16.22 ± 3.2	15.88 ± 1.9	-2.10	14.23 ± 0.7	13.56 ± 1.1	-4.71
	LOIS	12.47	12.37	-0.80	11.18	11.01	-1.52
	LARD	17.99	17.17	-4.56	16.34	16.21	-0.80
12	LOIS	15.31	14.92	-2.55	13.78	13.67	-0.80
	LARD	21.06	24.03	14.10	20.91		N/A
15	LOIS	20.50	19.77	-3.56	17.86	18.18	1.79
	LARD	29.69	29.82	-33.24	29.62		N/A

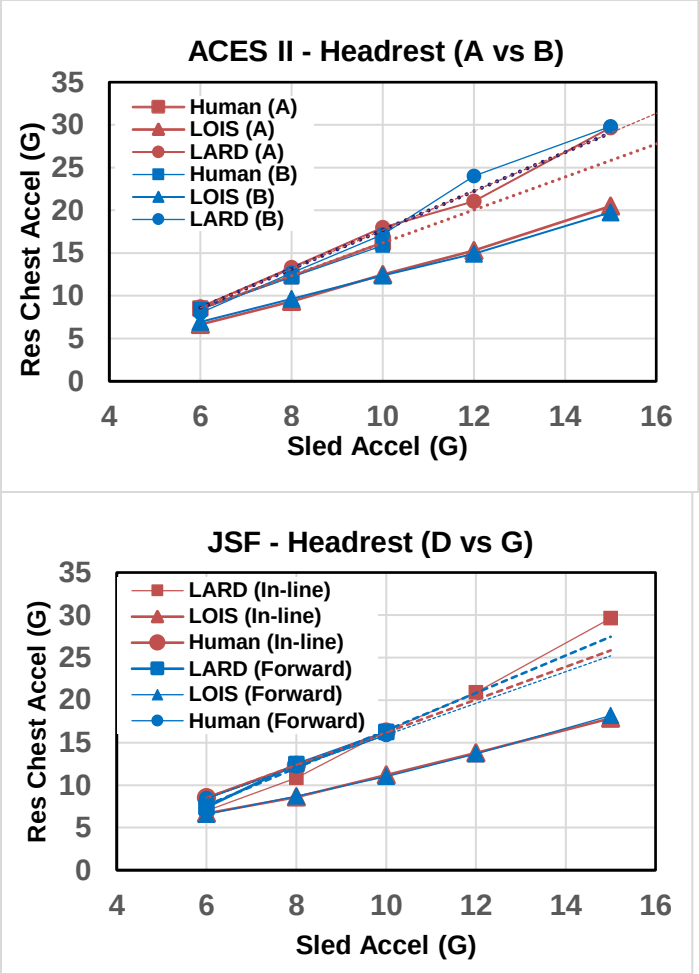

Figure 9. Headrest Comparison – Ressultant Cest Acceleration

Head +Ry Angular Acceleration (ATDs Only). In the ACES II configuration, neither ATD demonstrated consistent differences in head angular +Ry angular acceleration (forward flexion) between the in-line headrest (Cell A) and the forward headrest (Cell B) conditions, as shown in Figure 10 and Table 5. In the JSF configuration, the +Ry angular accelerations were higher in the forward headrest condition (Cell G) compared to the in-line headrest (Cell D) for LOIS, but the results were inconsistent for LARD. The -Ry angular accelerations (not shown here) were also inconsistent with the exception of larger LOIS accelerations in the JSF forward headrest condition, similar to the trend in the +Ry angular accelerations.

Table 5. Headrest Comparison (A vs B and D vs G) – Head + Ry Angular Accel (Rad/Sec²)

G Level	Test Subject	ACES II In-line (A)	ACES II Forward (B)	ACES II % Diff	JSF In-line (D)	JSF Forward (G)	JSF % Diff
6	LOIS	63.88	68.78	7.67	62.87	87.74	39.56
	LARD	141.5	157.5	11.30	61.59	86.04	39.70
8	LOIS	130.0	150.4	15.69	59.18	100.7	70.19
	LARD	333.1	286.1	-14.12	154.7	216.7	40.07
10	LOIS	244.5	275.2	12.52	110.8	118.1	6.54
	LARD	501.9	405.1	-19.29	311.4	298.0	-4.30
12	LOIS	373.4	366.2	-1.93	145.4	177.0	21.78
	LARD	545.2	599.2	9.90	539.5		N/A
15	LOIS	569.1	525.4	-7.68	239.8	330.3	37.76
	LARD	793.5	654.4	-17.53	757.9		N/A

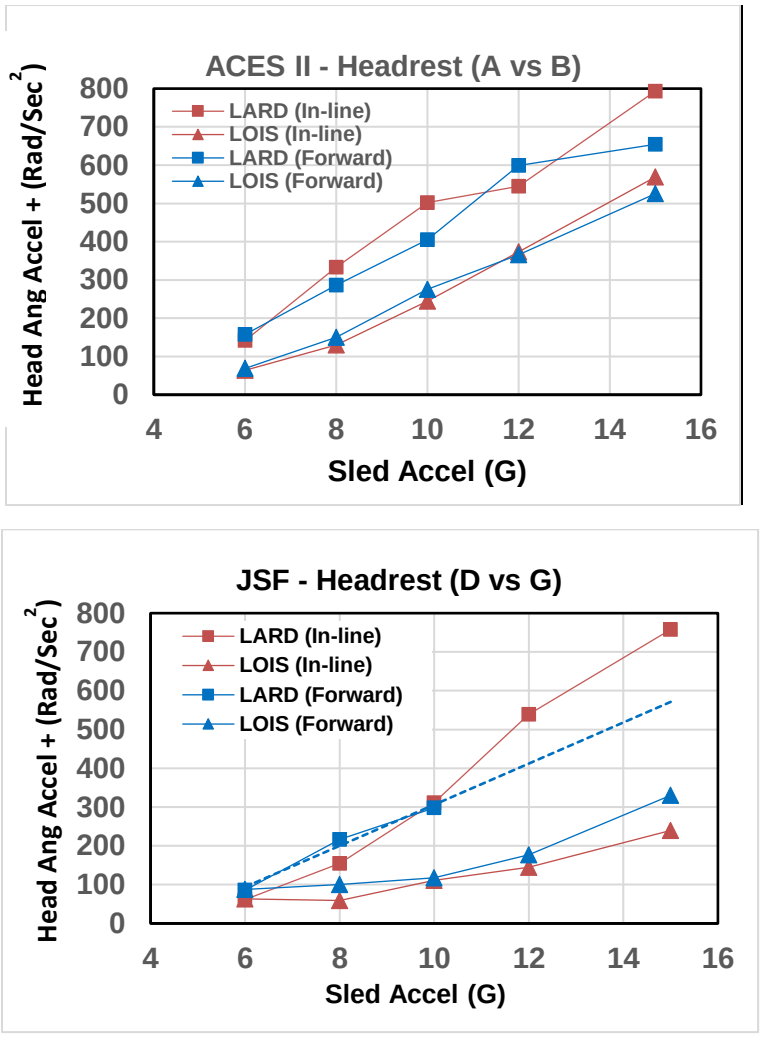

Figure 10. Headrest Comparison – Head RY Angular Acceleration

Neck Z Loads (ATDs Only). As shown in Figure 11 and Table 6, the neck z loads for the in-line and forward headrest configurations were very similar in linearity and magnitude in comparisons for both the ACES II seat (Cell A vs B) and the JSF seat (Cell D vs G).

Table 6. Headrest Comparison (A vs B and D vs G) – Neck Z Load (lb)

G Level	Test Subj	ACES II			JSF		
		In-line(A)	Forward(B)	% Diff	In-line(D)	Forward(G)	% Diff
6	LOIS	67.78	68.02	0.35	71.54	69.89	-2.31
	LARD	98.56	93.42	-5.22	89.46	93.72	4.76
8	LOIS	92.14	91.54	-0.65	91.96	94.34	2.59
	LARD	136.5	131.8	-3.39	124.7	148.4	19.04
10	LOIS	123.7	118.2	-4.42	117.9	113.3	-3.95
	LARD	180.2	175.4	-2.65	180.8	173.0	-4.29
12	LOIS	150.9	145.4	-3.63	138.5	140.4	1.38
	LARD	213.6	244.5	14.46	222.6		N/A
15	LOIS	199.4	191.7	-3.84	182.6	181.3	-0.74
	LARD	312.9	316.8	1.24	317.0		N/A

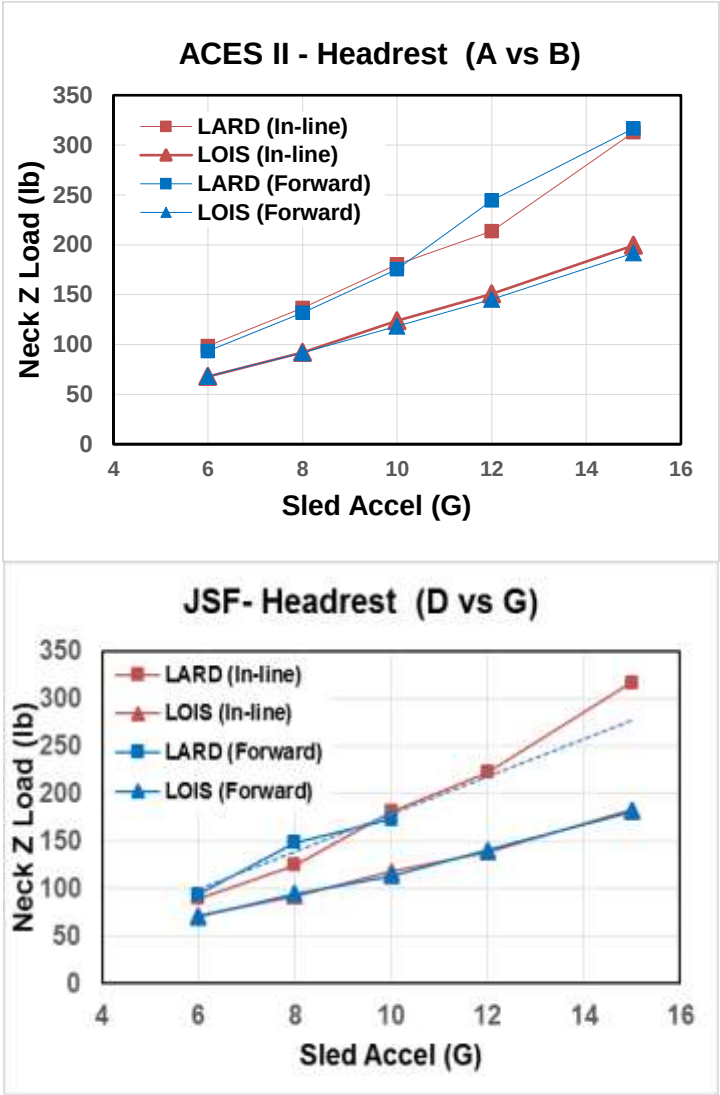

Figure 11. Headrest Comparison – Neck Z Load

Neck X Loads (ATDs Only). As shown in Figure 12 and Table 7, in the ACES II seat at the higher carriage acceleration levels, the neck loads were larger for both ATDs in the forward headrest configuration than the in-line headrest (Cell A vs B). In the JSF seat, the neck loads were substantially higher with the forward headrest for LOIS (Cell D vs G), but the data were inconsistent for LARD.

Table 7. Headrest Comparison (A vs B and D vs G) – Neck X Load (lb)

G Level	Test Subj	ACES II			JSF		
		In-line(A)	Forward(B)	% Diff	In-line(D)	Forward(G)	% Diff
6	LOIS	27.56	18.19	-34.00	6.60	13.44	103.6
	LARD	61.13	50.34	-17.65	23.77	29.61	24.57
8	LOIS	32.10	32.94	2.62	11.94	22.95	92.21
	LARD	84.56	80.93	-4.29	50.54	54.56	7.95
10	LOIS	50.79	53.85	6.02	19.39	31.49	62.40
	LARD	97.59	101.2	3.70	65.32	60.62	-7.20
12	LOIS	58.51	67.69	15.69	25.76	40.27	56.33
	LARD	98.39	110.5	12.30	73.28		N/A
15	LOIS	67.39	79.26	17.61	33.09	54.31	64.13
	LARD	120.1	127.6	6.30	86.72		N/A

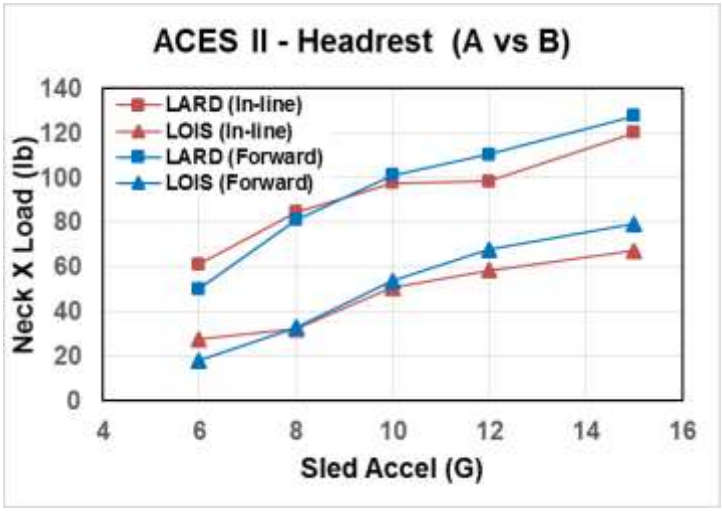

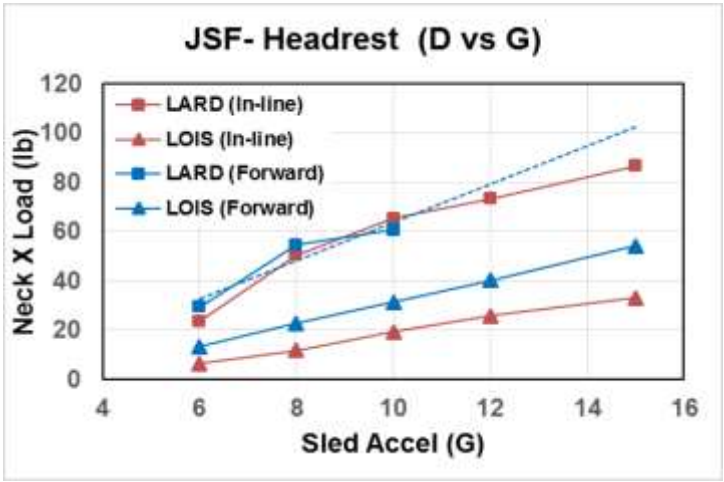

Figure 12. Headrest Comparison – Neck X Load

Neck My Torque (ATDs Only). As shown in Figure 13, the measured neck My torque (forward rotation) generally increased with increasing carriage acceleration level in tests with the ACES II seat, while some non-linearity was present in the JSF seat tests, especially at the higher levels. LARD generated larger neck torques than LOIS, with the exception of tests with the forward headrest in the JSF seat (Cell G) where the responses were similar between the two ATDs. As shown in Table 8, in the ACES II seat the neck torques were generally higher with the forward headrest compared to the in-line headrest (Cell A vs B) for LARD but lower for LOIS. The results of the headrest comparisons for the JSF configuration (Cell D vs G) were inconclusive for both ATDs.

Table 8. Headrest Comparison (a vs B and D vs G) – Neck My Torque (in-lb)

G Level	Test Subj	ACES II			JSF		
		In-line(A)	Forward(B)	% Diff	In-line(D)	Forward(G)	% Diff
6	LOIS	67.68	70.31	3.89	42.68	54.11	26.78
	LARD	78.17	74.95	-4.12	38.99	51.72	32.65
8	LOIS	84.00	82.85	-1.37	59.96	85.01	41.78
	LARD	120.0	127.1	5.93	76.99	77.00	0.01
10	LOIS	88.56	83.75	-5.43	78.16	91.23	16.72
	LARD	174.0	206.1	18.48	90.68	86.59	-4.51
12	LOIS	91.29	73.02	-20.01	96.97	90.51	-6.66
	LARD	175.6	245.3	39.72	95.33		N/A
15	LOIS	97.48	84.04	-13.79	107.4	91.69	-14.62
	LARD	263.2	302.0	14.73	151.9		N/A

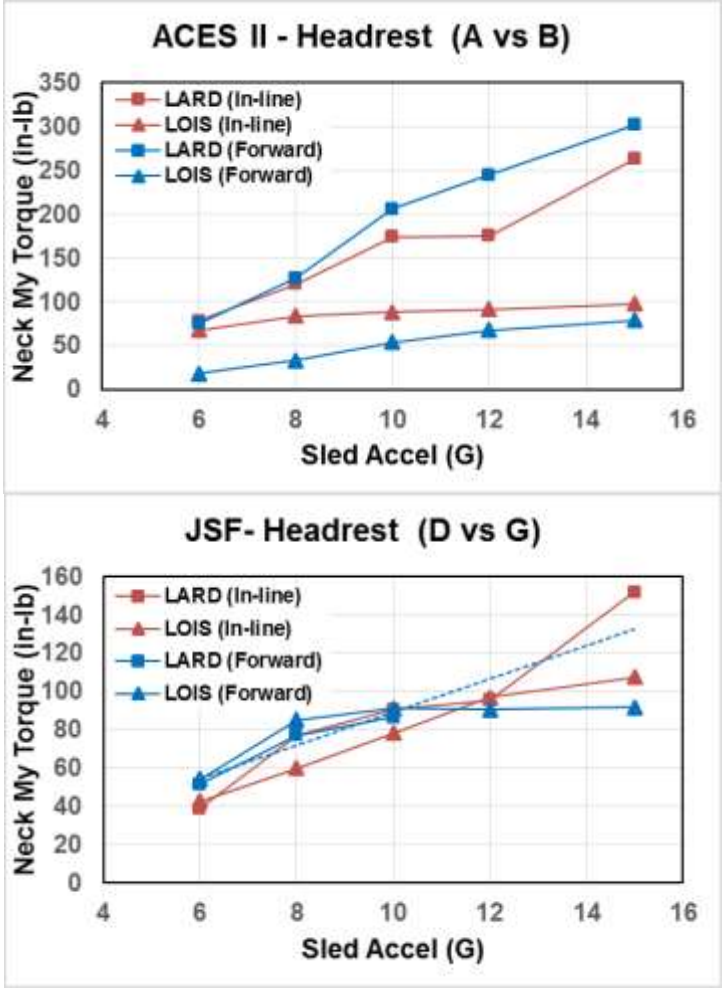

Figure 13. Headrest Comparison – Neck My Torque

Lumbar Z Loads (ATDs Only). As shown in Table 9 and Figure 14, in the ACES II seat at the higher carriage acceleration levels the lumbar z loads for LARD with the forward headrest (Cell B) were generally lower than with the in-line headrest (Cell A), but similar with LOIS. In the JSF seat, the lumbar z loads were similar for both headrests (Cell D vs G). However, the lumbar z load for LARD in the JSF seat at the 15 G carriage acceleration level with in-line headrest (Cell D) was substantially greater than for LARD in the ACES II seat under either headrest condition (Cell A or B).

Table 9. Headrest Comparison (A vs B and D vs G) – Lumbar Z Load (lb)

G Level	Test Subj	ACES II			JSF		
		In-line(A)	Forward(B)	% Diff	In-line(D)	Forward(G)	% Diff
6	LOIS	300.3	312.1	3.93	313.4	308.8	-1.45
	LARD	517.9	573.1	10.64	556.5	591.1	6.21
8	LOIS	429.7	437.2	1.75	402.4	417.7	3.80
	LARD	821.7	755.0	-8.12	872.7	785.8	-9.97
10	LOIS	585.9	566.2	-3.37	524.5	546.9	4.27
	LARD	974.5	832.8	-14.54	1021	967.3	-5.25
12	LOIS	703.7	675.2	-4.05	642.7	687.4	6.96
	LARD	1149	857.0	-25.44	1223		N/A
15	LOIS	946.1	902.5	-4.61	840.0	894.3	6.45
	LARD	1142	984.1	-13.80	1586		N/A

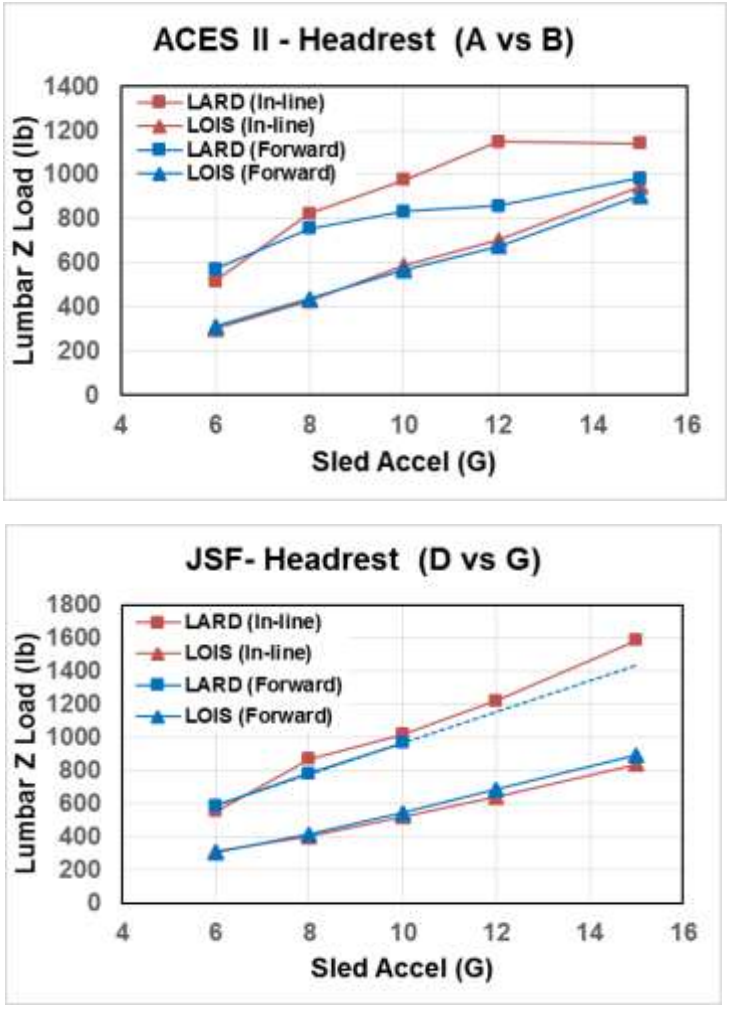

Figure 14. Headrest Comparison – Lumbar Z Load

Lumbar My Torque (ATDs Only). The measured lumbar My torque (forward rotation) increased linearly for LARD as shown in Figure 15, while the responses were relatively flat for LOIS. The magnitude of the lumbar My torque at higher carriage acceleration levels for LOIS was generally higher with the forward headrest compared to the in-line headrest configuration in both the ACES II seat (Cell A vs B) and the JSF seat (Cell D vs G), as shown in Table 10, but was inconclusive for the LARD data in both seats.

Table 10. Headrest Comparison (A vs B and D vs G) – Lumbar My Torque (in-lb)

G Level	Test Subj	ACES II			JSF		
		In-line(A)	Forward(B)	% Diff	In-line(D)	Forward(G)	% Diff
6	LOIS	65.59	179.8	174.1	274.3	329.8	20.24
	LARD	1237	1064	-14.00	677.9	1005	48.20
8	LOIS	154.3	298.1	93.16	353.1	351.9	-0.33
	LARD	1746	1574	-9.82	1270	1606	26.49
10	LOIS	349.5	363.4	3.99	403.4	406.1	0.66
	LARD	2290	2090	-8.74	1879	1601	-14.82
12	LOIS	450.0	511.6	13.70	449.6	466.0	3.65
	LARD	2561	2620	2.30	1932		N/A
15	LOIS	659.0	765.2	16.11	402.0	531.2	32.13
	LARD	3174	3209	1.10	2864		N/A

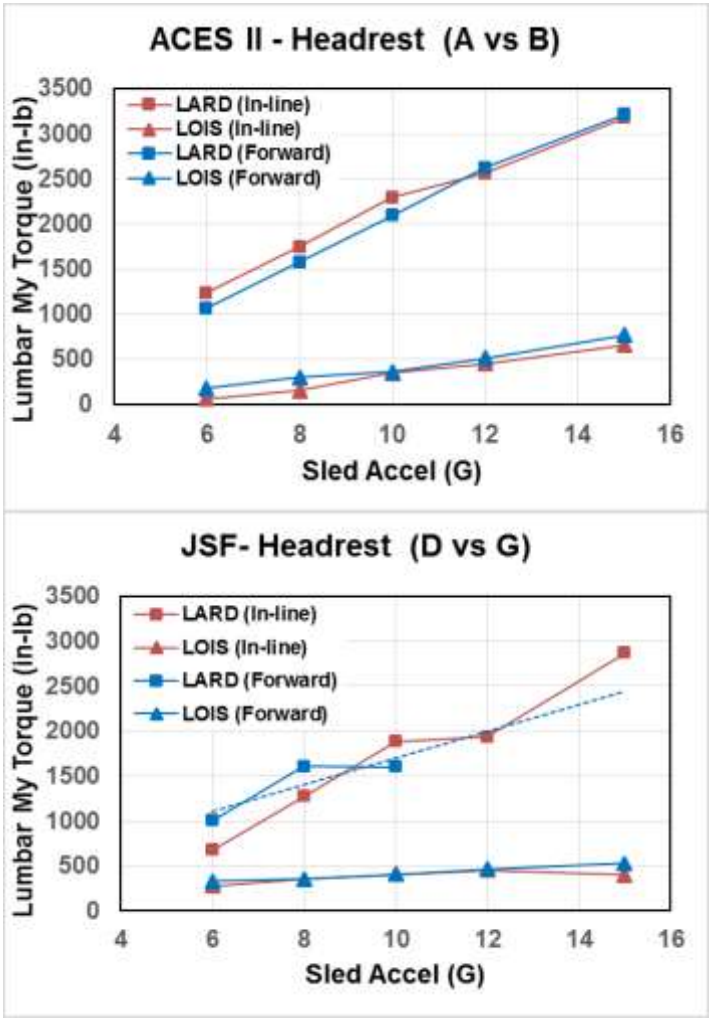

Figure 15. Headrest Comparison – Lumbar My Torque

7.2 VDT Parametric Assessment: Restraint System

A comparative assessment of data from impact acceleration tests with varying restraint configurations was conducted to determine the effects on human and ATD response of the different restraint configurations. Data from tests in an ACES II seat with a standard torso-mounted PCU-15/P harness were compared to tests in the JSF seat with a seat-mounted SCH harness (Cell A vs D). The comparisons were conducted with both configurations using a standard HGU-55/P helmet and in-line headrest. Comparisons between the restraint systems were also conducted with the headrests positioned 2.5" forward for both the ACES II seat and the JSF seat (Cell B vs G).

The measured accelerations and loads generally increased linearly for both humans and ATDs for all conditions as a function of impact acceleration, as shown in Figures 16-24. The LARD acceleration responses were generally larger than LOIS at all levels.

Head Z Acceleration. The human head z accelerations in both the in-line and forward headrest conditions were slightly lower in tests with the SCH harness compared to the PCU harness (significant at all carriage acceleration levels), as shown in Table 11 and Figure 16. In tests with the ATD subjects, LOIS generated slightly lower head z accelerations with the SCH harness for both headrest configurations, while results for LARD were inconclusive.

Table 11. Harness Comparison (A vs B and D vs G) – Head Z Accel (G)

G Level	Test Subject	In-line Headrest PCU (A)	In-line Headrest SCH (D)	In-line Headrest % Diff	Forward Headrest PCU (B)	Forward Headrest SCH (G)	Forward Headrest % Diff
6	Human	7.99 ± 0.5	6.98 ± 0.3	-12.64*	7.98 ± 1.0	6.87 ± 0.7	-13.91*
	LOIS	6.45	6.68	3.57	6.66	6.36	-4.50
	LARD	7.94	6.90	-13.10	7.54	7.24	-3.98
8	Human	11.45 ± 1.1	9.84 ± 1.6	-14.06*	11.27 ± 1.4	9.59 ± 1.2	-14.91*
	LOIS	8.93	8.64	-3.25	9.01	8.39	-6.88
	LARD	11.90	10.45	-12.18	11.28	11.79	4.52
10	Human	14.95 ± 1.5	12.85 ± 1.5	-14.05*	14.23 ± 2.0	11.60 ± 1.5	-18.48*
	LOIS	12.13	11.06	-8.82	11.70	10.54	-9.91
	LARD	16.15	15.66	-3.03	15.74	14.58	-7.37
12	LOIS	14.88	13.35	-10.28	14.11	13.15	-6.80
	LARD	18.98	19.63	3.42	21.22		N/A
15	LOIS	19.60	17.58	-10.31	18.94	17.13	-9.56
	LARD	27.44	28.75	4.77	26.99		N/A

* denotes statistical significance

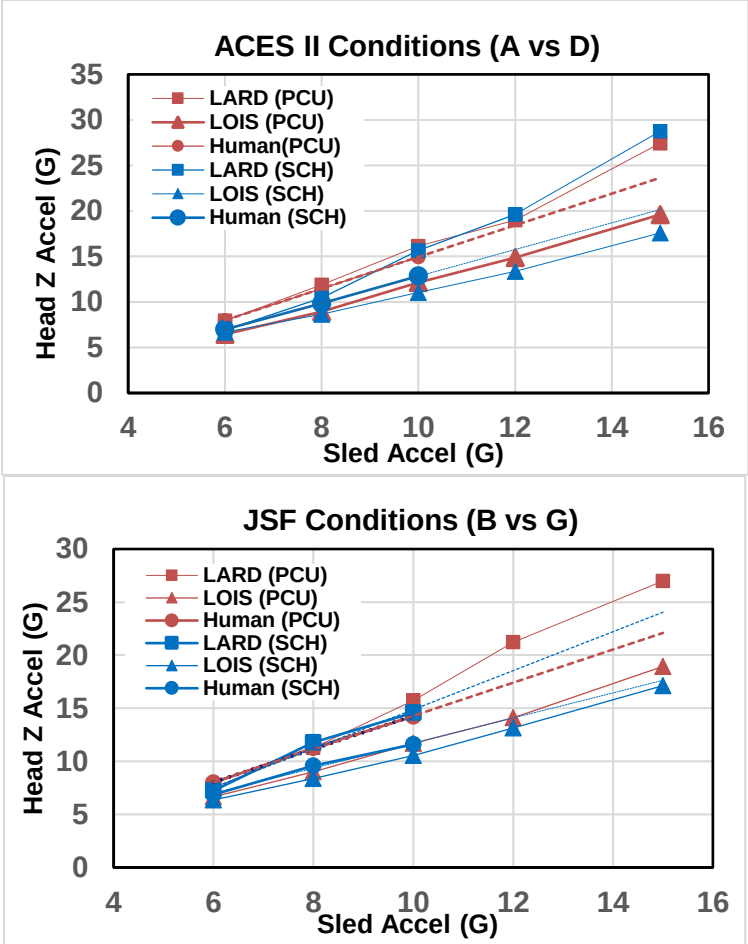

Figure 16. Harness Comparison – Head Z Acceleration

Head X Acceleration. As shown in Figure 17, the human head x accelerations tended to be more similar to LOIS than LARD under most conditions. As shown in Table 12, the human head x accelerations were lower in tests with the SCH harness for the in-line headrest condition (cells A vs D, not significant), and also lower for the SCH harness in the forward headrest condition (cells B vs G, significant at 6 G and 10 G). The head x accelerations for the ATD tests were also consistently lower when using the SCH versus the PCU harness for both headrest conditions.

Table 12. Harness Comparison (A vs D abd B vs G) – Head X Accel (G)

G Level	Test Subject	In-line Headrest PCU (A)	SCH (D)	% Diff	Forward Headrest PCU (B)	SCH (G)	% Diff
6	Human	1.52 ± 0.8	1.09 ± 0.6	-28.29	2.36 ± 1.1	1.65 ± 1.0	-30.08*
	LOIS	2.77	0.77	-72.20	2.86	1.82	-36.36
	LARD	4.45	1.90	-57.30	3.88	2.26	-41.75
8	Human	2.28 ± 1.0	1.90 ± 0.8	-16.67	3.05 ± 2.5	2.28 ± 1.2	-25.25
	LOIS	3.46	1.42	-58.96	4.10	2.85	-30.49
	LARD	6.10	3.72	-39.02	6.20	3.96	-36.13
10	Human	2.36 ± 1.1	1.94 ± 1.6	-17.80	4.61 ± 1.5	3.45 ± 1.7	-25.16*
	LOIS	4.77	2.26	-52.62	5.16	3.68	-28.68
	LARD	7.30	4.69	-35.75	7.84	4.74	-39.54
12	LOIS	5.29	2.88	-45.56	6.24	4.30	-31.09
	LARD	7.41	5.18	-30.09	8.98		N/A
15	LOIS	6.00	3.53	-41.17	7.25	5.10	-29.66
	LARD	9.83	5.39	-45.17	10.57		N/A

* denotes statistical significance

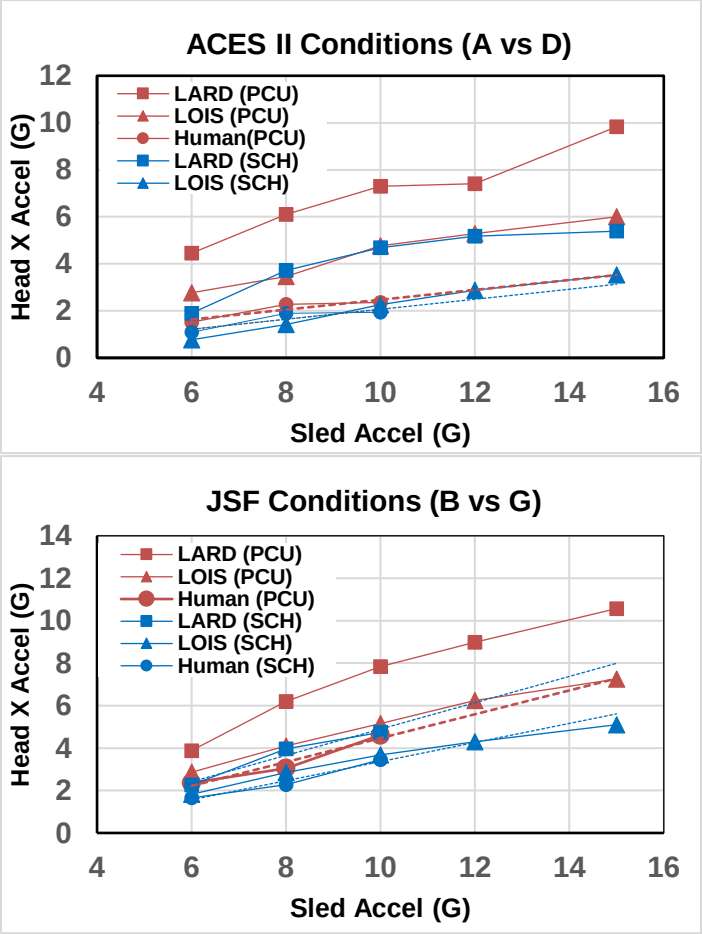

Figure 17. Harness Comparison – Head X Acceleration

Resultant Chest Acceleration. As shown in Table 13 and Figure 18, the resultant chest accelerations for the human subjects were slightly lower in tests with the SCH harness compared to the PCU harness for both seat configurations (cells A vs D and cells B vs G), with all but one condition significant. The ATD chest accelerations were also lower (0-20%) at nearly all carriage accelerations levels for the SCH harness in both headrest conditions.

Table 13. Harness Comparison (A vs D and B vs G) – Res Chest Accel (G)

G Level	Test Subject	In-line Headrest			Forward Headrest		
		PCU (A)	SCH (D)	% Diff	PCU (B)	SCH (G)	% Diff
6	Human	8.53 ± 0.8	7.46 ± 0.3	-12.54*	8.28 ± 0.5	7.26 ± 0.3	-12.32*
	LOIS	6.65	6.67	0.30	6.95	6.57	-5.47
	LARD	8.70	6.99	-19.66	8.01	7.40	-7.62
8	Human	12.06 ± 1.4	10.51 ± 0.7	-12.85*	12.03 ± 0.8	10.41 ± 0.6	-13.47*
	LOIS	9.36	8.58	-8.33	9.65	8.72	-9.64
	LARD	13.31	10.85	-18.48	12.66	12.47	-1.50
10	Human	15.82 ± 3.1	14.20 ± 0.8	-10.24	15.38 ± 1.5	13.47 ± 1.2	-12.42*
	LOIS	12.47	11.18	-10.34	12.37	11.01	-10.99
	LARD	17.99	16.34	-9.17	17.17	16.21	-5.59
12	LOIS	15.31	13.78	-9.99	14.92	13.67	-8.38
	LARD	21.06	20.91	-0.71	24.03		N/A
15	LOIS	20.50	17.86	-12.88	19.77	18.18	-8.04
	LARD	29.69	29.62	-0.24	29.72		N/A

* denotes statistical significance

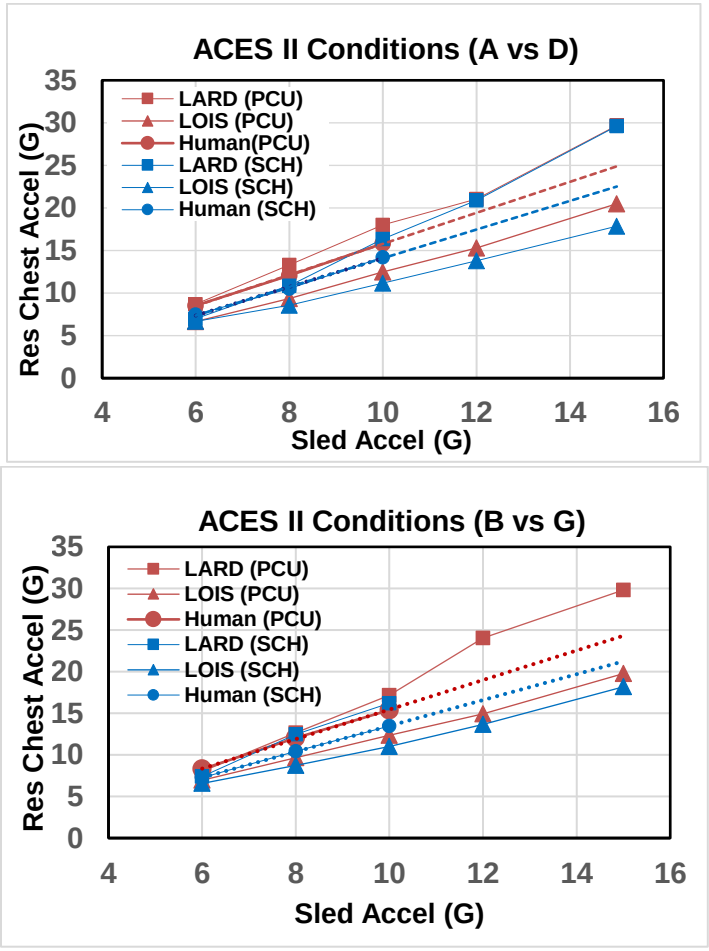

Figure 18. Harness Comparison – Resultant Chest Acceleration

Head +Ry Angular Acceleration (ATDs Only). As shown in Table 14 and Figure 19, both the LOIS and LARD demonstrated lower accelerations for the SCH harness under nearly all conditions, with the differences in tests with LOIS more pronounced at the higher carriage acceleration levels. In general, trends for the –Ry head angular accelerations (not shown here) were very similar to the +Ry responses for both ATDs.

Table 14. Harness Comparison (A vs D and B vs G) – Head +Ry Angular Accel (Rad/Sec²)

G Level	Test Subject	In-line Headrest PCU (A)	SCH (D)	% Diff	Forward Headrest PCU (B)	SCH (G)	% Diff
6	LOIS	63.88	62.87	-1.58	68.78	87.7	27.57
	LARD	141.5	61.59	-56.46	157.5	86.0	-45.36
8	LOIS	130.0	59.18	-54.47	150.4	100.7	-33.02
	LARD	333.1	154.7	-53.56	286.1	216.7	-24.25
10	LOIS	244.5	110.8	-54.68	275.2	118.1	-57.09
	LARD	501.9	311.4	-37.96	405.1	298.0	-26.43
12	LOIS	373.4	145.4	-61.07	366.2	177.0	-51.65
	LARD	545.2	539.5	-1.04	599.2		N/A
15	LOIS	569.1	239.8	-57.87	525.4	330.3	-37.13
	LARD	793.5	757.9	-4.49	654.4		N/A

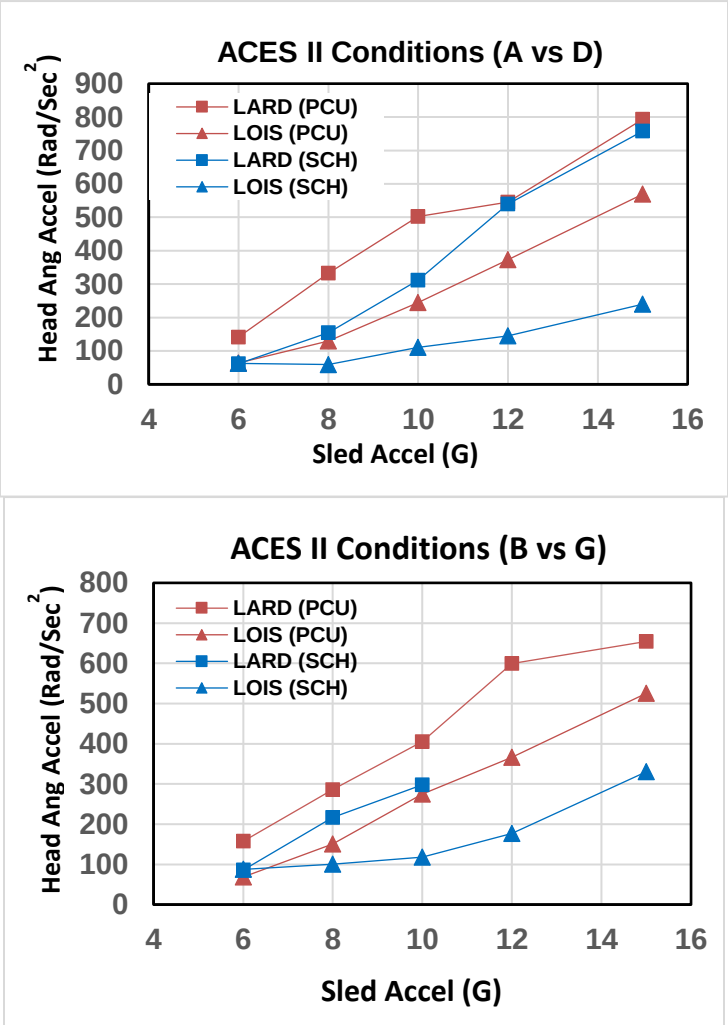

Figure 19. Harness Comparison – Head Ry Angular Acceleration

Neck Z Loads (ATDs Only). As shown in Table 15 and Figure 20, the neck loads for the PCU and SCH harnesses were very similar for both the in-line (cells A vs D) and forward headrest configurations (cells B vs G) at all carriage acceleration levels.

Table 15. Harness Comparison (A vs D and B vs G) – Neck Z Load (lb)

G Level	Test Subj	In-line Headrest			Forward Headrest		
		PCU (A)	SCH (D)	% Diff	PCU (B)	SCH (G)	% Diff
6	LOIS	67.78	71.54	5.55	68.02	69.89	2.75
	LARD	98.56	89.46	-9.23	93.42	93.72	0.32
8	LOIS	92.14	91.96	-0.20	91.54	94.34	3.06
	LARD	136.5	124.7	-8.64	131.8	148.4	12.57
10	LOIS	123.7	117.9	-4.67	118.2	113.3	-4.20
	LARD	180.2	180.8	0.34	175.4	173.0	-1.35
12	LOIS	150.9	138.5	-8.24	145.4	140.4	-3.47
	LARD	213.6	222.6	4.19	244.5		N/A
15	LOIS	199.4	182.6	-8.43	191.7	181.3	-5.47
	LARD	312.9	317.0	1.30	316.8		N/A

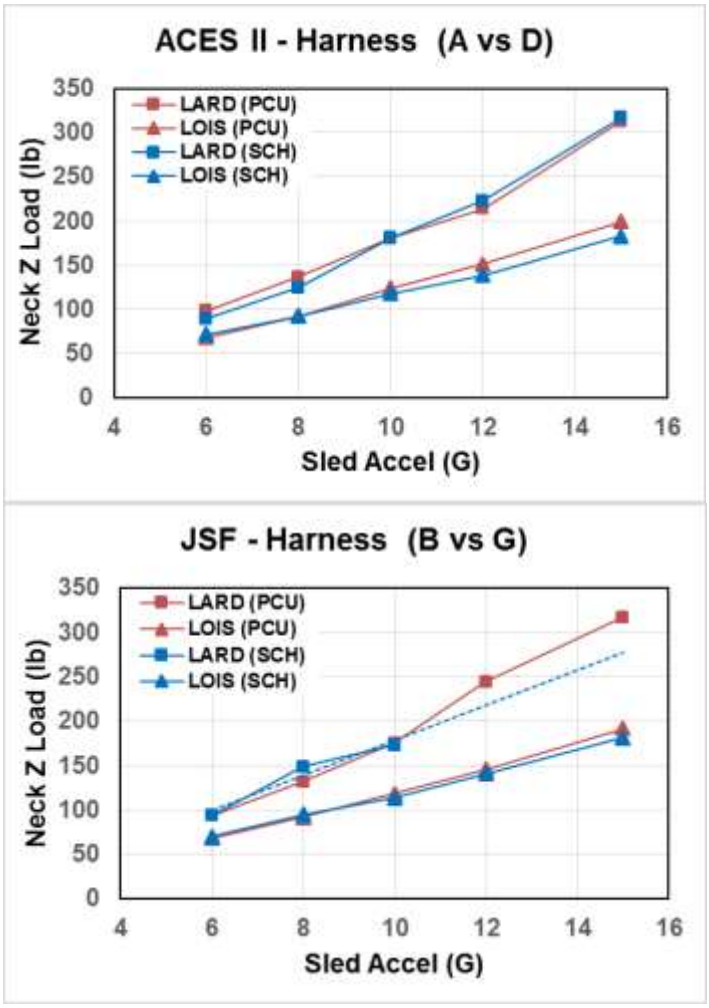

Figure 20. Harness Comparison – Neck Z Load

Neck X Loads (ATDs Only). As shown in Table 16 and Figure 21, the SCH harness generated substantially lower neck x loads with both ATDs for both the in-line and forward headrest configurations.

Table 16. Harness Comparison (A vs D and B vs G) – Neck X Load (lb)

G Level	Test Subj	In-line Headrest			Forward Headrest		
		PCU (A)	SCH (D)	% Diff	PCU (B)	SCH (G)	% Diff
6	LOIS	27.56	6.60	-76.05	18.19	13.44	-26.11
	LARD	61.13	23.77	-61.12	50.34	29.61	-41.18
8	LOIS	32.10	11.94	-62.80	32.94	22.95	-30.33
	LARD	84.56	50.54	-40.23	80.93	54.56	-32.58
10	LOIS	50.79	19.39	-61.82	53.85	31.49	-41.52
	LARD	97.59	65.32	-33.07	101.2	60.62	-40.10
12	LOIS	58.51	25.76	-55.97	67.69	40.27	-40.51
	LARD	98.39	73.28	-25.52	110.5		N/A
15	LOIS	67.39	33.09	-50.90	79.26	54.31	-31.48
	LARD	120.1	86.72	-27.78	127.6		N/A

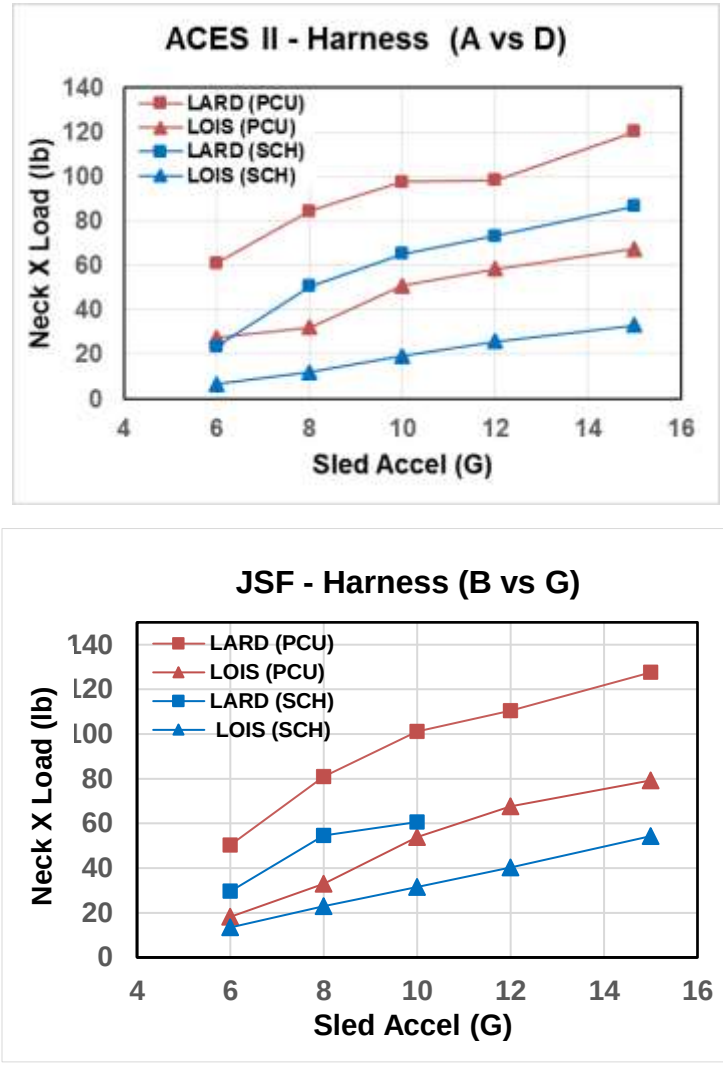

Figure 21. Harness Comparison – Neck X Load

My Neck Torque (ATDs Only). The measured My neck torque increased substantially with increasing carriage acceleration level for LARD with PCU harness in both the in-line configuration (Cell A) and forward headrest configuration (Cell B) as shown in Figure 22. The neck torques for LARD and LOIS in the other configurations remained relatively flat and lower in magnitude. As shown in Table 17, the LARD with SCH harness produced substantially smaller neck torques than the PCU harness for both headrest configurations, while LOIS with the SCH harness produced slightly higher neck torques than the PCU but only at the higher sled acceleration levels.

Table 17. Harness Comparison (A vs D and B vs G) – Neck My Torque (in-lb)

G Level	Test Subj	In-line Headrest			Forward Headrest		
		PCU (A)	SCH (D)	% Diff	PCU (B)	SCH (G)	% Diff
6	LOIS	67.68	42.68	-36.94	70.31	54.11	-23.04
	LARD	78.17	38.99	-50.12	74.95	51.72	-30.99
8	LOIS	84.00	59.96	-28.62	82.85	85.01	2.61
	LARD	120.0	76.99	-35.85	127.1	77.00	-39.44
10	LOIS	88.56	78.16	-11.74	83.75	91.23	8.93
	LARD	174.0	90.68	-47.88	206.1	86.59	-57.99
12	LOIS	91.29	96.97	6.22	73.02	90.51	23.95
	LARD	175.6	95.33	-45.71	245.3		N/A
15	LOIS	97.48	107.4	10.17	84.04	91.69	9.10
	LARD	263.2	151.9	-42.29	302.0		N/A

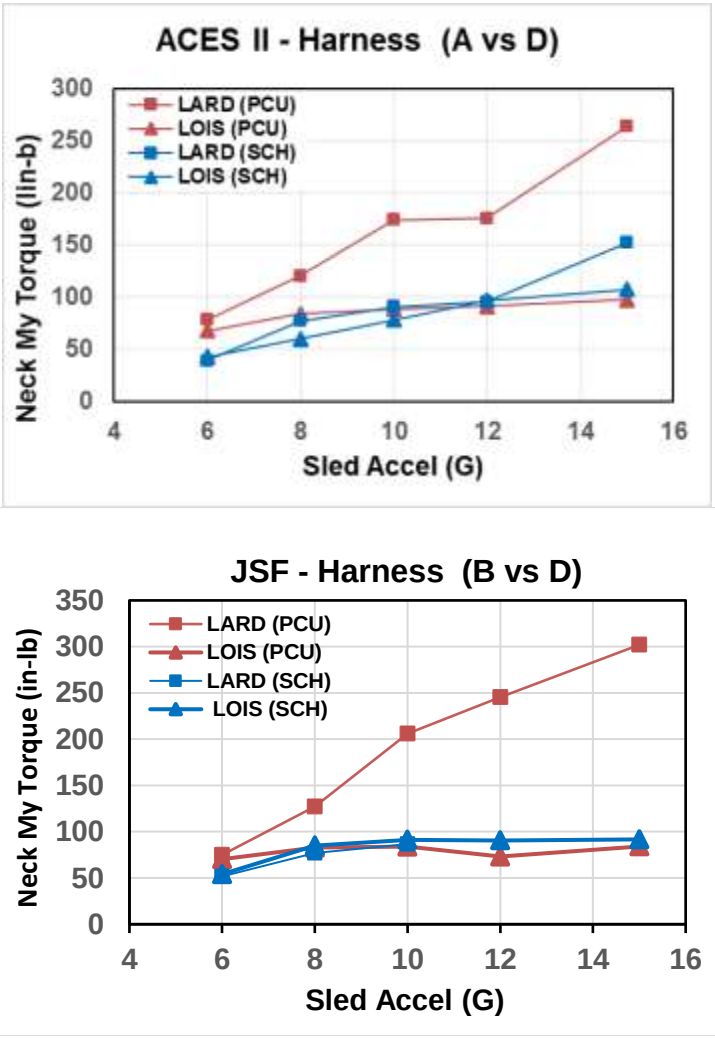

Figure 22. Harness Comparison – My Neck Torque

Lumbar Z Load (ATDs Only). In general, the measured lumbar z loads increased linearly with increasing carriage acceleration level, as shown in Figure 23, although the LARD with PCU harness showed some flatness in response in both seat configurations at the higher carriage acceleration levels. As shown in Table 18, the lumbar z loads for both the PCU and SCH harness tests were very similar, with the LARD generating slightly higher loads with the SCH harness, and the LOIS generating slightly lower loads with the SCH harness under most conditions. An exception was at 15 G where LARD generated loads in the in-line headrest/SCH condition (Cell D) that were substantially greater than at any other 15 G conditions.

Table 18. Harness Comparison (A vs D and B vs G) – Lumbar Z Load (lb)

G Level	Test Subj	In-line Headrest			Forward Headrest		
		PCU(A)	SCH(D)	% Diff	PCU (B)	SCH (G)	% Diff
6	LOIS	300.3	313.4	4.35	312.1	308.8	-1.05
	LARD	517.9	556.5	7.45	573.1	591.1	3.15
8	LOIS	429.7	402.4	-6.35	437.2	417.7	-4.45
	LARD	821.7	872.7	6.21	755.0	785.8	4.08
10	LOIS	585.9	524.5	-10.49	566.2	546.9	-3.41
	LARD	974.5	1021	4.75	832.8	967.3	16.14
12	LOIS	703.7	642.7	-8.67	675.2	687.4	1.80
	LARD	1150	1223	6.36	857.0		N/A
15	LOIS	946.1	840.0	-11.21	902.5	894.3	-0.91
	LARD	1142	1586	38.90	984.1		N/A

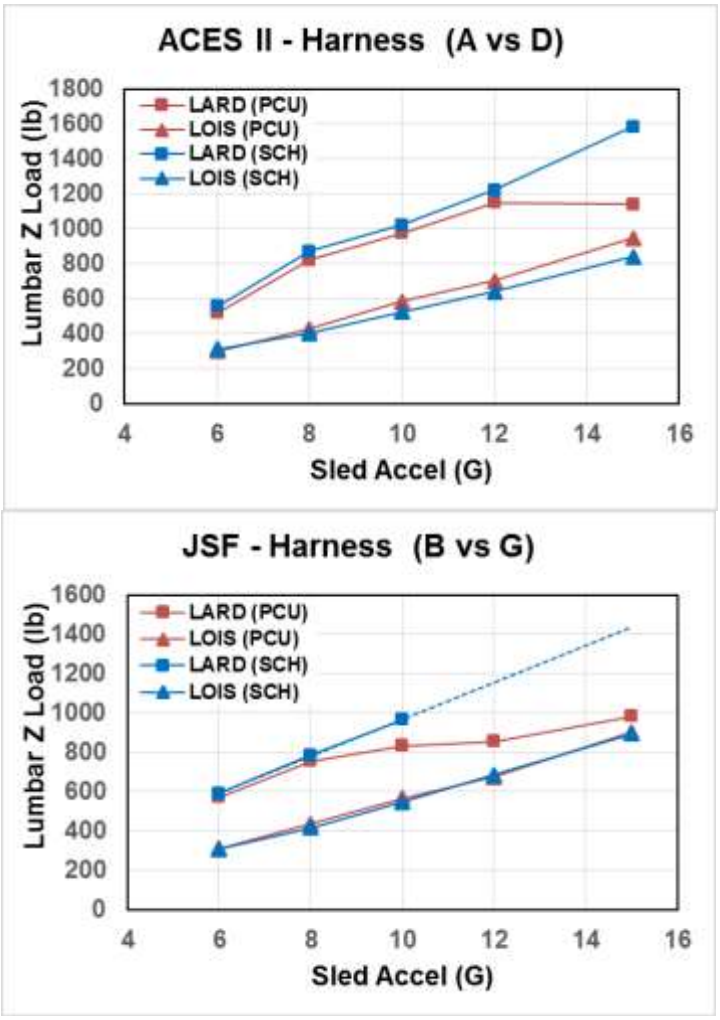

Figure 23. Harness Comparison – Lumbar Z Load

Lumbar My Torque (ATDs Only). The measured lumbar My torque increased linearly with increasing carriage acceleration levels for LARD tests with both PCU and SCH harnesses in the ACES II configuration, as shown in Figure 24, although lumbar torque increases were relatively small for tests with LOIS. The results for tests in the JSF configuration were similar (increasing LARD torque and smaller increases in LOIS torque), with the exception of a slight decrease in lumbar torque for the LARD with SCH harness at 10 G. As shown in Table 19, the lumbar torques for both ATDs were generally lower with the SCH at the higher carriage accelerations in both configurations as compared to the PCU harness. Under all conditions, tests with the LARD generated much larger lumbar torques than those with the LOIS.

Table 19. Harness Comparison (a vs D and B vs G) – Lumbar My Torque (in-lb)

G Level	Test Subj	In-line Headrest			Forward Headrest		
		PCU (A)	SCH (D)	% Diff	PCU (B)	SCH (G)	% Diff
6	LOIS	65.59	274.3	318.2	179.8	329.8	83.45
	LARD	1237	677.9	-45.20	1064	1005	-5.58
8	LOIS	154.3	353.1	128.8	298.1	351.9	18.08
	LARD	1746	1270	-27.26	1574	1606	2.03
10	LOIS	349.5	403.4	15.43	363.4	406.1	11.74
	LARD	2290	1879	-17.94	2090	1601	-23.40
12	LOIS	450	449.6	-0.08	511.6	466.0	-8.91
	LARD	2561	1932	-24.56	2620		N/A
15	LOIS	659.0	402.0	-39.00	765.2	531.2	-30.58
	LARD	3174	2864	-9.76	3209		N/A

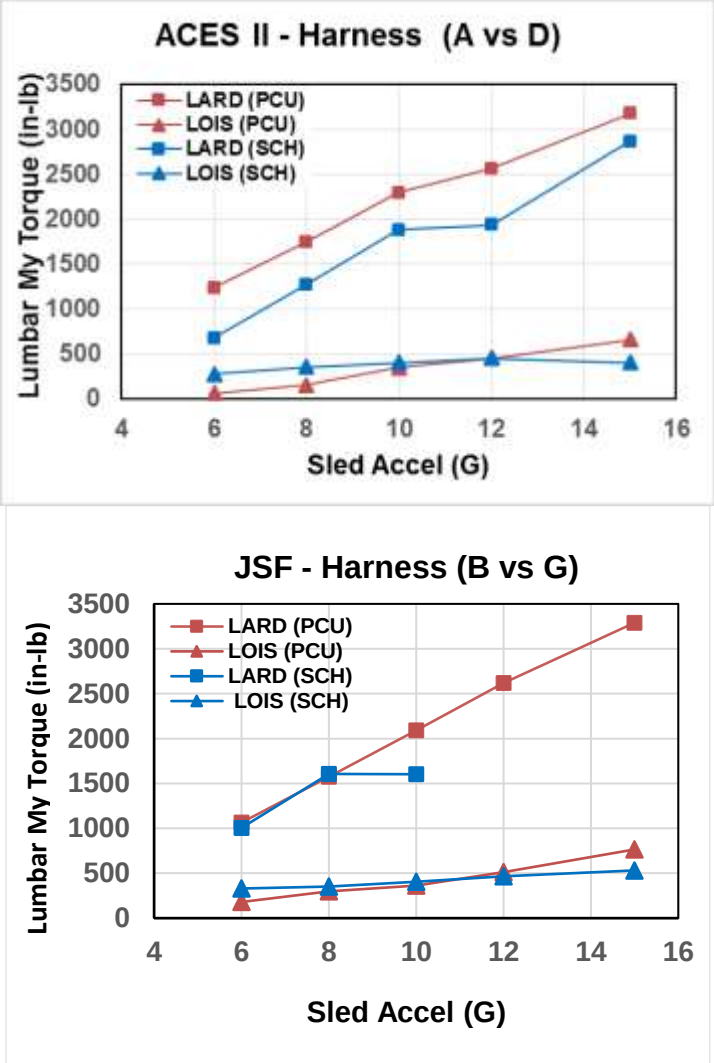

Figure 24. Harness Comparison – Lumbar My Torque

7.3 VDT Parametric Assessment: Helmet Effects.

Comparative assessments of data from impact acceleration tests with two helmet systems were conducted to determine variations in human and ATD response due to the effects of the helmet properties. Results of tests with the JSF Gen II helmet (approximately 4.6 lbs including MBU-20/P mask) with forward shifted CG were compared to the HGU-55/P baseline helmet configuration (approximately 2.4 lbs including MBU-20/P mask). The helmets were tested under identical conditions in both the ACES II seat configuration with PCU harness and in-line headrest (cells A and C) and JSF seat configuration with SCH harness and 2.5" forward headrest (cells G and E).

The measured accelerations and loads generally increased linearly for both humans and ATDs for all conditions as a function of impact acceleration, as shown in Figures 25-33, although the neck and lumbar My torque measurements for LOIS were relatively flat. The LARD acceleration responses were larger than LOIS at all levels, with the human data generally falling in-between.

Head Z Acceleration. The measured human head z accelerations were closer to LARD for both helmet conditions in the ACES II seat, and closer to LOIS for both helmets in the JSF seat, as shown in Figure 25. As shown in Table 20, both the Gen II and the HGU-55/P helmets produced similar head z accelerations, with the differences being less than 5% for humans and less than 10% for ATDs (with the one exception at 8 G with LARD in ACES II configuration) for both seats.

Table 20. Helmet Comparison (a vs C and G vs E) – Head Z Accel (G)

G Level	Test Subject	ACES II			JSF		
		HGU-55P (A)	Gen II (C)	% Diff	HGU-55P (G)	Gen II (E)	% Diff
6	Human	8.16 ± 0.6	8.46 ± 1.1	3.68	6.78 ± 0.6	6.86 ± 0.5	1.18
	LOIS	6.45	6.28	-2.64	6.36	6.36	0.00
	LARD	7.94	7.82	-1.51	7.24	7.14	-1.38
8	Human	11.67 ± 1.0	11.71 ± 0.8	0.34	9.38 ± 1.1	9.24 ± 0.8	-1.49
	LOIS	8.93	8.89	-0.45	8.39	8.36	-0.36
	LARD	11.90	10.29	-13.53	11.79	11.72	-0.59
10	Human	14.99 ± 1.4	14.72 ± 1.9	-1.80	11.85 ± 1.4	11.45 ± 0.7	-3.38
	LOIS	12.13	11.68	-3.71	10.54	10.35	-1.80
	LARD	16.15	15.55	-3.72	14.58	15.27	4.73
12	LOIS	14.88	14.55	-2.22	13.15	12.38	-5.86
	LARD	18.98	20.69	9.01		20.21	N/A
15	LOIS	19.60	19.45	-0.77	17.13	17.05	-0.47
	LARD	27.44	28.40	3.50		26.07	N/A

* denotes statistical significance

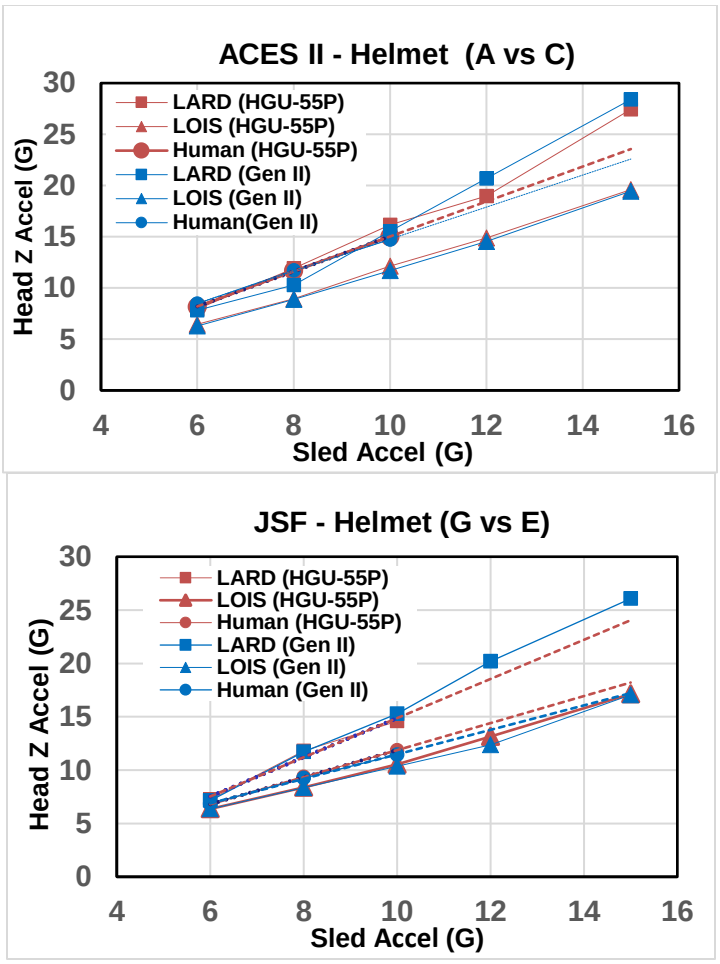

Figure 25. Helmet Comparison – Head Z Acceleration

Head X Acceleration. As shown in Figure 26, the measured human head x accelerations were lower than both LOIS and LARD accelerations for both helmets, while the LARD accelerations were greater than LOIS. As shown in Table 21, for the human subjects, the Gen II helmet generated larger head x accelerations than the HGU-55P helmet for both the ACES II and JSF seats at all levels, but only the 10 G level (Cell A vs C) was statistically significant. In the ACES II configuration, the head x accelerations with the Gen II helmet were generally lower than the HGU-55/P helmet with LARD, but higher with LOIS (Cell A vs C). In the JSF configuration, the Gen II helmet generated higher head x accelerations than the HGU-55/P helmet at nearly all levels for both LARD and LOIS (Cell G vs E).

Table 21. Helmet Comparison (A vs C and G vs E) – Head X Accel (G)

G Level	Test Subject	ACES II			JSF		
		HGU-55P (A)	Gen II (C)	% Diff	HGU-55P (G)	Gen II (E)	% Diff
6	Human	1.45 ± 0.8	1.76 ± 0.9	21.38	1.42 ± 1.0	1.88 ± 0.9	32.39
	LOIS	2.77	2.95	6.50	1.82	2.36	29.67
	LARD	4.45	3.98	-10.56	2.26	2.41	6.64
8	Human	2.01 ± 1.0	2.34 ± 1.2	16.42	2.31 ± 1.3	2.39 ± 1.0	3.46
	LOIS	3.46	3.93	13.58	2.85	3.87	35.79
	LARD	6.10	4.62	-24.26	3.96	3.57	-9.85
10	Human	2.51 ± 1.2	3.23 ± 1.2	28.69*	2.92 ± 1.6	3.62 ± 1.4	23.97
	LOIS	4.77	4.87	2.10	3.68	4.25	15.49
	LARD	7.30	6.08	-16.71	4.74	4.90	3.38
12	LOIS	5.29	5.25	-0.76	4.30	5.12	19.07
	LARD	7.41	6.57	-11.34		5.76	N/A
15	LOIS	6.00	6.88	14.67	5.10	5.94	16.47
	LARD	9.83	8.57	-12.82		7.57	N/A

* denotes statistical significance

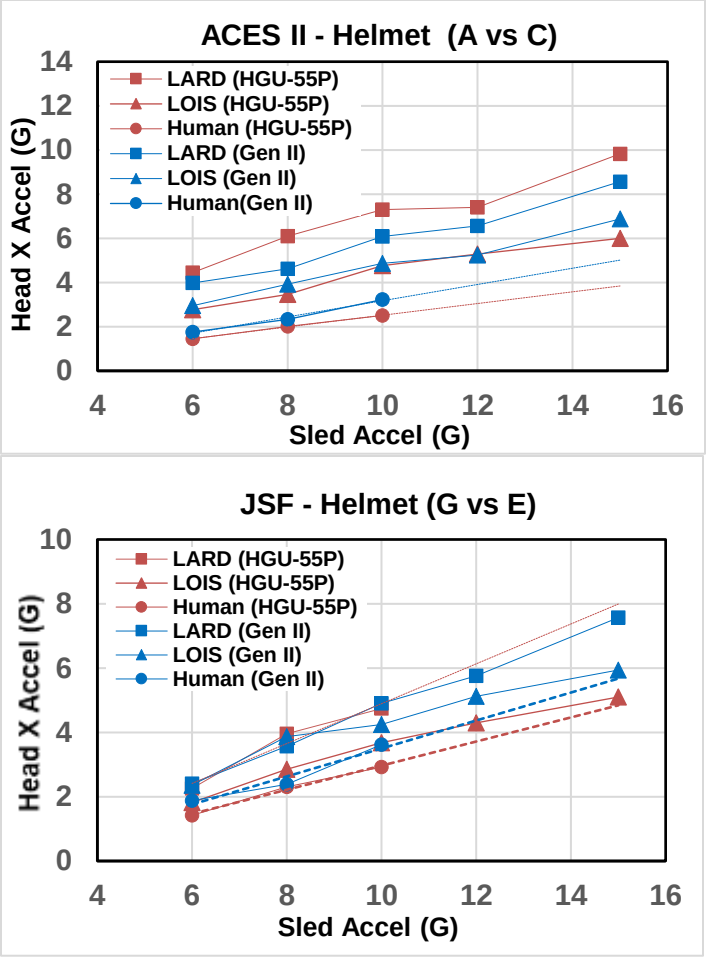

Figure 26. Helmet Comparison – Head X Acceleration

Resultant Chest Acceleration. The human resultant chest acceleration data generally fell in-between the LOIS and LARD accelerations for both seats as shown in Figure 27, with the LARD accelerations being greater than LOIS. As shown in Table 22, for both human and ATD subjects, there was very little difference in the acceleration responses generated by the Gen II and the HGU-55/P helmets under all conditions.

Table 22. Helmet Comparison (A vs C and G vs E) – Res Chest Accel (G)

G Level	Test Subject	ACES II HGU-55P (A)	ACES II Gen II (C)	ACES II % Diff	JSF HGU-55P (G)	JSF Gen II (E)	JSF % Diff
6	Human	8.49 ± 0.7	8.56 ± 0.7	0.82	7.11 ± 0.4	7.40 ± 0.5	4.08
	LOIS	6.65	6.53	-1.80	6.57	6.70	1.98
	LARD	8.70	8.61	-1.03	7.40	7.52	1.62
8	Human	12.26 ± 1.6	12.17 ± 1.1	-0.73	10.42 ± 0.5	10.53 ± 0.7	1.06
	LOIS	9.36	9.23	-1.39	8.72	9.04	3.67
	LARD	13.31	12.89	-3.16	12.47	12.49	0.16
10	Human	16.17 ± 3.1	16.45 ± 2.4	1.73	13.62 ± 1.1	14.03 ± 1.1	3.01
	LOIS	12.47	12.10	-2.97	11.01	11.43	3.81
	LARD	17.99	17.08	-5.06	16.21	16.68	2.90
12	LOIS	15.31	15.16	-0.98	13.67	13.62	-0.37
	LARD	21.06	22.60	7.31		21.89	N/A
15	LOIS	20.50	20.20	-1.46	18.18	18.58	2.20
	LARD	29.69	29.99	1.01		27.02	N/A

* denotes statistical significance

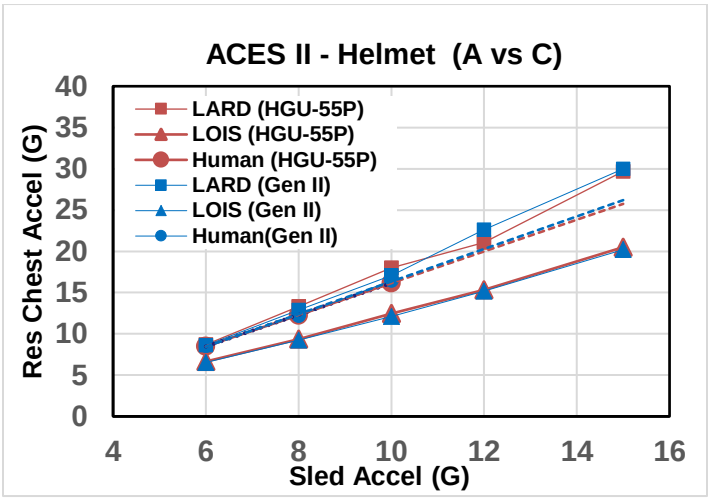

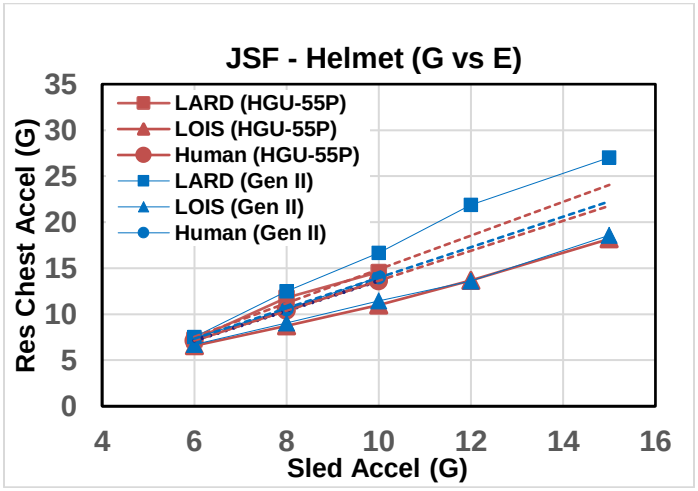

Figure 27. Helmet Comparison – Resultant Chest Acceleration

Head +Ry Angular Acceleration (ATDs Only). The measured +Ry angular accelerations generally increased with increasing carriage acceleration, with the LARD accelerations being larger than LOIS, as shown in Figure 28, although some non-linearity was present for LARD at the higher levels in the ACES II condition. As shown in Table 23, at the higher carriage acceleration levels, both ATDs generated lower accelerations with the Gen II helmet than the HGU-55/P helmet in the ACES II configuration, but higher accelerations for the Gen II in the JSF configuration. The –Ry results (not shown here) were generally similar.

Table 23. Helmet Comparison (A vs C and G vs E) – Head +RY Angular Accel (Rad/Sec²)

G Level	Test Subject	ACES II HGU-55P (A)	ACES II Gen II (C)	ACES II % Diff	JSF HGU-55P (G)	JSF Gen II (E)	JSF % Diff
	LOIS	63.88	84.74	32.65	87.74	75.19	-14.30
	LARD	141.5	144.2	1.90	86.04	78.68	-8.55
8	LOIS	130.0	149.7	15.14	100.7	126.8	25.88
	LARD	333.1	221.7	-33.44	216.7	220.9	1.95
10	LOIS	244.5	220.6	-9.80	118.1	181.2	53.52
	LARD	501.9	410.0	-18.32	298.0	380.6	27.70
12	LOIS	373.4	298.3	-20.11	177.0	259.2	46.40
	LARD	545.2	547.0	0.33		493.7	N/A
15	LOIS	569.1	433.9	-23.76	330.3	401.2	21.46
	LARD	793.5	575.3	-27.50		643.4	N/A

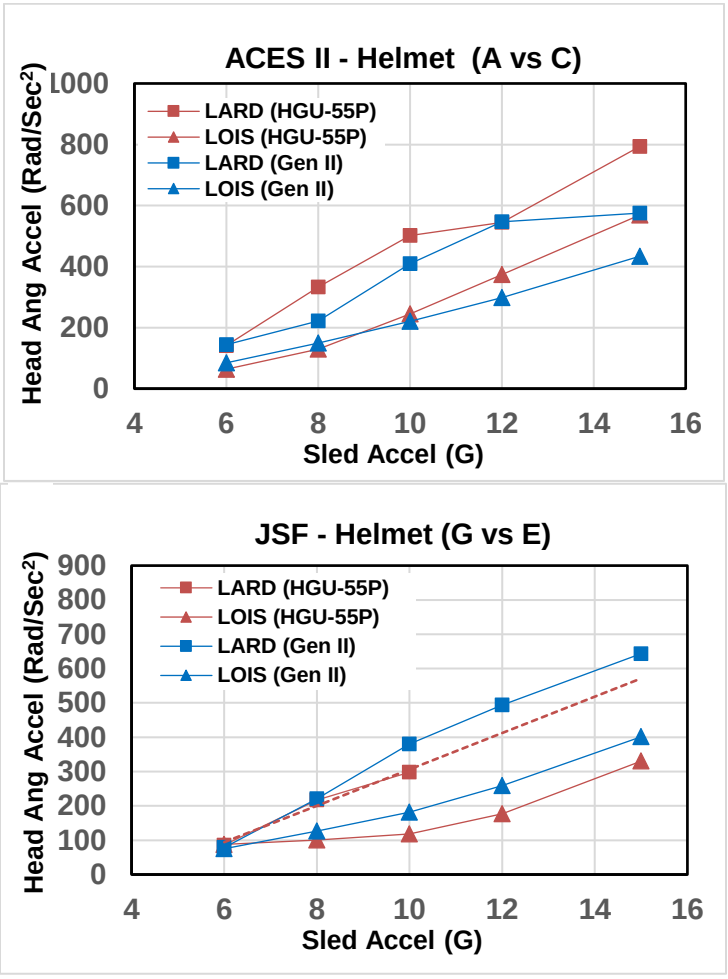

Figure 28. Helmet Comparison – Head Ry Angular Acceleration

Neck Z Load (ATDs Only). The measured neck z loads were higher for LARD than LOIS for all conditions as shown in Figure 29. The Gen II helmet generated higher neck z loads than the HGU-55P helmet under all conditions as shown in Table 24.

Table 24. Helmet Comparison (A vs C and G vs E) – Neck Z Load (lb)

G Level	Test Subj	ACES II			JSF		
		HGU-55P(A)	Gen II(C)	% Diff	HGU-55P(G)	Gen II(E)	% Diff
6	LOIS	67.78	76.51	12.88	69.89	84.24	20.53
	LARD	98.56	115.2	16.89	93.72	113.6	21.22
8	LOIS	92.14	107.2	16.31	94.34	108.1	14.59
	LARD	136.5	149.1	9.26	148.4	172.3	16.11
10	LOIS	123.7	141.1	14.08	113.3	130.6	15.33
	LARD	180.2	209.6	16.32	173.0	225.9	30.56
12	LOIS	150.9	177.8	17.82	140.4	159.3	13.48
	LARD	213.6	279.3	30.72		282.2	N/A
15	LOIS	199.4	240.3	20.51	181.3	216.9	19.65
	LARD	312.9	392.6	25.46		373.7	N/A

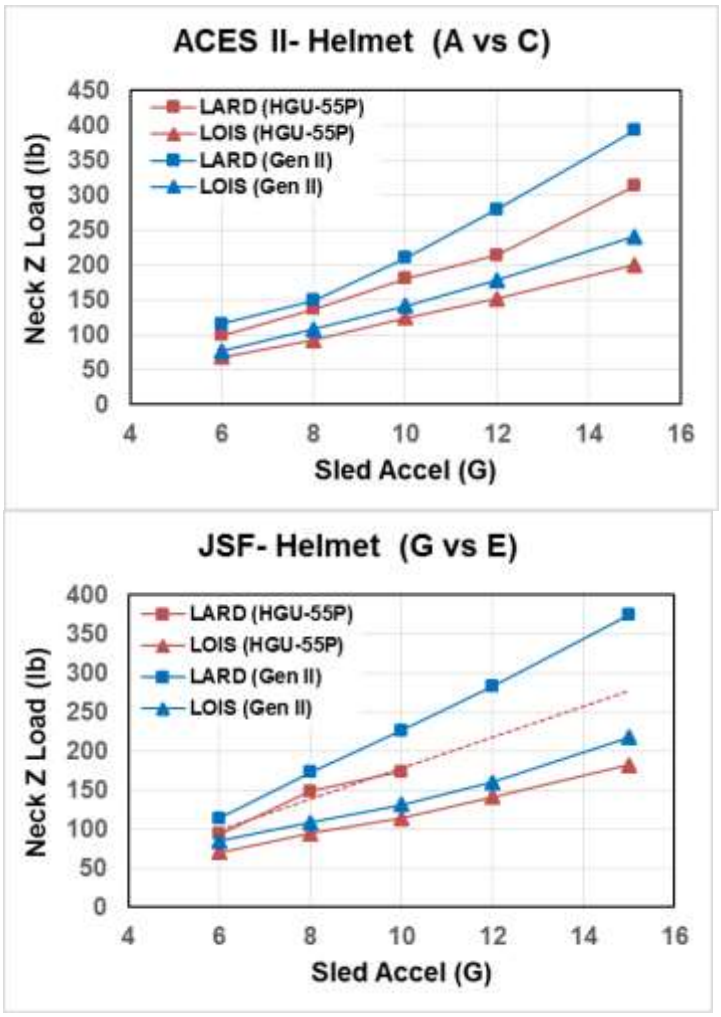

Figure 29. Helmet Comparison – Neck Z Load

Neck X Load (ATDs Only). The measured neck x loads generally increased with increasing carriage acceleration levels as shown in Figure 30, with the exception of LARD responses with the Gen II helmet in the ACES II configuration, with the loads for LARD being mostly higher than LOIS. The Gen II helmet generated higher neck x loads than the HGU-55P helmet under all conditions, with the increases being greater for LOIS than LARD, as shown in Table 25.

Table 25. Helmet Comparison (A vs C and G vs E) – Neck X Load (lb)

G Level	Test Subj	ACES II			JSF		
		HGU-55P(A)	Gen II(C)	% Diff	HGU-55P(G)	Gen II(E)	% Diff
6	LOIS	27.56	39.70	44.05	13.44	26.37	96.21
	LARD	61.13	71.88	17.59	29.61	44.75	51.13
8	LOIS	32.10	57.16	78.07	22.95	47.26	105.9
	LARD	84.56	103.2	21.98	54.56	65.28	19.65
10	LOIS	50.79	72.40	42.55	31.49	61.67	95.84
	LARD	97.59	97.66	0.07	60.62	78.72	29.86
12	LOIS	58.51	77.49	32.44	40.27	77.17	91.63
	LARD	98.39	98.49	0.10		90.53	N/A
15	LOIS	67.39	94.36	40.02	54.31	86.70	59.64
	LARD	120.1	130.9	9.04		111.3	N/A

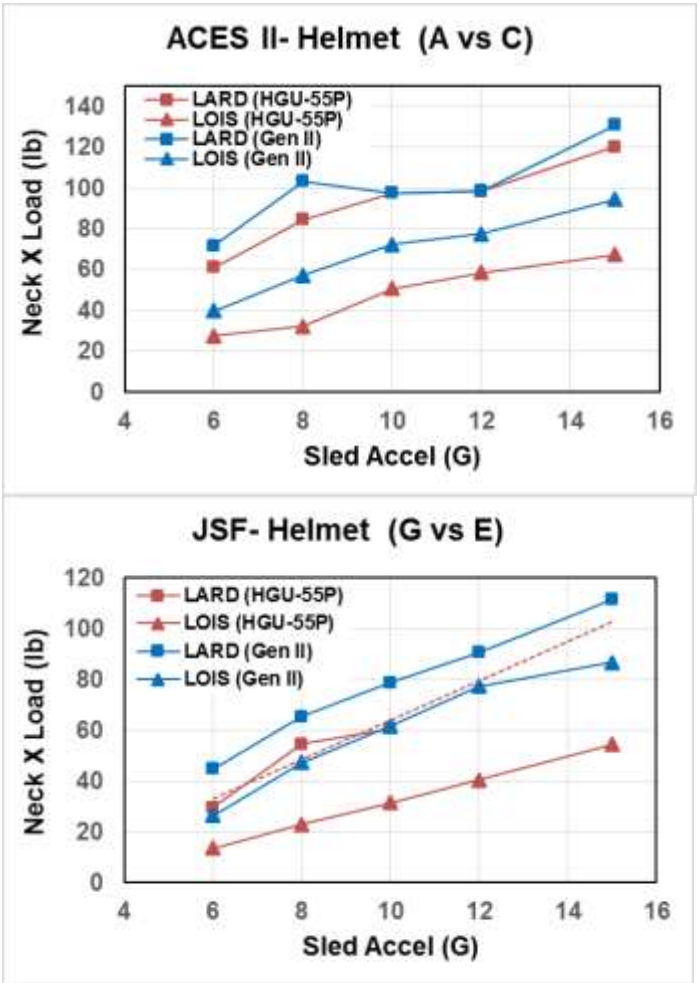

Figure 30. Helmet Comparison – Neck X Load

Neck My Torque (ATDs Only). The measured neck My torque increased linearly with increasing carriage acceleration at all levels with the ACES II seat but not the JSF seat, as shown in Figure 31. The LARD generated larger torques than LOIS in the ACES II seat, but in the JSF seat this was true only for the Gen II helmet configuration. As shown in Table 26, the Gen II helmet produced larger torques (9-130%) than the HGU-55/P helmet at all levels in both seats. The differences were especially substantial with LARD in the JSF seat.

Table 26. Helmet Comparison (A vs C and G vs E) – Neck My Torque (in-lb)

G Level	Test Subj	ACES II			JSF		
		HGU-55P(A)	Gen II(C)	% Diff	HGU-55P(G)	Gen II(E)	% Diff
6	LOIS	67.78	76.51	12.88	54.11	83.42	54.17
	LARD	98.56	115.2	16.89	51.72	91.26	76.45
8	LOIS	92.14	107.2	16.31	85.01	99.27	16.77
	LARD	136.5	149.1	9.26	77.00	125.5	62.95
10	LOIS	123.7	141.1	14.08	91.23	103.4	13.32
	LARD	180.2	209.6	16.32	86.59	198.9	129.6
12	LOIS	150.9	177.8	17.82	90.51	109.6	21.08
	LARD	213.6	279.3	30.72		216.0	N/A
15	LOIS	199.4	240.3	20.51	91.69	116.6	27.17
	LARD	312.9	392.6	25.46		266.9	N/A

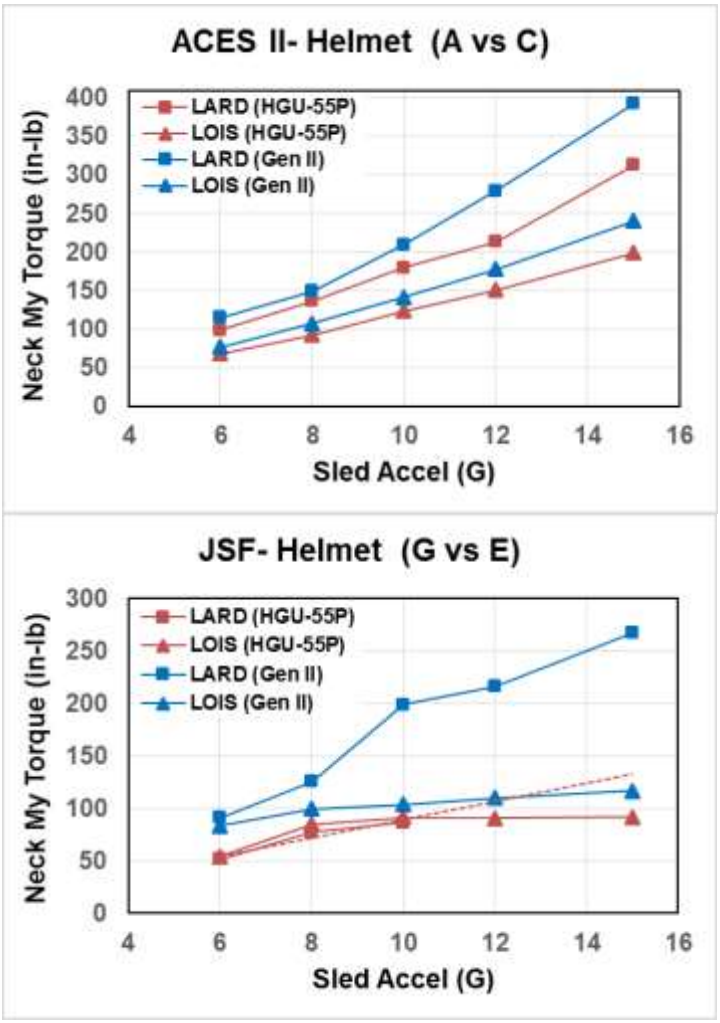

Figure 31. Helmet Comparison – Neck My Torque

Lumbar Z Loads (ATDs Only). The measured lumbar z loads as shown in Figure 32 were greater for LARD than LOIS in all conditions. The loads for the HGU-55/P and Gen II helmets were very similar under all conditions as shown in Table 27, with all differences being less than 12%. An exception was at 15 G where LARD with the Gen II helmet generated lumbar loads in the JSF seat (Cell E) that were substantially greater than at any 15 G conditions with the ACES II seat.

Table 27. Helmet Comparison (A vs C and G vsE) – Lumbar Z Load (lb)

G Level	Test Subj	ACES II			JSF		
		HGU-55P(A)	Gen II(C)	% Diff	HGU-55P(G)	Gen II(E)	% Diff
6	LOIS	300.3	304.6	1.42	308.8	344.8	11.64
	LARD	517.9	528.4	2.02	591.1	557.6	-5.67
8	LOIS	429.7	441.7	2.78	417.7	462.0	10.59
	LARD	821.7	791.6	-3.66	785.8	759.0	-3.40
10	LOIS	585.9	585.5	-0.07	546.9	582.4	6.50
	LARD	974.5	984.8	1.05	967.3	979.4	1.25
12	LOIS	703.7	729.2	3.63	687.4	689.2	0.26
	LARD	1150	1007	-12.38		1200	N/A
15	LOIS	946.1	963.1	1.80	894.3	957.5	7.07
	LARD	1142	1200	5.13		1630	N/A

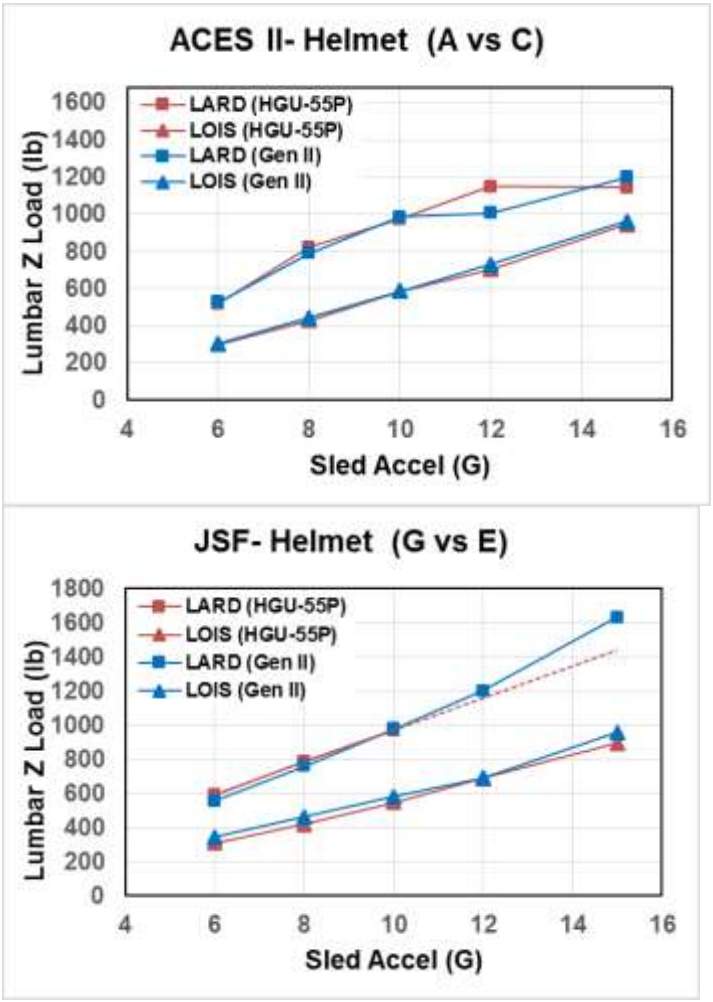

Figure 32. Helmet Comparison – Lumbar Z Load

Lumbar My Torque (ATDs Only). The lumbar My torque measured with both helmets increased linearly with increasing carriage acceleration level for the ACES II seat conditions but not JSF seat conditions, as shown in Figure 33. LARD generated substantially larger torques than LOIS at all levels for both seats. As shown in Table 28, LOIS with the Gen II helmet generated larger torques than the HGU-55/P helmet in tests with the ACES II seat at all levels; however, the torques generated by LARD in the ACES II seat were similar between the helmets at lower levels but slightly greater for the Gen II at the higher levels. In the JSF seat, LOIS generated slightly lower torques with the Gen II helmet at all levels, while the LARD data were inconclusive.

Table 28. Helmet Comparison (A vs C and G vs E) – Lumbar My Torque (in-lb)

G Level	Test Subj	ACES II			JSF		
		HGU-55P(A)	Gen II(C)	% Diff	HGU-55P(G)	Gen II(E)	% Diff
6	LOIS	65.59	155.43	136.9	329.8	323.4	-1.96
	LARD	1237	1197	-3.24	1005	1033	2.83
8	LOIS	154.3	286.7	85.79	351.9	328.4	-6.68
	LARD	1746	1637	-6.25	1606	1455	-9.42
10	LOIS	349.5	426.3	21.98	406.1	318.6	-21.54
	LARD	2290	2264	-1.15	1601	1852	15.69
12	LOIS	450	545.8	21.30	466.0	456.7	-1.99
	LARD	2561	2753	7.50		1743	N/A
15	LOIS	659.0	852.5	29.36	531.2	440.6	-17.07
	LARD	3174	3469	9.31		2628	N/A

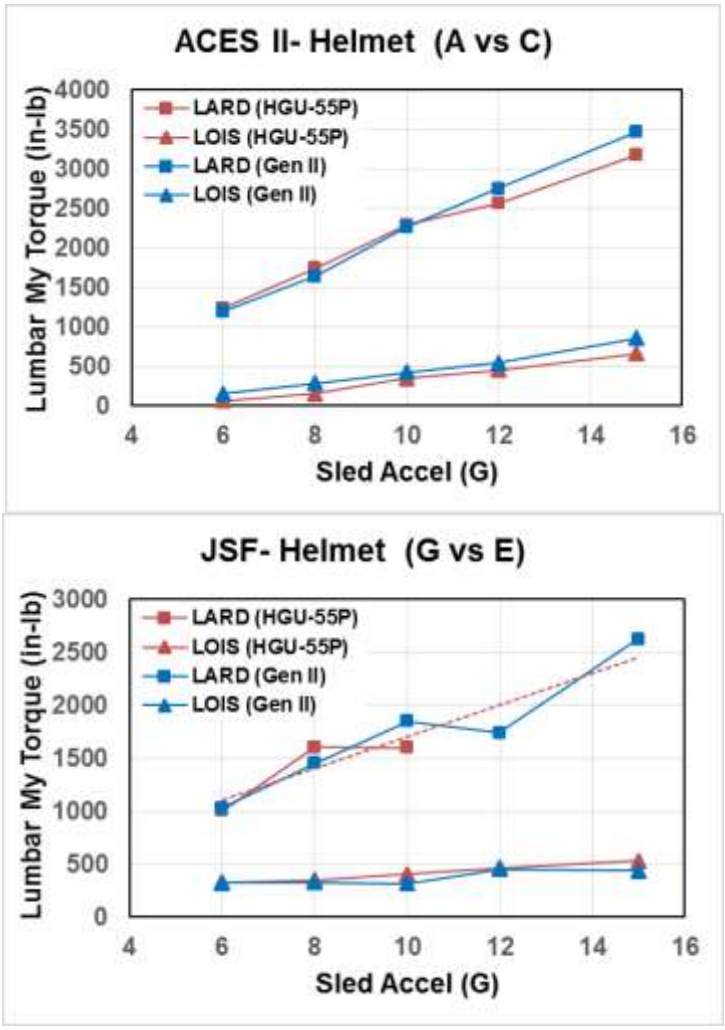

Figure 33. Helmet Comparison – Lumbar My Torque

7.4 VDT Parametric Assessment: Neck Protection Device (NPD)

A comparative assessment of data from impact acceleration tests was conducted to evaluate the effects of the Neck Protection Device (NPD) compared to the baseline tests without NPD. Test Cell E was conducted with standard JSF seat configuration including the 2.5" forward headrest and SCH, while Cell F was conducted under the same conditions except for use of the pre-inflated NPD.

The measured accelerations and loads generally increased for both humans and ATDs for all conditions as a function of impact acceleration, as shown in Figures 34-37, although the neck My torque measurements for LOIS in the JSF configuration without NPD (Cell E) were relatively flat. The LARD acceleration responses were larger than LOIS at all levels, with the human data generally falling in-between.

Resultant Head Acceleration. As shown in Figure 34, larger resultant head accelerations were generated by LARD compared to the humans and LOIS, particularly in the non-NPD baseline condition (Cell E). As shown in Table 29, the resultant head acceleration was lower for both humans and ATDs at all acceleration levels with the NPD (Cell F) compared to baseline (Cell E), with the results significant for human tests at 6 G and 8 G.

Table 29. NPD Comparison (E vsF) – Res Head Accel (G)

G Level	Test Subject	JSF Baseline (E)	JSF NPD (F)	% Diff
4	Human	N/A	4.04	N/A
	LOIS	N/A	N/A	N/A
	LARD	N/A	N/A	N/A
6	Human	6.84	5.79	-15.35*
	LOIS	6.43	5.98	-7.00
	LARD	7.15	7.07	-1.12
8	Human	9.37	7.56	-19.32*
	LOIS	8.47	7.70	-9.10
	LARD	11.73	9.76	-16.80
10	Human	11.37	N/A	N/A
	LOIS	10.49	9.31	-11.25
	LARD	15.40	12.36	-19.74
12	LOIS	12.17	10.93	-10.19
	LARD	20.12	16.14	-19.78
15	LOIS	16.95	13.29	-21.59
	LARD	25.95	20.68	-20.31

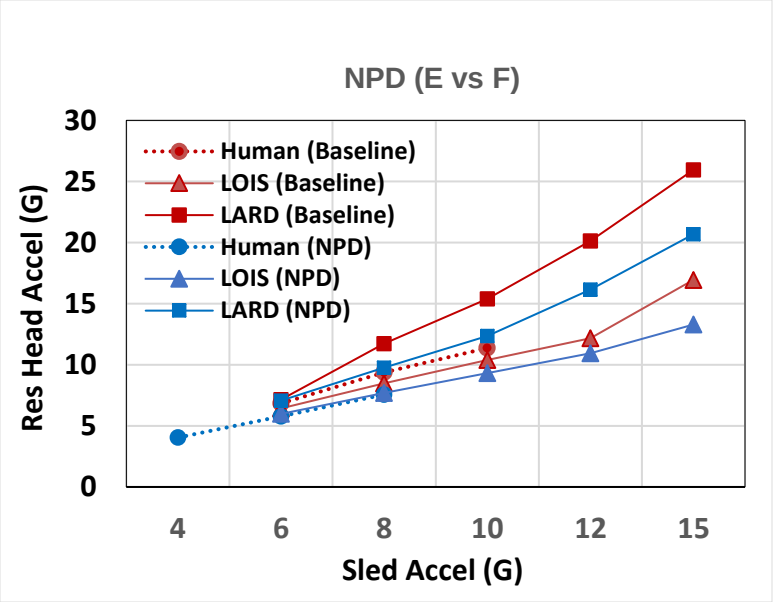

Figure 34. NPD Comparison – Resultant Head Acceleration

Resultant Chest Acceleration. As shown in Figure 35, the human resultant chest accelerations generally fell in between the LARD and LOIS accelerations. As shown in Table 30, the humans generated resultant chest accelerations that were nearly identical with and without the NPD (Cell E vs F), while the ATDs also demonstrated no consistent differences in the accelerations between the two conditions.

Table 30. NPD Comparison (E vs F) – Res Chest Accel (G)

G Level	Test Subject	JSF Baseline (E)	JSF NPD (F)	JSF % Diff
4	Human	N/A	4.45	N/A
	LOIS	N/A	N/A	N/A
	LARD	N/A	N/A	N/A
6	Human	7.27	7.27	0.00
	LOIS	6.66	6.36	-4.50
	LARD	7.49	7.92	5.74
8	Human	10.52	10.33	-1.81
	LOIS	9.04	8.61	-4.76
	LARD	12.46	11.49	-7.78
10	Human	13.80	N/A	N/A
	LOIS	11.43	10.82	-5.34
	LARD	16.63	15.38	-7.52
12	LOIS	13.57	13.61	0.29
	LARD	21.82	20.66	-5.32
15	LOIS	18.47	18.26	-1.14
	LARD	26.91	27.04	0.48

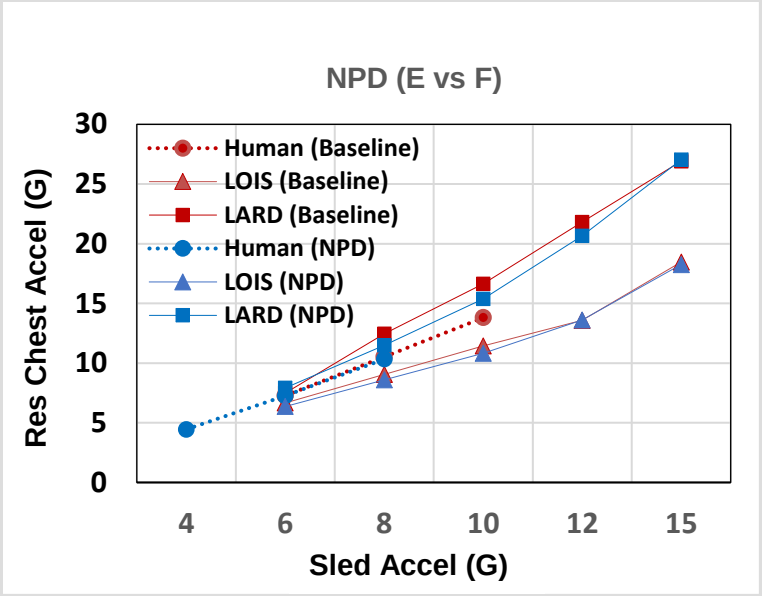

Figure 35. NPD Comparison – Resultant Chest Acceleration

Resultant Neck Load (ATDs Only). As shown in Table 31 and Figure 36, the LARD manikin generated substantially larger resultant neck loads than LOIS at all carriage acceleration levels. Both LARD and LOIS generated lower neck loads in the NPD condition (Cell F) versus the non-NPD baseline condition (Cell E) at all carriage acceleration levels, with the decreases more pronounced with LARD in most cases.

Table 31. NPD Comparison (E vs F) – Res Neck Load (lb)

G Level	Test Subj	JSF		
		Baseline (E)	NPD (F)	% Diff
6	LOIS	75.74	38.16	-49.7
	LARD	111.36	63.46	-43.0
8	LOIS	96.03	64.20	-33.1
	LARD	161.92	101.352	-37.4
10	LOIS	120.23	92.31	-23.2
	LARD	214.48	127.36	-40.6
12	LOIS	155.54	130.852	-15.9
	LARD	266.51	172.10	-35.4
15	LOIS	210.32	174.28	-17.1
	LARD	366.18	228.48	-37.6

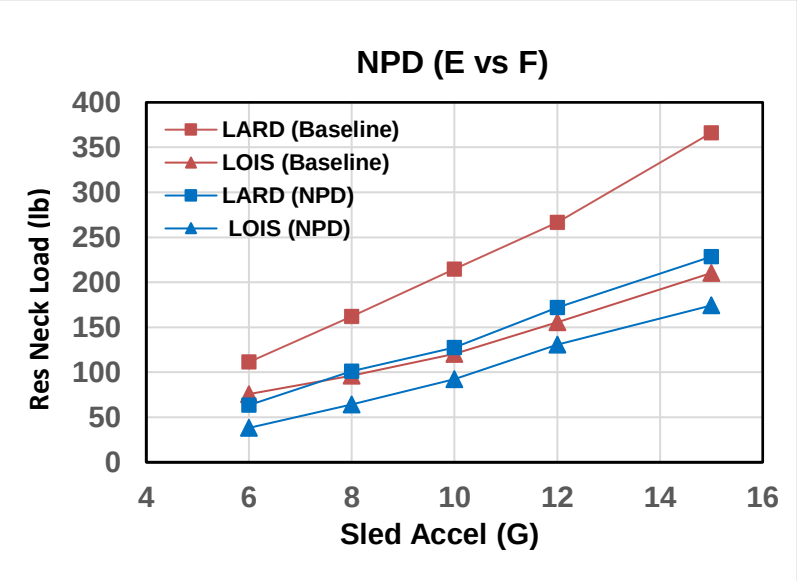

Figure 36. NPD Comparison – Resultant Neck Load

Neck My Torque (ATDs Only). As shown in Table 32 and Figure 37, the LARD manikin generated substantially larger neck My torque than LOIS at all carriage acceleration levels. Neck My torque was greater in the NPD condition (Cell F) vs. baseline (Cell E) at all acceleration levels for LARD, but lower in the NPD condition for LOIS.

Table 32. NPD Comparison (E vs F) – Neck My Torque (in-lb)

G Level	Test Subj	JSF		
		Baseline (E)	NPD (F)	% Diff
6	LOIS	83.42	16.46	-80.3
	LARD	91.26	112.46	23.2
8	LOIS	99.27	28.25	-71.5
	LARD	125.50	227.36	81.2
10	LOIS	103.40	42.56	-58.8
	LARD	198.90	277.45	14.4
12	LOIS	109.60	60.91	-44.4
	LARD	216.00	325.84	50.9
15	LOIS	116.60	97.37	-16.5
	LARD	266.90	387.31	45.1

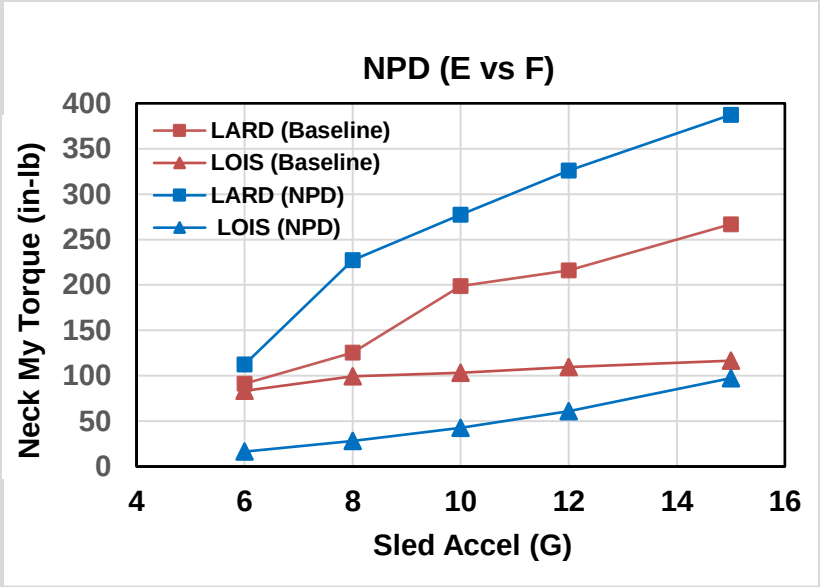

Figure 37. NPD Comparison – Neck My Torque

7.5 VDT Parametric Assessment: 2-Factor Analysis (Harness and Headrest)

Data were compared to evaluate the combined effects of the ACES II harness (PCU) and in-line headrest compared to the JSF harness (SCH) and 2.5" forward headrest. Test cell A was conducted using the ACES II seat with PCU harness, in-line headrest, and HGU-55/P helmet, while test cell G used the US16E seat with SCH harness, 2.5" forward headrest, and HGU-55/P helmet. Test cells C and E were also evaluated, and were the same as cells A and G except for the use of the Gen II helmet in both cells.

The measured accelerations and loads generally increased for both humans and ATDs for all conditions as a function of impact acceleration, as shown in Figures 38-46, although the neck and lumbar My torque measurements for LOIS in all configurations were relatively flat. The LARD acceleration responses were larger than LOIS at all levels, with the human data generally falling in-between. An exception was the head x accelerations which were lower than LOIS for the human subjects.

Head Z Acceleration. As shown in Figure 38 and Table 33, head z accelerations for the human subjects were significantly lower at all levels with the JSF configuration (SCH/forward headrest), compared to the ACES II configuration (PCU harness/in-line headrest). This was true for tests with both the HGU-55/P helmet (cells A vs G) and Gen II helmet (cells C vs E). Both ATDs also generated lower head z accelerations with the JSF configuration at nearly all acceleration levels.

Table 33. 2-factor Comparison (A vs G and C vs E) – Head Z Accel (G)

G Level	Test Subject	ACES II (A)	JSF (G)	% Diff	ACES II (C)	JSF (E)	% Diff
6	Human	7.99 ± 0.5	6.88 ± 0.6	-13.89*	8.49 ± 1.0	6.87 ± 0.5	-19.08*
	LOIS	6.45	6.36	-1.40	6.28	6.36	1.27
	LARD	7.94	7.24	-8.82	7.82	7.14	-8.70
8	Human	11.45 ± 1.1	9.52 ± 1.2	-16.86*	11.43 ± 0.7	9.48 ± 0.6	-17.06*
	LOIS	8.93	8.39	-6.05	8.89	8.36	-5.96
	LARD	11.90	11.79	-0.92	10.29	11.72	13.90
10	Human	14.95 ± 1.5	11.63 ± 1.4	-22.21*	13.75 ± 1.3	11.59 ± 0.7	-15.71*
	LOIS	12.13	10.54	-13.11	11.68	10.35	-11.39
	LARD	16.15	14.58	-9.72	15.55	15.27	-1.80
12	LOIS	14.88	13.15	-11.63	14.55	12.38	-14.91
	LARD	18.98		N/A	20.69	20.21	-2.32
15	LOIS	19.60	17.13	-12.60	19.45	17.05	-12.34
	LARD	27.44		N/A	28.40	26.07	-8.20

* denotes statistical significance

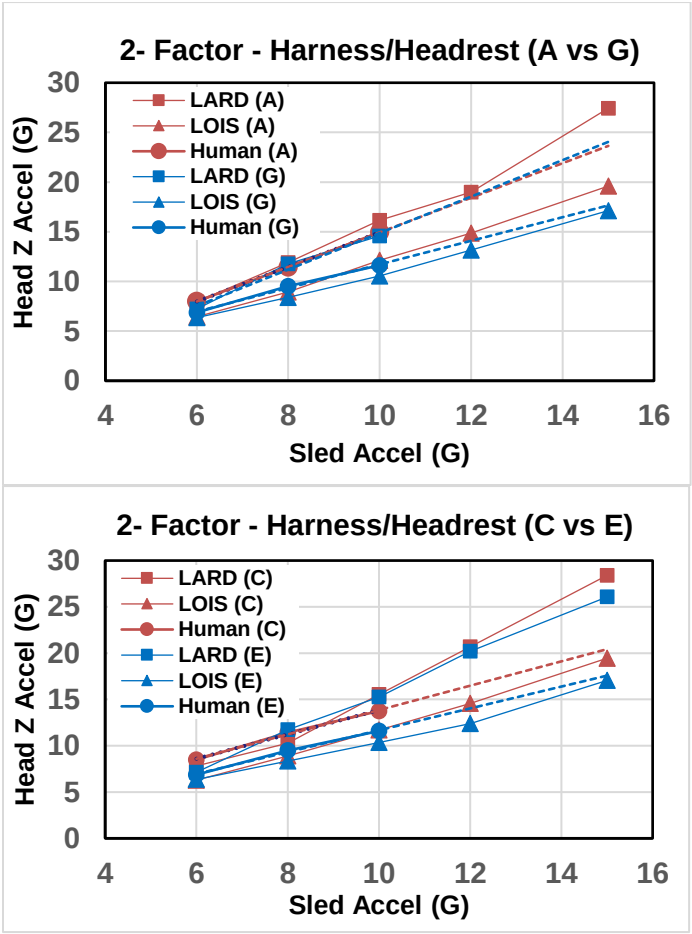

Figure 38. 2-Factor Comparison – Head Z Acceleration

Head X Acceleration. As shown in Figure 39, the human head x accelerations were generally lower than the ATD accelerations for all conditions. As shown in Table 34, head x accelerations for the human subjects were higher at all levels with the JSF configuration (SCH/forward headrest) compared to the ACES II configuration (PCU harness/in-line headrest), and this was significant at the 10 G level. This was true for tests with both the HGU-55/P helmet (Cell A vs G) and the Gen II helmet (Cell C vs E). Conversely, both ATDs generated lower head x accelerations at all levels with the JSF configuration, regardless of helmet.

Table 34. 2-Factor Comparison (A vs G and C vs E) – Head X Accel (G)

G Level	Test Subject	ACES II (A)	JSF (G)	% Diff	ACES II (C)	JSF (E)	% Diff
6	Human	1.52 ± 0.8	1.57 ± 1.0	3.29	1.87 ± 0.8	1.99 ± 1.0	6.42
	LOIS	2.77	1.82	-34.30	2.95	2.36	-20.00
	LARD	4.45	2.26	-49.21	3.98	2.41	-39.45
8	Human	2.28 ± 1.0	2.63 ± 1.2	15.35	2.39 ± 1.2	2.46 ± 1.2	2.93
	LOIS	3.46	2.85	-17.63	3.93	3.87	-1.53
	LARD	6.10	3.96	-35.08	4.62	3.57	-22.73
10	Human	2.36 ± 1.1	3.34 ± 1.6	41.53*	3.13 ± 1.0	3.84 ± 1.4	22.68*
	LOIS	4.77	3.68	-22.85	4.87	4.25	-12.73
	LARD	7.30	4.74	-35.07	6.08	4.90	-19.41
12	LOIS	5.29	4.30	-18.71	5.25	5.12	-2.48
	LARD	7.41		N/A	6.57	5.76	-12.33
15	LOIS	6.00	5.10	-15.00	6.88	5.94	-13.66
	LARD	9.83		N/A	8.57	7.57	-11.67

* denotes statistical significance

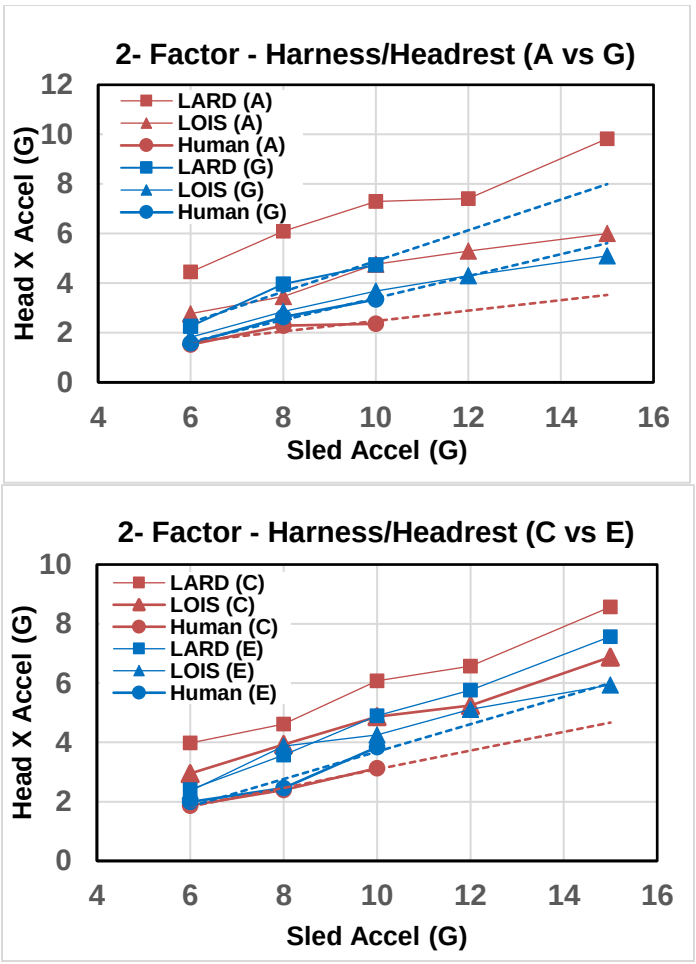

Figure 39. 2 Factor Comparison – Head X Acceleration

Resultant Chest Acceleration. As shown in Figure 40, the human accelerations generally fell in-between the LARD and LOIS responses. As shown in Table 35, the human chest accelerations were significantly lower at all levels with the JSF configuration (SCH harness/forward headrest) than for the ACES II configuration (PCU harness/in-line headrest), and this was true for tests with both the HGU-55/P helmet (Cell A vs G) and Gen II helmet (Cell C vs. E). Both ATDs also generated lower resultant chest accelerations with the JSF configuration at nearly all acceleration levels.

Table 35. 2- Factor Comparison (A vs G and C vs E) – Res Chest Accel (G)

G Level	Test Subject	ACES II (A)	JSF (G)	% Diff	ACES II (C)	JSF (E)	% Diff
6	Human	8.53 ± 0.8	7.20 ± 0.4	-15.59*	8.61 ± 0.6	7.44 ± 0.6	-13.59*
	LOIS	6.65	6.57	-1.20	6.53	6.70	2.60
	LARD	8.70	7.40	-14.94	8.61	7.52	-12.66
8	Human	12.06 ± 1.4	10.38 ± 0.5	-13.93*	11.88 ± 1.0	10.58 ± 0.8	-10.94*
	LOIS	9.36	8.72	-6.84	9.23	9.04	-2.06
	LARD	13.31	12.47	-6.31	12.89	12.49	-3.10
10	Human	15.82 ± 3.1	13.56 ± 1.2	-14.29*	15.92 ± 2.4	14.04 ± 1.2	-11.81*
	LOIS	12.47	11.01	-11.71	12.10	11.43	-5.54
	LARD	17.99	16.21	-9.89	17.08	16.68	-2.34
12	LOIS	15.31	13.67	-10.71	15.16	13.62	-10.16
	LARD	21.06		N/A	22.60	21.89	-3.14
15	LOIS	20.50	18.18	-11.32	20.20	18.58	-8.02
	LARD	29.69		N/A	29.99	27.02	-9.90

* denotes statistical significance

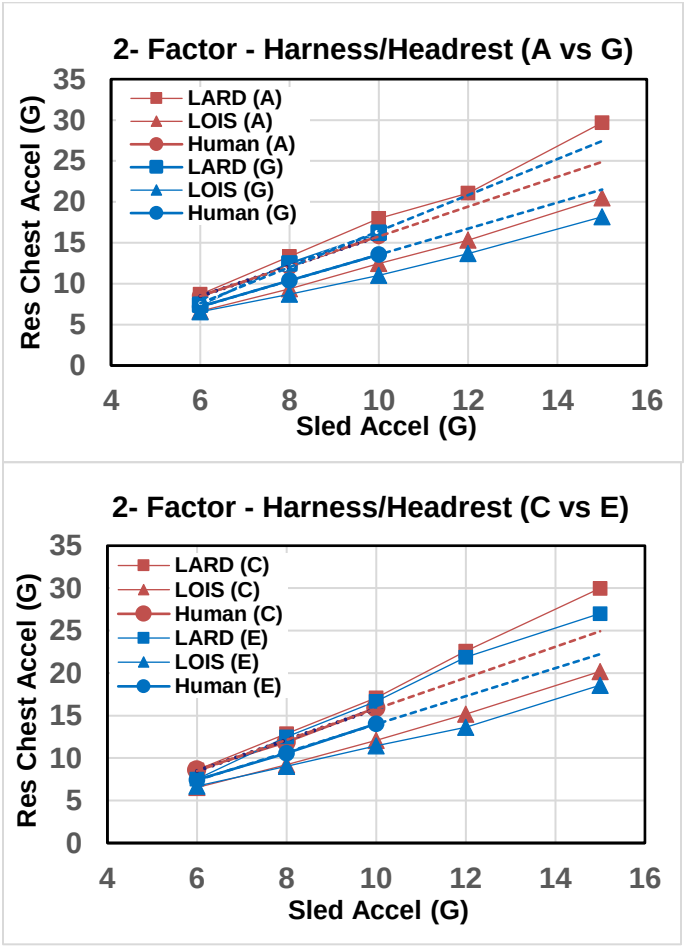

Figure 40. 2-Factor Comparison – Resultant Chest Acceleration

Head +Ry Angular Acceleration (ATDs Only). The measured +Ry head angular accelerations generally increased linearly with increasing carriage acceleration level for both ATDs as shown in Figure 41, although some non-linearity was present in the LOIS responses in the JSF configuration (Cell G). The measured +Ry head angular accelerations for LOIS fell well below the LARD responses in most instances. As shown in Table 36, both ATDs generally demonstrated lower angular accelerations with the JSF configuration compared to the ACES II configuration, and this was true regardless of helmet type. The results were also similar for comparisons of the –Ry angular accelerations (not shown here).

Table 36. 2-Factor Comparison (A vs G and C vs E) – Head + Ry Angular Accel (Rad/Sec²)

G Level	Test Subject	ACES II (A)	JSF (G)	% Diff	ACES II (C)	JSF (E)	% Diff
	LOIS	63.88	87.74	37.35	84.74	75.19	-11.27
	LARD	141.5	86.04	-39.18	144.2	78.68	-45.42
8	LOIS	130.0	100.7	-22.52	149.7	126.8	-15.29
	LARD	333.1	216.7	-34.95	221.7	220.9	-0.36
10	LOIS	244.5	118.1	-51.72	220.6	181.2	-17.83
	LARD	501.9	298.0	-40.63	410.0	380.6	-7.17
12	LOIS	373.4	177.0	-52.59	298.3	259.2	-13.12
	LARD	545.2		N/A	547.0	493.7	-9.74
15	LOIS	569.1	330.3	-41.96	433.9	401.2	-7.53
	LARD	793.5		N/A	575.3	643.4	11.83

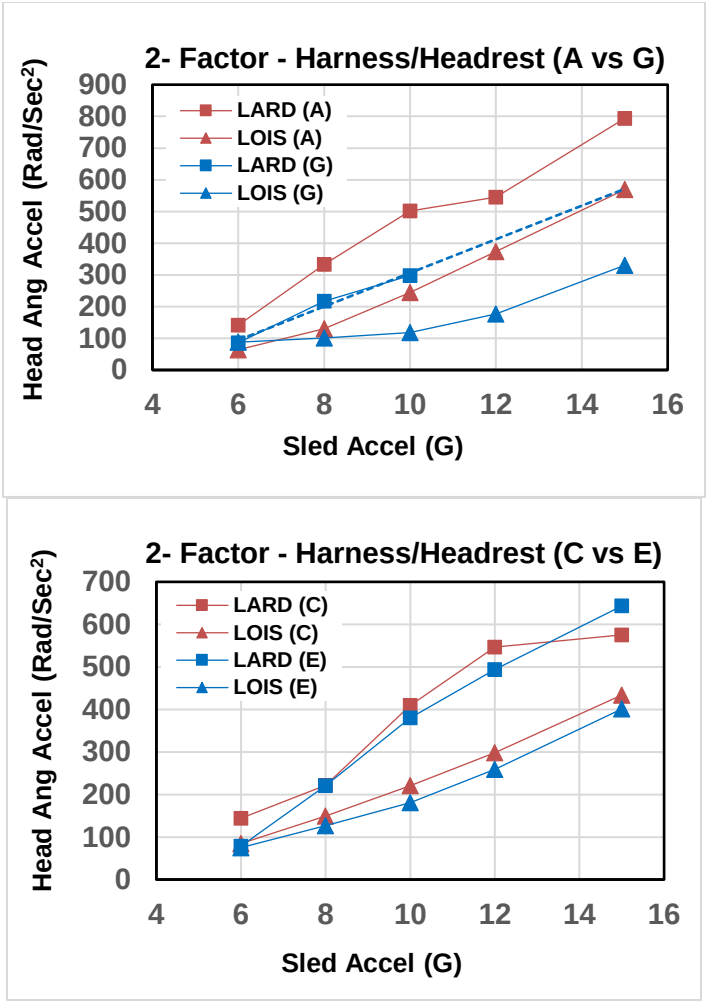

Figure 41. 2-Factor Comparison – Head Ry Angular Acceleration

Neck Z Load (ATDs Only). As shown in Figure 42, LARD generated substantially higher neck z loads than LOIS at all acceleration levels. As shown in Table 37, both ATDs generated slightly lower neck loads (< 10%) at the higher carriage acceleration levels with the JSF configuration (SCH harness/forward headrest) than the ACES II configuration (PCU harness/in-line headrest) in cells with the HGU-55/P helmet (Cell A vs G). This was also the case in cells with the Gen II helmet (Cell C vs E) for LOIS, while the LARD comparisons were inconclusive.

Table 37. 2-Factor Comparison (A vs G and C vs E) – Neck Z Load (lb)

G Level	Test Subj	ACES II (A)	JSF (G)	% Diff	ACES II (C)	JSF (E)	% Diff
6	LOIS	67.78	69.89	3.11	76.51	84.24	10.10
	LARD	98.56	93.72	-4.91	115.2	113.6	-1.39
8	LOIS	92.14	94.34	2.39	107.2	108.1	0.87
	LARD	136.5	148.4	8.75	149.1	172.3	15.58
10	LOIS	123.7	113.3	-8.44	141.1	130.6	-7.43
	LARD	180.2	173.0	-3.96	209.6	225.9	7.80
12	LOIS	150.9	140.4	-6.97	177.8	159.3	-10.40
	LARD	213.6		N/A	279.3	282.2	1.05
15	LOIS	199.4	181.3	-9.10	240.3	216.9	-9.75
	LARD	312.9		N/A	392.6	373.8	-4.80

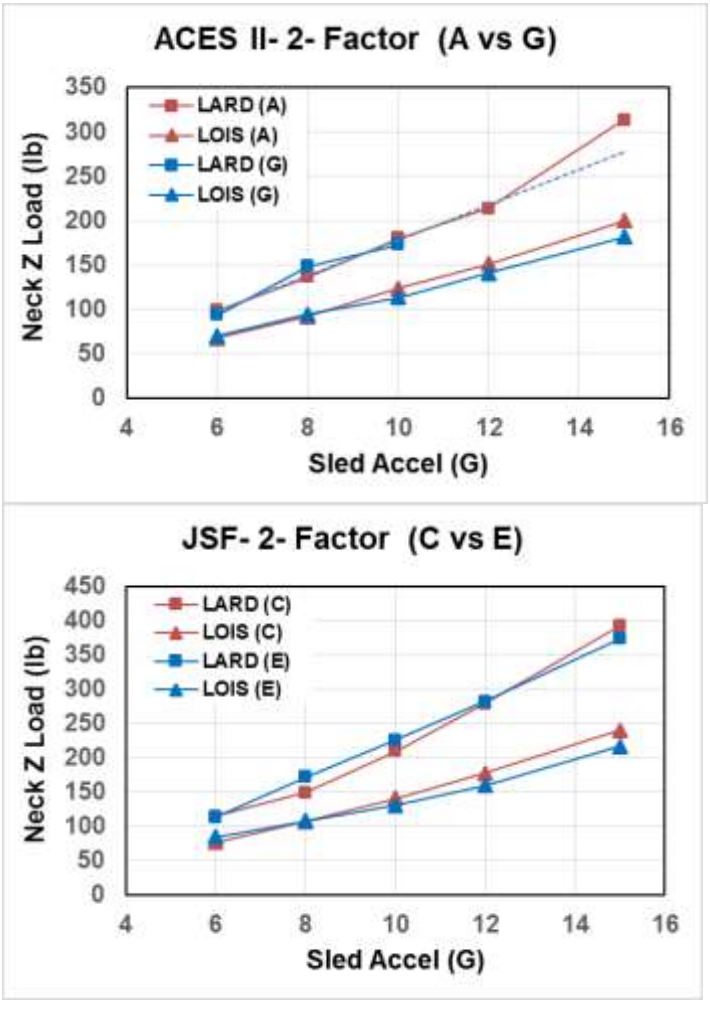

Figure 42. 2-Factor Comparison – Neck Z Load

Neck X Load (ATDs Only). The measured neck x loads generally increased with increasing carriage acceleration level, although non-linearity was present in LARD tests between 8-12 G for the JSF condition, as shown in Figure 43. LARD generated higher neck loads than LOIS for all test conditions in this comparison. As shown in Table 38, both ATDs generated lower neck loads at all acceleration levels with the JSF configuration (SCH harness/forward headrest) than the ACES II configuration (PCU harness/in-line headrest) regardless of helmet type. The differences were especially large (20-50%) in tests with the HGU-55/P helmet (Cells A vs G).

Table 38. 2-Factor Comparison (a vs G and C vs E) – Neck X Load (lb)

G Level	Test Subj	ACES II (A)	JSF (G)	% Diff	ACES II (C)	JSF (E)	% Diff
6	LOIS	27.56	13.44	-51.23	39.70	26.37	-33.58
	LARD	61.13	29.61	-51.56	71.88	44.75	-37.74
8	LOIS	32.10	22.95	-28.50	57.16	47.26	-17.32
	LARD	84.56	54.56	-35.48	103.2	65.28	-36.74
10	LOIS	50.79	31.49	-38.00	72.40	61.67	-14.82
	LARD	97.59	60.62	-37.88	97.66	78.72	-19.39
12	LOIS	58.51	40.27	-31.17	77.49	77.17	-0.41
	LARD	98.39		N/A	117.3	90.53	-22.8
15	LOIS	67.39	54.31	-19.41	94.36	86.70	-8.12
	LARD	120.1		N/A	130.9	111.3	-14.97

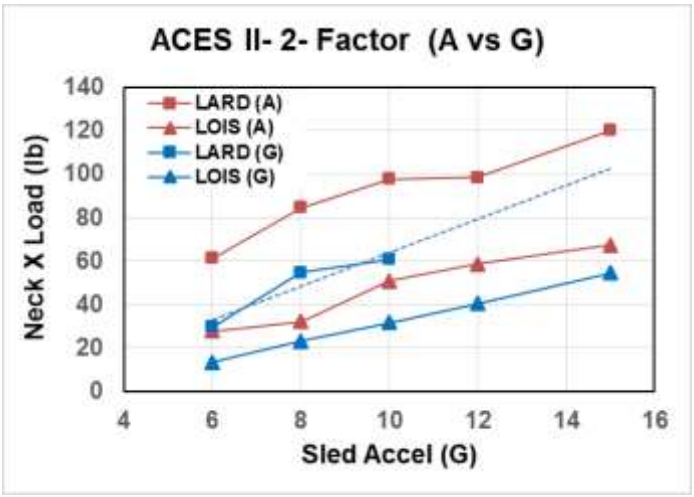

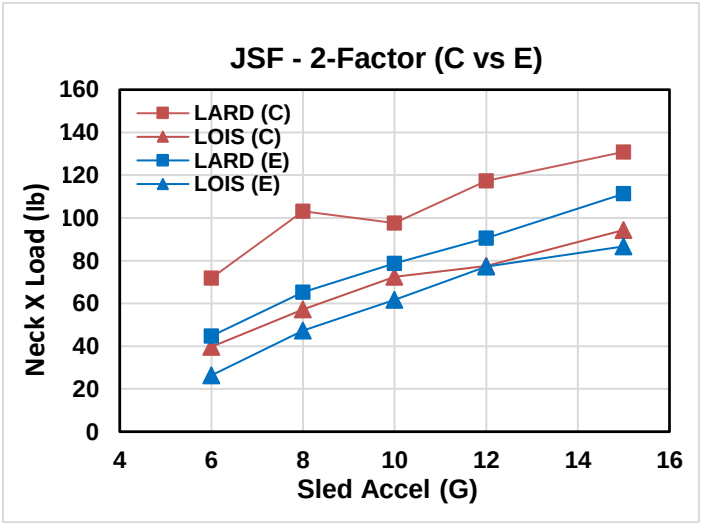

Figure 43. 2-Factor Comparison – Neck X Load

Neck My Torque (ATDs Only). Correlations between measured neck My torques and increasing carriage acceleration level were generally non-linear as shown in Figure 44. As shown in Table 39, LARD generated consistently lower torques for the JSF configuration (SCH harness/forward headrest) than the ACES II configuration (PCU harness/in-line headrest) regardless of helmet type. The neck torques for LOIS were nearly identical for both the ACES II and JSF configurations when wearing the HGU-55/P helmet (Cell A vs G), and inconsistent between the ACES II and JSF configurations with the Gen II helmet (Cell C vs E).

Table 39. 2-Factor Comparison (A vs G and C vs E) – Neck My Torque (in-lb)

G Level	Test Subj	ACES II (A)	JSF (G)	% Diff	ACES II (C)	JSF (E)	% Diff
6	LOIS	67.68	54.11	-20.05	93.39	83.42	-10.68
	LARD	78.17	51.72	-33.84	142.8	91.26	-36.11
8	LOIS	84.00	85.01	1.20	95.87	99.27	3.55
	LARD	120.0	77.00	-35.84	238.5	125.5	-47.40
10	LOIS	88.56	91.23	3.01	94.57	103.4	9.32
	LARD	174.0	86.59	-50.23	228.7	198.9	-13.04
12	LOIS	91.29	90.51	-0.85	88.83	109.6	23.37
	LARD	175.6		N/A	263.6	216.0	-18.05
15	LOIS	97.48	91.69	-5.94	119.7	116.6	-2.57
	LARD	263.2		N/A	290.3	266.9	-15.02

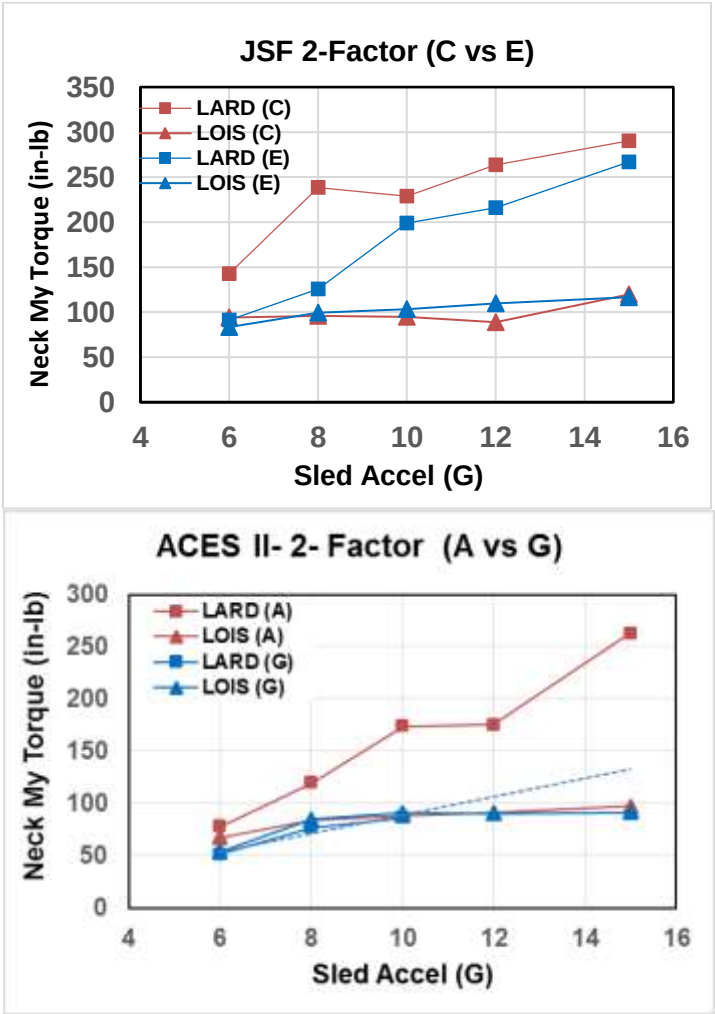

Figure 44. 2-Factor Comparison – Neck My Torque

Lumbar Z Load (ATDs Only). The measured lumbar z load generally increased linearly with increasing carriage acceleration level, although the LARD plots tended to demonstrate non-linearity in the ACES II configuration at the higher acceleration levels, as shown in Figure 45. LARD generated loads that were substantially larger than LOIS under all conditions. The ATD loads were similar between the ACES II configuration (PCU harness/in-line headrest) and the JSF configuration (SCH harness/forward headrest) with both HGU-55/P helmet (Cell A vs G) and the Gen II helmet (Cell C vs E). The exception to this was higher lumbar loads for the JSF configuration with the Gen II helmet for LARD at the 12 G and 15 G carriage acceleration levels, as shown in Table 40.

Table 40. 2-Factor Comparison (A vs G and C vs E) – Lumbar Z Load (lb)

G Level	Test Subj	ACES II (A)	JSF (G)	% Diff	ACES II (C)	JSF (E)	% Diff
6	LOIS	300.3	308.8	2.84	304.6	344.8	13.21
	LARD	517.9	591.1	14.12	528.4	557.6	5.51
8	LOIS	429.7	417.7	-2.78	441.7	462.0	4.60
	LARD	821.7	785.8	-4.37	791.6	759.0	-4.11
10	LOIS	585.9	546.9	-6.66	585.5	582.4	-0.52
	LARD	974.5	967.3	-0.74	984.8	979.4	-0.55
12	LOIS	703.7	687.4	-2.32	729.2	689.2	-5.49
	LARD	1150		N/A	1007	1200	19.16
15	LOIS	946.1	894.3	-5.48	963.1	957.5	-0.59
	LARD	1142		N/A	1200	1630	35.82

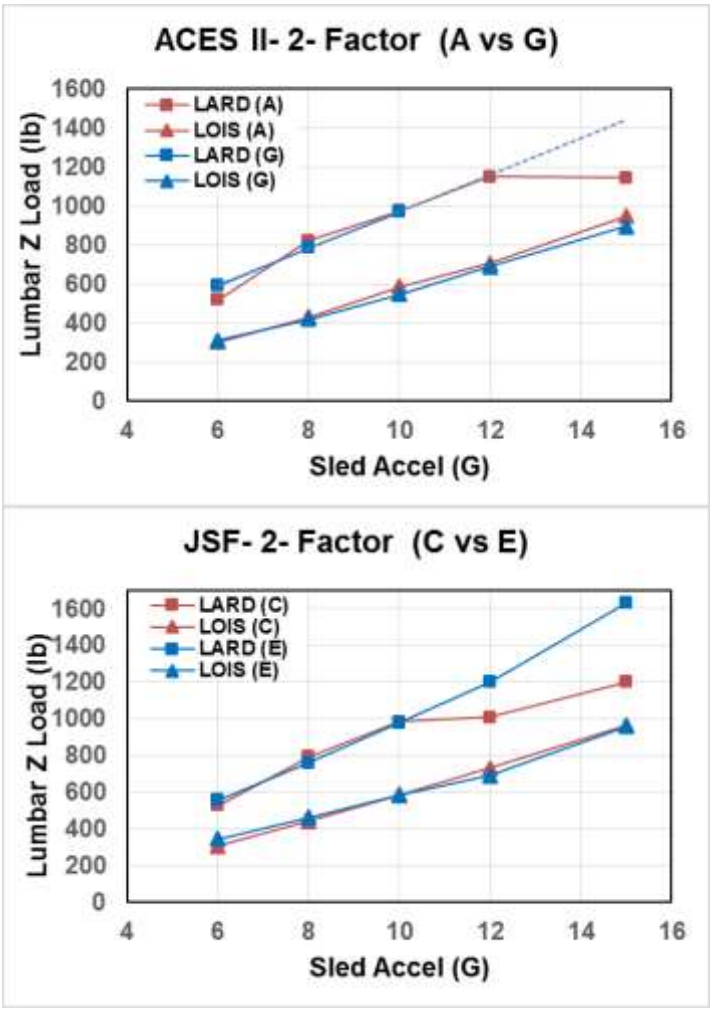

Figure 45. 2-Factor Comparison – Lumbar Z Load

Lumbar My Torque (ATSs Only). As shown in Figure 46, the measured lumbar My torque generally increased with increasing carriage acceleration level, with the exception of LARD in Cell G (10 G) and Cell E (12 G). The LARD torques were substantially larger than LOIS for all conditions, while the LOIS plots were much lower in magnitude and relatively flat. As shown in Table 41, the lumbar torques for both ATDs were generally lower in tests with the JSF configuration (SCH harness/forward headrest) than with the ACES II configuration (PCU harness/in-line headrest) with the Gen II helmet (Cell C vs E). This was also true for LARD tests with the HGU-55/P helmet (Cell A vs G), but not consistently with LOIS.

Table 41. 2-Factor Comparison (A vs G and C vs E) – Lumbar My Torque (in-lb)

G Level	Test Subj	ACES II (A)	JSF (G)	% Diff	ACES II (C)	JSF (E)	% Diff
6	LOIS	65.59	329.8	402.88	155.4	323.4	108.05
	LARD	1237	1005	-18.79	1197	1033	-13.69
8	LOIS	154.3	351.9	128.07	286.7	328.4	14.56
	LARD	1746	1606	-7.99	1637	1455	-11.10
10	LOIS	349.5	406.1	16.19	426.3	318.6	-25.26
	LARD	2290	1601	-30.10	2264	1852	-18.19
12	LOIS	450.0	466.0	3.56	545.8	456.7	-16.32
	LARD	2561		N/A	2753	1743	-36.70
15	LOIS	659.0	531.2	-19.39	852.5	440.6	-48.32
	LARD	3174		N/A	3469	2628	-24.26

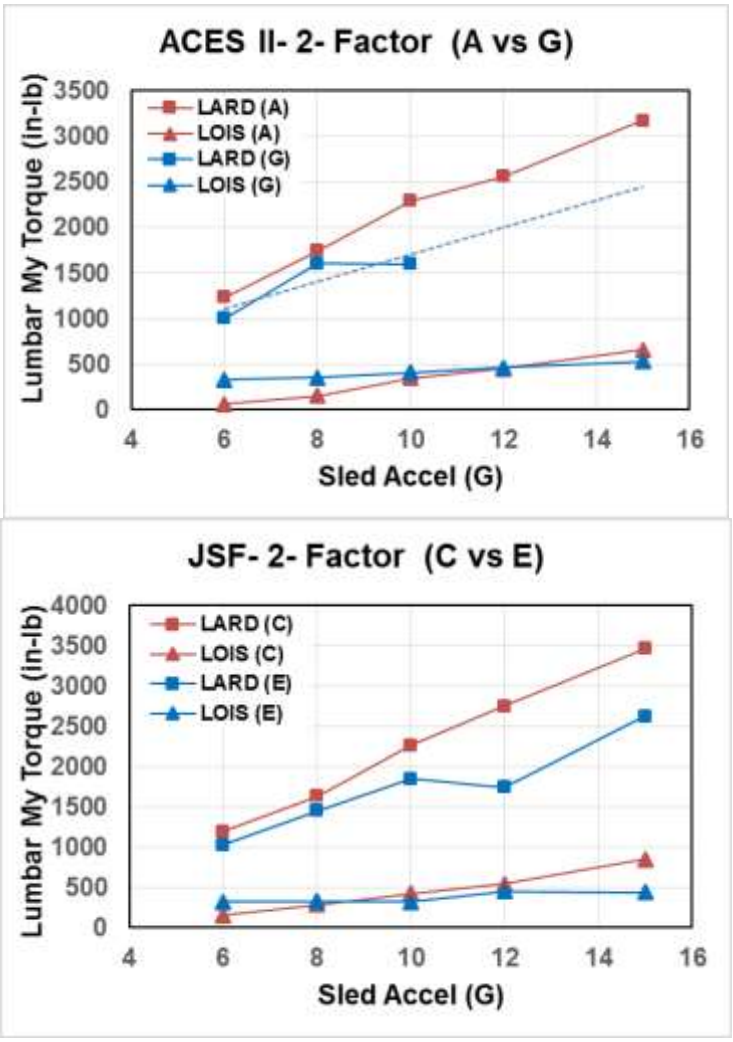

Figure 46. 2-Factor Comparison – Lumbar My Torque

7.6 VDT Parametric Assessment: 3-Factor Analysis (Helmet, Headrest Position, Harness)

A comparative assessment was conducted to evaluate the effects of the JSF ejection seat configuration (Cell E) compared to the baseline ejection seat configuration (Cell A). The baseline seat configuration is defined as the ACES II seat with in-line headrest, HGU-55/P helmet, and PCU torso harness. The JSF seat configuration is defined as the US16E seat with forward headrest (2.5”), JSF Gen II mock-up helmet, and SCH seat-mounted harness.

Head and chest accelerations (linear and angular) were collected for both human and ATD subjects. Neck and lumbar forces and torque were also collected for the ATDs. In addition, the ATD data were also evaluated for comparison with human tests and to ascertain responses at the higher acceleration levels. Data tables and plots showing the response of the instrumented humans and ATDs as a function of impact level for specific measured variables were developed and assessed.

Head Z Acceleration. As shown in Figure 47, the measured head z acceleration responses were consistently higher for LARD than LOIS, while the human accelerations tended to fall in-between the LOIS and LARD for both seat configurations. As shown in Table 42, the JSF configuration (Cell E) generally produced lower head z accelerations than the JSF configuration (Cell A) for both human and ATD subjects, and these were statistically significant for the human subjects at all G levels.

Table 42. 3-Factor Comparison (A vs E) – Head Z Acceleration (G)

G Level	Test Subject	ACES II (A)	JSF (E)	% Diff
6	Human	7.99 ± 0.5	6.87 ± 0.5	-14.02*
	LOIS	6.45	6.36	-1.40
	LARD	7.94	7.14	-10.08
8	Human	11.43 ± 1.1	9.48 ± 0.6	-17.06*
	LOIS	8.93	8.36	-6.38
	LARD	11.90	11.72	-1.51
10	Human	15.09 ± 1.6	11.59 ± 0.7	-23.19*
	LOIS	12.13	10.35	-14.67
	LARD	16.15	15.27	-5.45
12	LOIS	14.88	12.38	-16.80
	LARD	18.98	20.21	6.48
15	LOIS	19.60	17.05	-13.01
	LARD	27.44	26.07	-4.99

* denotes statistical significance

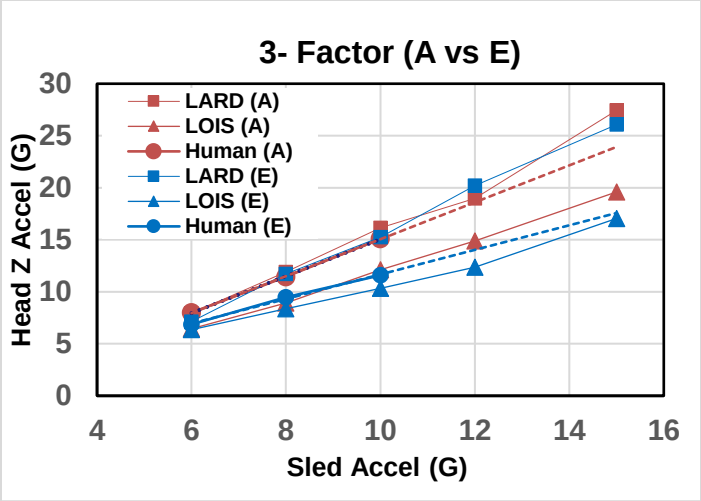

Figure 47. 3-Factor Comparison – Head Z Acceleration

Head X Acceleration. The measured head x acceleration generally increased linearly for all subjects as a function of increasing carriage acceleration, as shown in Figure 48, although in the ACES II configuration the increases in acceleration response for the human subjects were flat at 8-10 G and flat for the LARD response at 10-12 G. The LARD acceleration responses were generally higher than LOIS, while the human responses tended to be lower than the ATDs at all levels for both configurations. As shown in Table 43, the JSF configuration (Cell E) produced larger head x accelerations for the human subjects with the differences significant at the 10 G level, while the ATDs generally produced larger accelerations in the ACES II configuration (Cell A).

Table 43. 3-Factor Comparison (A vs E) – Head Z Acceleration (G)

G Level	Test Subject	ACES II (A)	JSF (E)	% Diff
6	Human	1.55 ± 0.9	1.99 ± 1.0	28.39
	LOIS	2.77	2.36	-14.80
	LARD	4.45	2.41	-45.84
8	Human	2.32 ± 1.0	2.46 ± 1.2	6.03
	LOIS	3.46	3.87	11.85
	LARD	6.10	3.57	-41.48
10	Human	2.41 ± 1.2	3.84 ± 1.4	59.34*
	LOIS	4.77	4.25	-10.90
	LARD	7.30	4.90	-32.88
12	LOIS	5.29	5.12	-3.21
	LARD	7.41	5.76	-22.27
15	LOIS	6.00	5.94	-1.00
	LARD	9.83	7.57	-22.99

* denotes statistical significance

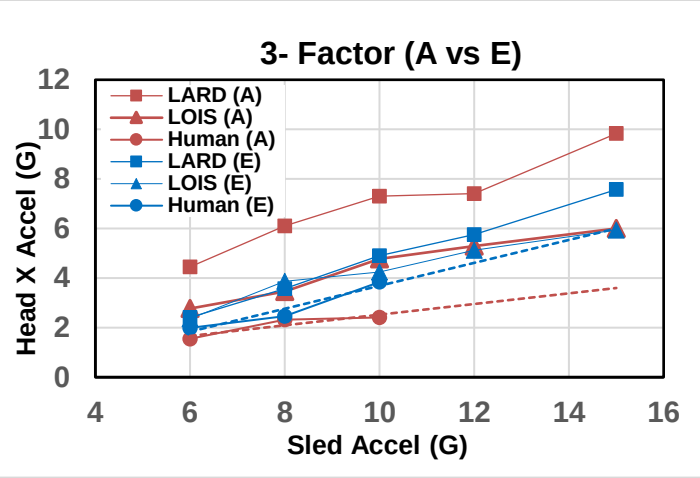

Figure 48. 3-Factor Comparison – Head X Acceleration

Resultant Chest Acceleration. As shown in Figure 49, the measured resultant chest accelerations for LARD were larger than LOIS with the human responses falling in-between. As shown in Table 44, the JSF configuration (Cell E) generally produced lower resultant chest accelerations for the human and ATD subjects than the ACES II configuration (Cell A), with the differences being significant for the human subjects at all levels.

Table 44. 3-Factor Comparison (A vs E) – Resultant Chest Accel (G)

G Level	Test Subject	ACES II (A)	JSF (E)	% Diff
6	Human	8.55 ± 0.8	7.44 ± 0.6	-12.98*
	LOIS	6.65	6.70	0.75
	LARD	8.70	7.52	-13.56
8	Human	12.16 ± 1.5	10.58 ± 0.8	-12.99*
	LOIS	9.36	9.04	-3.42
	LARD	13.31	12.49	-6.16
10	Human	16.17 ± 3.1	14.04 ± 1.2	-13.17*
	LOIS	12.47	11.43	-8.34
	LARD	17.99	16.68	-7.28
12	LOIS	15.31	13.62	-11.04
	LARD	21.06	21.89	3.94
15	LOIS	20.50	18.58	-9.37
	LARD	29.69	27.02	-8.99

* denotes statistical significance

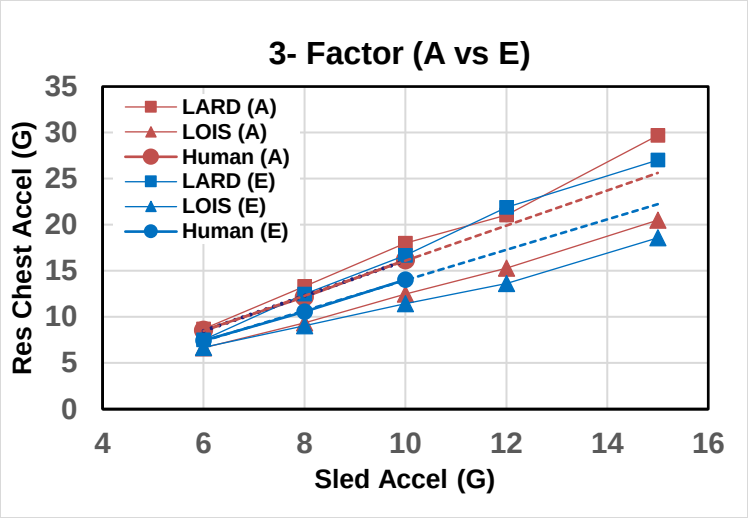

Figure 49. 3-Factor Comparion – Resultant Chest Acceleration

Head +Ry Angular Acceleration (ATDs only). As shown in Figure 50, the measured head +Ry angular accelerations for LARD were substantially higher than LOIS. As shown in Table 45, the JSF configuration (Cell E) generally produced lower angular accelerations for the ATDs, as compared to the ACES II configuration (Cell A). The results were similar for the head -Ry angular accelerations (not shown here).

Table 45. 3-Factor Comparison (A vs E) – Head +RY Angular Accel (Rad/Sec²)

G Level	Test Subject	ACES II (A)	JSF (E)	% Diff
6	LOIS	63.88	75.19	17.71
	LARD	141.5	78.68	-44.38
8	LOIS	130.0	126.8	-2.46
	LARD	333.1	220.9	-33.68
10	LOIS	244.5	181.2	-25.88
	LARD	501.9	380.6	-24.18
12	LOIS	373.4	259.2	-30.59
	LARD	545.2	493.7	-9.44
15	LOIS	569.2	401.2	-29.50
	LARD	793.5	643.4	-18.92

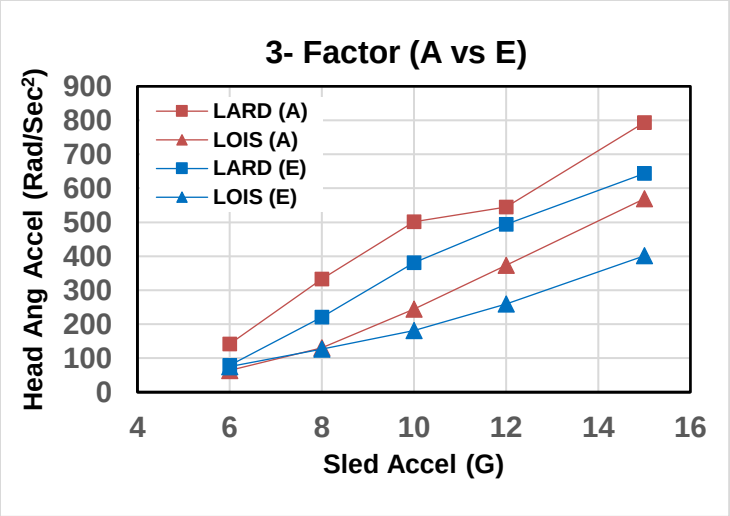

Figure 50. 3-Factor Comparison – Head +RY Angular Acceleration

Neck Z Load (ATDs Only). As shown in Figure 51, with LARD generated substantially higher neck z loads than LOIS at all levels. As shown in Table 46, both ATDs generated larger neck z loads with the JSF configuration (Cell E) than the ACES II configuration (Cell A), with the differences generally being more pronounced for LARD than LOIS.

Table 46. 3-Factor Comparison (A vs E) – Neck Z Load (lb)

G Level	Test Subject	ACES II (A)	JSF (E)	% Diff
6	LOIS	67.78	84.24	24.28
	LARD	98.56	113.6	15.27
8	LOIS	92.14	108.1	17.32
	LARD	136.5	172.3	26.27
10	LOIS	123.7	130.6	5.59
	LARD	180.2	225.9	25.39
12	LOIS	150.9	159.3	5.57
	LARD	213.6	282.2	32.09
15	LOIS	199.4	216.9	8.76
	LARD	312.9	373.7	19.45

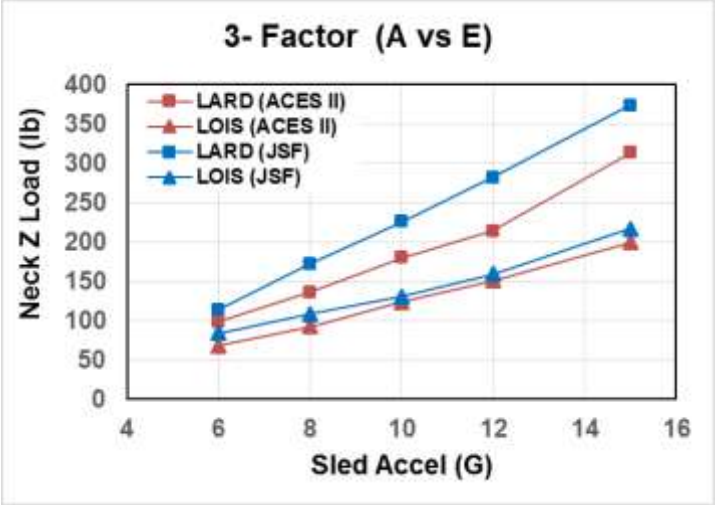

Figure 51. 3-Factor Comparison – Neck Z Load

Neck X Load (ATDs Only). As shown in Figure 52, the measured neck x load generally increased linearly with increasing carriage acceleration, with some non-linearity present in the ACES II configuration. LARD generated substantially higher neck loads than LOIS at all levels. As shown in Table 47, LARD generated smaller neck loads with the JSF configuration (Cell E) than the ACES II configuration (Cell A), while LOIS generally demonstrated substantially larger neck loads with the JSF configuration.

Table 47. 3-Factor Comparison (A vs E) – Neck X Load (lb)

G Level	Test Subject	ACES II (A)	JSF (E)	% Diff
6	LOIS	27.56	26.37	-4.32
	LARD	61.13	44.75	-26.80
8	LOIS	32.10	47.26	47.23
	LARD	84.56	65.28	-22.80
10	LOIS	50.79	61.67	21.42
	LARD	97.59	78.72	-19.34
	LOIS	58.51	77.17	31.89
12	LARD	98.39	90.53	-7.99
	LOIS	67.39	86.70	28.65
15	LARD	120.1	111.3	-7.34

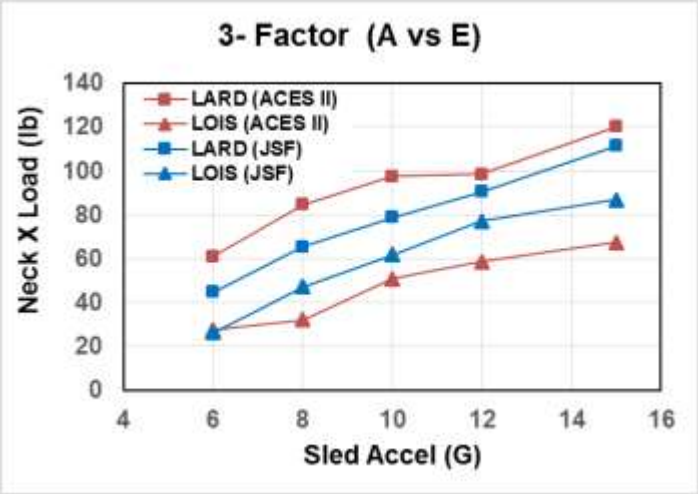

Figure 52. 3-Factor Comparison – Neck X Load

Neck My Torque (ATDs Only). The measured neck My torque increased with increasing carriage acceleration, as shown in Figure 53, with LARD generating substantially higher neck torque and greater slope than LOIS. As shown in Table 48, both ATDs generated larger neck torque with the JSF configuration (Cell E) than the ACES II configuration (Cell A) at all acceleration levels.

Table 48. 3-Factor Comparison (A vs E) – Neck My Torque (in-lb)

G Level	Test Subject	ACES II (A)	JSF (E)	% Diff
6	LOIS	67.68	83.42	23.26
	LARD	78.17	91.26	16.75
8	LOIS	84.00	99.27	18.18
	LARD	120.0	125.5	4.54
10	LOIS	88.56	103.4	16.73
	LARD	174.0	198.9	14.31
12	LOIS	91.29	109.6	20.05
	LARD	175.6	216.0	23.02
15	LOIS	97.48	116.6	19.61
	LARD	263.2	266.9	1.39

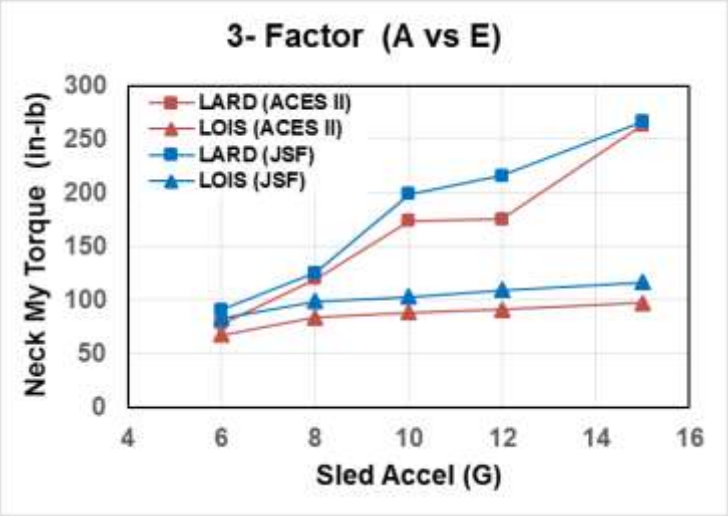

Figure 53. 3-Factor Comparison – Neck My Torque

Lumbar Z Load (ATDs Only). As shown in Figure 54, the measured lumbar z load increased linearly with increasing carriage acceleration for both ATDs, with the exception of a decrease in load for LARD with the ACES II configuration (Cell A) at 12-15 G. LARD generated substantially higher lumbar loads than the LOIS at all levels. As shown in Table 49, the JSF and ACES II configurations produced similar responses with the exception of a large increase in load (43%) for LARD at 15 G with the JSF configuration (Cell E).

Table 49. 3-Factor Comparison (A vs E) - Lumbar Z Load (lb)

G Level	Test Subject	ACES II (A)	JSF (E)	% Diff
6	LOIS	300.3	344.8	14.81
	LARD	517.9	557.6	7.65
8	LOIS	429.7	462.0	7.51
	LARD	821.7	759.0	-7.62
10	LOIS	585.9	582.4	-0.60
	LARD	974.5	979.4	0.49
12	LOIS	703.7	689.2	-2.06
	LARD	1149	1200	4.40
15	LOIS	946.1	957.5	1.20
	LARD	1142	1630	42.78

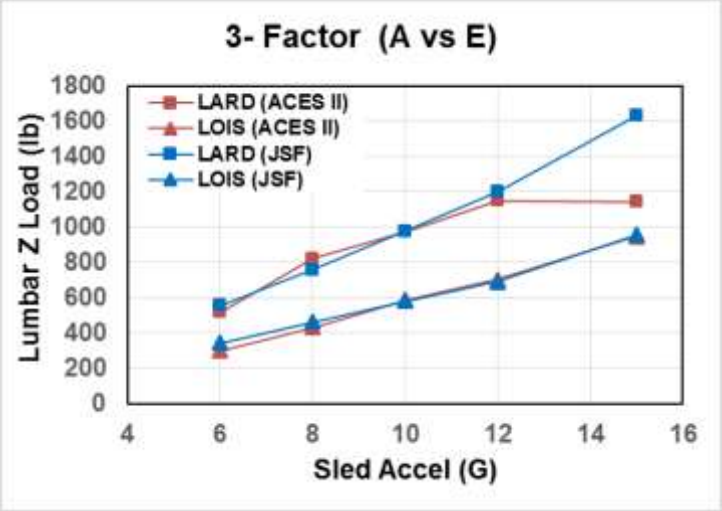

Figure 54. 3-Factor Comparison – Lumbar Z Load

Lumbar My Torque (ATDs Only). As shown in Figure 55, the measured lumbar My torque generally increased with increasing carriage acceleration for both ATDs, although the plot for LOIS with the JSF configuration was relatively flat. LARD generated substantially higher lumbar My torque than LOIS at all levels. As shown in Table 50, the JSF configuration (Cell E) produced lower torques than the ACES II configuration (Cell A) in tests with LARD, but the results were inconclusive with LOIS.

Table 50. 3-Factor Comparison (A vs E) – Lumbar My Torque (in-lb)

G Level	Test Subject	ACES II (A)	JSF (E)	% Diff
6	LOIS	65.59	323.4	393.02
	LARD	1237	1033	-16.49
8	LOIS	154.3	328.4	112.84
	LARD	1746	1455	-16.66
10	LOIS	349.5	318.6	-8.83
	LARD	2290	1852	-19.13
12	LOIS	450.0	456.7	1.50
	LARD	2561	1743	-31.95
15	LOIS	659.0	440.6	-33.15
	LARD	3174	2628	-17.21

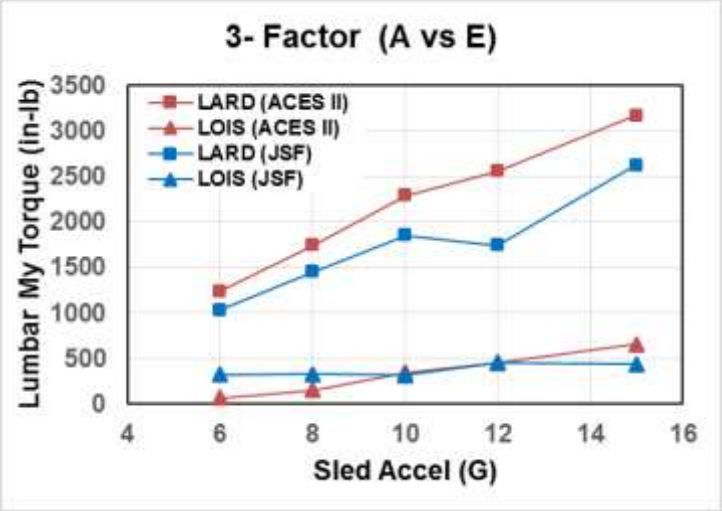

Figure 55. 3-Factor Comparison – Lumbar My Torque

8.0 DISCUSSION

8.1 VDT Parametric Assessment: Headrest Position

The position of the headrest did not have a substantial effect on human head downward (z-axis) accelerations as measured in either seat configuration during vertical impact, but did have a significant effect on horizontal (x-axis) acceleration. When the headrest was positioned forward (JSF configuration) the head acceleration decreased slightly in the z-axis but increased significantly in the x-axis. Since the x-axis accelerations were much smaller, the overall resultant effect on neck loading would not be significantly different between the forward and in-line conditions. With the headrest positioned forward, it was more difficult for the head to remain stationary against the headrest during the impact event, resulting in increased forward displacement and acceleration. This is consistent with findings by Brinkley, Hearon, Raddin, McGowan, and Powers (1982) who measured increased forward and downward displacements with the headrest positioned 2.25" forward of the seat back during human subject accelerations. No discernable differences were present in the resultant human or ATD chest acceleration measurements between the in-line and forward headrest conditions in either seat configuration.

In the JSF seat, the head angular accelerations for the ATDs were greater in the forward headrest condition compared to the in-line headrest condition, but no noticeable differences were present between the forward and in-line conditions in the ACES II seat. The ATD neck loads generally reflected the same pattern as the head accelerations, with very little difference in z-axis neck loading, but increased loading in the x-axis in the forward headrest position in both seats. The increase in neck x-axis loading for the forward headrest was particularly large for LOIS in the JSF seat. Increases in neck torque for LARD and decreases for LOIS were also recorded in the forward headrest position in the ACES II seat, with no discernable effect on neck torque due to the head position in the JSF seat configuration.

In the ACES II seat, the z-axis lumbar loads for LARD tended to decrease in the forward headrest position, while there were no discernable differences in loads between the headrest configurations in the JSF seat. The lumbar torque also tended to increase in the forward headrest condition for LOIS in both seat configurations, but not consistently for LARD.

8.2 VDT Parametric Assessment: Restraint System

The SCH restraint system consistently demonstrated significantly lower head linear accelerations than the PCU for the humans in both the x and z-axes during vertical impact. With the ATD subjects, this effect occurred primarily in the x-axis and was quite significant, with large decreases in forward linear head accelerations observed in tests with the SCH restraint. The chest accelerations were also significantly lower for the SCH restraint conditions for both human and ATD subjects. It is possible that the reduction of the head linear accelerations for the SCH harness conditions were due in part to the tightening of the upper rear cross strap firmly in place against the LPU. This procedure was subsequently modified for Phase II of the program on the HIA where the cross strap is now adjusted to touch the LPU, but not tightened.

The ATD angular accelerations were substantially lower as well with the SCH restraint under all conditions. The ATD neck loads generally reflected the same pattern as the human and ATD head accelerations, with similar z-axis neck loads in both restraint systems, but substantially lower x-axis neck loads observed with the SCH restraint. The neck torque was also substantially lower when using the SCH restraint in LARD tests, but the differences in neck torque were inconsistent for LOIS tests.

The z-axis lumbar loads were generally similar with both restraint configurations, with the exception of LARD lumbar loads with the in-line headrest/SCH harness configuration that were substantially greater at 15 G than with the PCU restraint. The lumbar load for this condition approached 1600 lbs, which was close to the maximum limits for the large ATD as defined by Desjardins (2008). However, the lumbar torque was lower in the SCH restraint configuration for LARD under all conditions, and for LOIS at the higher acceleration levels. This was likely due to the crotch strap in the SCH acting to control the forward pitch of the lumbar region in the LARD, while not being as apparent in the smaller LOIS which was more easily restrained by both harnesses.

8.3 VDT Parametric Assessment: Helmet Effects

The z-axis head accelerations for the humans were very similar for both the heavy Gen II helmet and the lightweight HGU-55/P helmet under both seat configurations, while the x-axis head accelerations and angular accelerations were generally higher with the Gen II helmet. This is likely due to the forward CG of the Gen II helmet pulling the head forward, which increased the horizontal acceleration and off-loaded some of the vertical acceleration of the head during the impact.

Similar to the humans, the ATDs also generated head z-axis accelerations that were similar for both helmets. However, the x-axis accelerations were somewhat dependent on the manikin, with decreases for the Gen II helmet worn by LARD in the ACES II seat, but increases for the Gen II helmet worn by LOIS in the JSF seat. ATD neck forces were consistently higher with the Gen II helmet compared to the HGU-55/P helmet for neck z-axis loads, neck x-axis loads, and neck torque for both seats. The increase in neck loads was expected due to the greater weight of the Gen II helmet. This was primarily concerning for LOIS tests at the highest carriage acceleration level (15 G) where the compressive neck loads slightly exceeded the JSF Neck Injury Criteria (NIC) limit of 200 lbs for the small occupant (Nichols, 2006). Although ejection seat acceleration levels during the catapult phase are normally less than 15 G, keeping the weight of the helmet at or below current levels will help minimize the risk of neck injury during ejection.

The head angular accelerations appeared to be dependent on the seat configuration, with generally lower angular accelerations for the Gen II helmet in the ACES II seat, but larger angular accelerations for the Gen II helmet in the JSF seat. Apparently, the forward headrest of the JSF seat in combination with the SCH harness allowed greater forward rotation of the forward weighted Gen II helmet compared to the ACES II seat configuration with the in-line headrest and chest strap, which was able to better control the forward rotations of the forward weighted helmet.

As expected, there was very little difference between the two helmets in the resultant chest accelerations and lumbar loads, since only the helmets were varied in the comparisons. However, differences in lumbar torque between the helmets were observed in the LOIS tests, with increased torque for the Gen II helmet in the ACES II seat, but decreased lumbar torque for the Gen II in the JSF seat. This could be due in part to differences inherent in the lumbar structure between the two ATDs, as demonstrated during tests in a previous study (Perry et al., 2017).

8.4 VDT Parametric Assessment: NPD Effects

Testing and analyses of the NPD were limited due to the challenges of pressurizing the device and maintaining the subject's head against the NPD for several minutes during test set-up while ensuring the subjects were avoiding neck fatigue. Since the head was inclined approximately 30° from the headrest during bracing and initial impact, it was difficult to separate out the z and x-axis accelerations, so only the resultant accelerations and neck loads are listed in this report. The resultant head accelerations for both humans and ATDs were lower for the NPD configuration compared to the baseline configuration, while the resultant chest accelerations were similar for both configurations. The ATD neck loads generally reflected the same pattern as the human and ATD head accelerations, with lower ATD neck forces measured with the NPD compared to the baseline condition. The lower head accelerations and neck loads in the NPD condition may have been due to the initial (pre-impact) 30° forward angle of the head which would have off loaded the head accelerations in the primary vertical axis, resulting in lower resultant head accelerations and neck loads. However, with the head rotated significantly forward during upward ejection, there is the potential for an increase in cervical torque due to the head-spine misalignment. The increased neck torque during the NPD condition was demonstrated by the LARD but not the LOIS.

8.5 Two-Factor Analysis (Harness and Headrest)

The SCH restraint system with forward headrest demonstrated significantly lower head z-axis accelerations and larger x-axis accelerations for humans than the PCU with in-line headrest, regardless of helmet weight. Since the tests were conducted in the vertical direction and the z-axis accelerations were considerably higher than the x-axis accelerations, the resultant accelerations would be lower for the SCH configuration compared to the PCU configuration. The increased head x-axis accelerations with the SCH configuration are similar to the effects seen with the single-factor forward headrest condition (Section 8.1), and had the effect of negating the reductions in head x-axis accelerations for the SCH harness seen in the single-factor restraint condition (Section 8.2). With the headrest positioned forward, it was more difficult for the head to remain stationary against the headrest during the impact event, resulting in increased forward displacement and acceleration, which was consistent with findings by Brinkley et al., (1982). The resultant chest accelerations were also significantly lower in tests with the SCH restraint system for both humans and ATDs, which was similar to the results of the single-factor restraint tests (Section 8.2).

The ATD results were similar to the human tests for the head z-axis accelerations, but the ATDs unexpectedly generated lower x-axis accelerations for the SCH configuration than the PCU,

which was opposite of the human results. The ATD z-axis neck loads were similar between the two configurations for LARD but slightly lower in the JSF configuration for LOIS. The ATD x-axis neck loads, neck toques (LARD only), and angular accelerations were substantially lower in the SCH configuration compared to the PCU. It was apparent that he ATDs were not able to simulate the complexities of human bracing and response in this configuration as the acceleration pulse translated upward from the vertical to the horizontal component of the head accelerations. This is due in part to the structure of the Hybrid III neck which was designed and validated primarily for automotive (frontal, rearward, and lateral) impact acceleration, but not necessarily vertical (compressive).

At higher carriage acceleration levels, the LARD ATD generated z-axis lumbar loads that were much greater in the SCH configuration compared to the PCU configuration. These loads are a concern since at the 15 G carriage acceleration level with the Gen II helmet, they came close to exceeding established lumbar load limits for the large occupant. The lumbar loads for LOIS with both configurations were smaller than LARD but they also came close to exceeding the lumbar load limits for the small occupant at 15 G for all conditions (Desjardins, 2008). However, it should be noted that the lumbar torques for the SCH configuration with LARD were lower than the PCU configuration, which would indicate good restraint of the lower torso during the impact, and that could help mitigate potential lumbar spine injury risk during actual ejections. This effect was likely due to the crotch strap present in the 5-point SCH harness which limited the displacement of the lower torso during the impact event.

8.6 Three-Factor Analysis (Harness, Headrest, and Helmet)

The JSF seat configuration (SCH restraint system with forward headrest and heavy helmet) demonstrated significantly lower z-axis head accelerations than the ACES II configuration (PCU with in-line headrest and light helmet) for humans, but demonstrated higher accelerations in the x-axis. Since the tests were conducted in the vertical direction, the z-axis accelerations were much higher than the x-axis accelerations for both configurations, thus the resultant acceleration was lower for the JSF configuration compared to the ACES II. The increased head x-axis accelerations with the SCH configuration were similar to the effects seen with the single-factor forward headrest condition (Section 8.1) and the two-factor analysis (Section 8.5). With the headrest positioned forward, it was more difficult for the subjects' heads to remain stationary against the headrest during the impact event, resulting in increased forward displacement and acceleration. As in the 2-factor results, the higher head accelerations in the x-axis for the JSF configuration was indicative of increased forward head flexion due to the combination of the V-shape of the harness shoulder straps and difficulty of bracing with the forward headrest.

The results for LOIS and to a lesser extent LARD were similar to the human tests for the head z-axis accelerations, with generally lower accelerations in the JSF configuration. However, the ATDs unexpectedly also generated lower x-axis accelerations for the JSF configuration than the ACES II, which was opposite of the human results. This was especially pronounced in the LARD tests. The ATD angular accelerations were also lower in the JSF configuration. As mentioned in the 2-factor analysis (Section 8.5), it was apparent that he ATDs were not able to adequately simulate the complexities of human bracing and response in this configuration (vertical acceleration pulse translating to horizontal head acceleration). This is due in part to the

structure of the Hybrid III neck, which was designed and validated primarily for the automotive impact acceleration environment (frontal, rearward, and lateral).

The resultant chest accelerations were also significantly lower in tests with the JSF configuration for both humans and to a lesser extent with the ATDs, which was similar to the results of the single-factor restraint analysis (Section 8.2) and two-factor analysis (Section 8.5), and indicates good restraint for the SCH restraint system in the primary vertical axis.

The neck z loads and torques were higher for both ATDs with the JSF configuration compared to the ACES II configuration. This was primarily the result of the heavier Gen II helmet used in the JSF configuration, since this was not the case in the 2-factor analysis which used only the lightweight helmet. The neck x loads were higher in the JSF configuration for LOIS, but lower in the JSF configuration for LARD, accentuating the differences between the manikin necks.

The lumbar loads were similar between the two configurations, with the exception of LARD showing a large increase in lumbar load with the JSF configuration compared to the ACES II configuration at 15 G. As discussed in Section 8.2, these loads came close to exceeding "conservative" maximum limits for the large ATD. This was also the case for LOIS in both configurations. However, the lumbar torques tended to be lower in the JSF configuration, particularly with the LARD ATD, again indicating good restraint in the lower torso region.

9.0 CONCLUSION

This research study investigated the effects on human and ATD response of varying factors and combinations of factors in the ACES II and JSF ejection seats during vertical acceleration, including the restraint system, headrest position, helmet system, and use of an inflatable neck stabilization device. These results are not intended to produce an overall evaluation of either seat system during ejection since they include only vertical seat accelerations in a controlled laboratory environment, and do not include the effects of windblast, drogue and parachute opening phases, and/or other off-axis accelerations due to head and spinal misalignment. The objective was to identify factors that could potentially have an effect on aircrew safety, and provide recommendations for risk mitigation of spinal injuries during upward aircraft ejection.

In general, both seats and systems performed well under most conditions. It appears that positioning of the headrest approximately 2.5" in the forward position (JSF head box) increases horizontal linear head acceleration, horizontal neck loading, and head angular accelerations during vertical impact acceleration, with very little effect on compressive acceleration or loading. The higher head accelerations in the x-axis for the forward headrest were indicative of increased forward head flexion due to the subjects' difficulty of bracing with the head leaning forward. However, the increased forward head accelerations were small compared to the primary vertical accelerations so these would not likely contribute to increased risk of neck injury during the vertical phase of ejection, provided the cervical displacement was not excessive.

The SCH harness generally performed better than the PCU in mitigating vertical and horizontal linear head and chest accelerations in the humans, and reducing head angular acceleration and neck horizontal loading in the ATDs. The exception was an increase in neck torque for the LOIS ATD for the SCH harness condition, accentuating the differences in neck response between the large and small ATDs. This may warrant additional precautions for the small occupant under some conditions. The SCH restraint system in combination with forward headrest also reduced the compressive head accelerations and resultant chest accelerations, but resulted in larger horizontal head accelerations for humans. However, the ATDs unexpectedly generated lower horizontal and angular accelerations for the SCH configuration than the PCU, demonstrating the inability of the ATDs to simulate the complexities of human bracing and response in this configuration.

The Gen II helmet generated larger forward linear head accelerations for the humans and LOIS ATD compared to the HGU-55/P helmet, which was likely due to the forward CG of the Gen II helmet pulling the head forward. ATD neck forces were consistently higher with the Gen II helmet in compression, shear, and torque for both seat configurations, which was expected due to the greater weight of the Gen II helmet. This would be of primary concern for the small occupant at seat acceleration levels of 15 G or greater, where the compressive neck loads slightly exceeded the JSF Neck Injury Criteria (NIC) limits. Although ejection seat acceleration levels during the catapult phase are normally less than 15 G, keeping the weight of the helmet at or below current levels will help minimize the risk of neck injury during ejection.

Another concern with the JSF configuration was the large compressive loads generated in the lumbar spine of the LARD ATD at the higher carriage acceleration levels. These loads in some

instances came close to exceeding recently proposed “conservative” lumbar load limits for the large occupant when tested at 15 G. However, the lumbar torques and shear lumbar loads for the JSF configurations were generally lower than the ACES II configurations, which would indicate good restraint of the lower torso during the impact, possibly due to the SCH crotch strap that could help mitigate potential lumbar spine injury risk during actual ejections.

Although testing and analyses of the NPD was limited, the resultant human and ATD head accelerations and ATD neck loads were lower for the NPD configuration compared to the non-NPD configuration, indicating no increased risk of neck injury during accelerations with static NPD pressurization. However, neck torque did increase for the LARD ATD with NPD indicating that the NPD should be evaluated separately for the small and large ATDs due to their different neck response characteristics. Also, the potential for injury risk due to cervical misalignment with forward inflation of the NPD in upward ejections was not evaluated in this program, and testing has not yet been accomplished to investigate the effects of dynamically pressurizing the NPD prior to or during impact accelerations, which could generate increased motion of the head during the impact event.

10.0 Summary and Recommendations

The analysis confirmed that both seat systems functioned properly within the constraints of their respective configurations and requirements, and did not appear to generate excessive injury risk during vertical-axis laboratory testing. One medical incident occurred out of several hundred exposures which consisted of a minor neck muscle tear in a male subject during a 10 G test with the ACES II configuration and lightweight helmet. After the exposure the subject reported feeling that his drop brace technique was poor and inadequate. The subject fully recovered and continued testing within three months.

Surprisingly, the SCH harness reduced head and torso acceleration and neck loading slightly compared to the PCU, since the chest strap on the PCU would have been expected to provide additional upper torso restraint. However, the combination of forward headrest and forward-weighted helmet generally increased head acceleration and neck loading in the JSF configuration, which would be a concern primarily for small occupants if the vertical seat pulse were to exceed 15 G. Neck strengthening exercises for smaller aircrew and moving the helmet center-of-mass rearward would help off-load the neck forces, as would re-positioning the helmet resting point in the head rest slightly rearward. Also at the higher acceleration levels in the JSF seat, the lumbar loads for the large occupant began to approach conservative limits, so mitigation strategies should include evaluation of cushioning material and optimal occupant positioning. Going forward, the effects of head and torso displacement should also be analyzed with respect to the effects on vertebral loading, particularly with NPD deployment, with the use of finite element models to more accurately determine risk of specific spinal compromise during vertical acceleration.

11.0 REFERENCES

Brinkley J.W., Hearon B.F., Raddin J.H., McGowan L.A., and Powers J.M. Vertical Impact Tests of a Modified F/FB-111 Crew Seat to Evaluate Headrest Position and Restraint Configuration Effects. AFRL Technical Report AFAMRL-TR-82-51, Aug 1982.

Brinkley J.W. and Shaffer J.T. Dynamic Simulation Techniques for the Design and Escape Systems: Current Applications and Future Air Force Requirements, AFAMRL-TR-71-29, 1971.

Buhrman J.R., Perry C.E., and Wright N.L. Ejection Back Injury Risk Factors for an Expanded Aircrew Population, 50th Annual SAFE Symposium, Reno, Oct 2012.

Cheng H., Mosher S.E., and Buhrman J.R. Development and Use of the Biodynamics Data Bank and its Web Interface, AFRL Technical Report AFRL-HE-WP-TR-2004-0147, Oct 2004.

Desjardins S. Establishing Lumbar Injury Tolerance for Energy Absorbing Seats: Criteria and Testing Limitations. American Helicopter Society 64th Annual Forum, Montreal, 2008.

Lewis M. Survivability and Injuries from Use of Rocket-Assisted Ejection Seats: Analysis of 232 Cases, Aviation, Space, and Environmental Medicine, 77(9), Sep 2006.

Martin-Baker Aircraft Co. LTD. US16E-4.6 Ejection Seat Aircrew Manual (unpublished), Oct 2013.

Nichols J. Overview of Ejection Neck Injury Criteria, 44th Annual SAFE Symposium, pp. 159-171, Reno, NV, 23-25 Oct 2006.

Perry C., Burneka C., Buhrman J., Christopher R., and Albery C. Comparative Assessment of Torso and Seat Mounted Restraint Systems using Manikins on the Vertical Deceleration Tower, AFRL Technical Report AFRL-RH-WP-TR-2017-0044, Mar 2017.

Strzelecki J.P. Characterization of the Vertical Deceleration Tower (VDT) Plunger Profiles, AFRL Technical Report AFRL-HE-WP-SR-2005-0005, Sep 2004.

Tulloch J. Ejection Seat Back Injuries During Catapult Phase. 49th Annual SAFE Symposium, Reno, Oct 2011.

APPENDIX: SENSOR CALIBRATION SHEET AND SAMPLE DATA PLOTS

PROGRAM: Aircrew Restraint Biodynamic Assessment (ACES II Seat)	TEST DATES: 16 Sept 2016 - 16 Mar 2017
STUDY NUMBER: 201507 (Part III)	TEST NUMBERS: 7436 - 7601
FACILITY: VERTICAL DROP TOWER	SAMPLE RATE: 1K
DATA COLLECTION SYSTEM: TDAS PRO	FILTER FREQUENCY: 120Hz
	TRANSDUCER RANGE (VOLTS): +/- 5 V

DATA CHANNEL	DATA POINT	TRANSDUCER MFG. & MODEL	SERIAL NUMBER	PRE-CAL		POST-CAL		% D	DAS SENSITIVITY	BRIDGE	FULL SCALE	NOTES
				DATE	SENS	DATE	SENS					
1	CARRIAGE X ACCEL (G)	ENTRAN EGA-125-100D	97I97I 19-A10	18-May-16	.8823 mv/g at 5V exc	16-Mar-17	.8891 mv/g at 10V exc	0.8	.17646 mv/v/g	FULL	50 G	Used on all tests.
2	CARRIAGE Y ACCEL (G)	ENTRAN EGA-125-100D	93F93F 11-P14	18-May-16	.9335 mv/g at 10V exc	16-Mar-17	.9448 mv/g at 10V exc	1.2	.18670 mv/v/g	FULL	50 G	Used on all tests.
3	CARRIAGE Z ACCEL (G)	MEAS SPEC EGCS-S425-250	R150VR	18-May-16	.2614 mv/g at 5V exc	16-Mar-17	.2639 mv/g at 10V exc	0.9	.05228 mv/v/g	FULL	50 G	Used on all tests.
4	SEAT PAN X ACCEL (G)	MEAS SPEC EGCS-S425-250	T13132	4-Jan-16	.2890 mv/g at 5V exc	24-Mar-17	.2930 mv/g at 5V exc	1.4	.05780 mv/v/g	FULL	100 G	Used on all tests.
5	SEAT PAN Y ACCEL (G)	MEAS SPEC EGCS-S425-250	R1307Y	4-Jan-16	.2767 mv/g at 5V exc	24-Mar-17	.2794 mv/g at 15V exc	1.0	.05534 mv/v/g	FULL	100 G	Used on all tests.
6	SEAT PAN Z ACCEL (G)	MEAS SPEC EGCS-S425-250	R13085	4-Jan-16	.3108 mv/g at 5V exc	24-Mar-17	.3142 mv/g at 5V exc	1.1	.06216 mv/v/g	FULL	100 G	Used on all tests.
7	SEAT CUSHION X ACCEL (G)	ENTRAN EGV3-F-250	M110LO (X)	24-Mar-16	.4044 mv/g at 5V exc	16-Mar-17	.4069 mv/g at 5V exc	0.6	.08088 mv/v/g	FULL	100 G	Used on all tests.
8	SEAT CUSHION Y ACCEL (G)	ENTRAN EGV3-F-250	M110LO (Y)	24-Mar-16	.4012 mv/g at 5V exc	16-Mar-17	.4036 mv/g at 5V exc	0.6	.08024 mv/v/g	FULL	100 G	Used on all tests.
9	SEAT CUSHION Z ACCEL (G)	ENTRAN EGV3-F-250	M110LO (Z)	24-Mar-16	.3667 mv/g at 5V exc	16-Mar-17	.3696 mv/g at 5V exc	0.8	.07334 mv/v/g	FULL	100 G	Used on all tests.
10	HEAD X ACCEL (G)	MEAS SPEC EGCS-S425-50	A013010	17-Jun-15	2.8670 mv/g at 10V exc	16-Mar-17	2.8885 mv/g at 10V exc	0.8	.28670 mv/v/g	FULL	50 G	Used on all tests.
11	HEAD Y ACCEL (G)	MEAS SPEC EGCS-S425-50	A013015	17-Jun-15	2.8837 mv/g at 10V exc	16-Mar-17	2.9301 mv/g at 10V exc	1.6	.28837 mv/v/g	FULL	50 G	Used on all tests.
12	HEAD Z ACCEL (G)	MEAS SPEC EGCS-S425-50	A013014	17-Jun-15	2.8410 mv/g at 10V exc	16-Mar-17	2.8602 mv/g at 10V exc	0.7	.28410 mv/v/g	FULL	50 G	Used on all tests.
13	HEAD Ry ANG RATE (RAD/SEC)	DTS ARS-1500	101	23-Jun-15	67.78 mv/rad/sec at 5V exc	17-Mar-17	67.95 mv/rad/sec at 5V exc	0.3	67.78 mv/v/rad/sec	FULL	30 RAD/SEC	Used on all tests.
14	CHEST X ACCEL (G)	MEAS SPEC EGCS-S425-250	S080AG	18-Jun-15	.4344 mv/g at 10V exc	16-Mar-17	.4386 mv/g at 10V exc	1.0	.04344 mv/v/g	FULL	50 G	Used on all tests.
15	CHEST Y ACCEL (G)	MEAS SPEC EGCS-S425-250	S080A7	1-Jun-15	.4386 mv/g at 10V exc	16-Mar-17	.4417 mv/g at 10V exc	0.7	.04386 mv/v/g	FULL	50 G	Used on all tests.
16	CHEST Z ACCEL (G)	MEAS SPEC EGCS-S425-250	S080AF	1-Jun-15	.4539 mv/g at 10V exc	16-Mar-17	.4570 mv/g at 10V exc	0.7	.04539 mv/v/g	FULL	50 G	Used on all tests.
17	CHEST Ry ANG RATE (RAD/SEC)	DTS ARS-1500	102	23-Jun-15	71.94 mv/rad/sec at 5V exc	17-Mar-17	71.97 mv/rad/sec at 5V exc	0.0	71.94 mv/v/rad/sec	FULL	30 RAD/SEC	Used on all tests.
18	LEFT LAP X FORCE (LB)	MICH SCI	110 (Z)	06-Jun-16	10.84 uv/lb at 10V exc	24-Mar-17	11.17 uv/lb at 10V exc	3.0	.001084 mv/v/lb	FULL	1500 LB	Used on all tests.
19	LEFT LAP Y FORCE (LB)	MICH SCI	110 (X)	06-Jun-16	13.12 uv/lb at 10V exc	24-Mar-17	13.22 uv/lb at 10V exc	0.8	.001312 mv/v/lb	FULL	1500 LB	Used on all tests.
20	LEFT LAP Z FORCE (LB)	MICH SCI	110 (Y)	06-Jun-16	13.39 uv/lb at 10V exc	24-Mar-17	13.33 uv/lb at 10V exc	-0.4	.001339 mv/v/lb	FULL	1500 LB	Used on all tests.
21	RIGHT LAP X FORCE (LB)	MICH SCI	3 (Z)	6-Jun-16	10.99 uv/lb at 10V exc	24-Mar-17	11.07 uv/lb at 10V exc	0.7	.001099 mv/v/lb	FULL	1500 LB	Used on all tests.
22	RIGHT LAP Y FORCE (LB)	MICH SCI	3(Y)	6-Jun-16	13.74 uv/lb at 10V exc	24-Mar-17	13.69 uv/lb at 10V exc	-0.4	.001374 mv/v/lb	FULL	1500 LB	Used on all tests.
23	RIGHT LAP Z FORCE (LB)	MICH SCI	3 (X)	6-Jun-16	13.85 uv/lb at 10V exc	24-Mar-17	13.78 uv/lb at 10V exc	-0.5	.001385 mv/v/lb	FULL	1500 LB	Used on all tests.

201507 Test: 7286 Test Date: 160511 Subj: A22 Wt: 132.0
Nom G: 10.0 Cell: D10

Data ID	Immediate Preimpact	Maximum Value	Minimum Value	Time Of Maximum	Time Of Minimum
Kodak Start Time (Ms)				-1991.0	
Reference Mark Time (Ms)				-114.0	
Drop Height (In)		84.65			
Impact Rise Time (Ms)				71.6	
Impact Duration (Ms)				154.7	
Velocity Change (Ft/Sec)		26.76			
CARRIAGE X ACCEL (G)	0.01	1.71	-1.61	19.0	24.0
CARRIAGE Y ACCEL (G)	-0.01	1.01	-0.69	95.0	90.0
CARRIAGE Z ACCEL (G)	0.01	9.88	0.25	72.0	0.0
CARRIAGE RESULTANT (G)	0.05	9.92	0.29	71.0	0.0
INTEGRATED ACCEL (FT/SEC)	26.08	26.76	1.49	12.0	266.0
SEAT PAN X ACCEL (G)	-0.01	1.31	-0.55	54.0	60.0
SEAT PAN Y ACCEL (G)	-0.05	0.85	-1.11	94.0	121.0
SEAT PAN Z ACCEL (G)	-0.01	10.82	0.10	77.0	0.0
SEAT PAN RESULTANT (G)	0.09	10.85	0.10	77.0	0.0
SEAT PAN DRZ	0.00	12.87	-1.89	100.0	171.0
SEAT CUSHION X ACCEL (G)	-0.04	0.48	-3.62	32.0	78.0
SEAT CUSHION Y ACCEL (G)	-0.06	2.38	-1.63	88.0	81.0
SEAT CUSHION Z ACCEL (G)	0.04	12.87	0.06	78.0	0.0
SEAT CUSHION RESULTANT (G)	0.09	13.39	0.10	78.0	0.0
SEAT CUSHION DRZ	0.01	16.10	-3.39	103.0	175.0
LEFT LAP X FORCE (LB)	-85.06	-67.55	-216.14	192.0	91.0
LEFT LAP Y FORCE (LB)	-0.57	17.93	-1.84	93.0	193.0
LEFT LAP Z FORCE (LB)	44.54	81.08	19.08	91.0	184.0
LEFT LAP RESULTANT (LB)	96.02	231.53	70.25	91.0	192.0
RIGHT LAP X FORCE (LB)	-59.21	-41.42	-156.90	206.0	98.0
RIGHT LAP Y FORCE (LB)	5.37	7.20	-6.36	216.0	106.0
RIGHT LAP Z FORCE (LB)	19.34	40.75	8.67	99.0	156.0
RIGHT LAP RESULTANT (LB)	62.52	162.20	43.32	98.0	206.0
HEAD X ACCEL (G)	0.09	1.87	-0.93	82.0	31.0
HEAD Y ACCEL (G)	-0.06	0.89	-0.50	102.0	169.0
HEAD Z ACCEL (G)	0.05	14.10	-0.08	84.0	169.0
HEAD RESULTANT (G)	0.12	14.22	0.04	84.0	4.0
HEAD Ry ANG VELOCITY (RAD/SEC)	0.04	2.06	-3.39	137.0	95.0
HEAD Ry ANG ACCEL (RAD/SEC2)	-1.29	246.97	-308.43	111.0	65.0

201507 Test: 7286 Test Date: 160511 Subj: A22 Wt: 132.0
Nom G: 10.0 Cell: D10

Data ID	Immediate Preimpact	Maximum Value	Minimum Value	Time Of Maximum	Time Of Minimum
CHEST X ACCEL (G)	0.04	3.15	-1.40	70.0	115.0
CHEST Y ACCEL (G)	0.02	0.66	-1.02	56.0	72.0
CHEST Z ACCEL (G)	-0.02	13.86	-0.81	78.0	168.0
CHEST RESULTANT (G)	0.06	13.87	0.06	78.0	0.0
CHEST Ry ANG VELOCITY (RAD/SEC)	0.06	4.99	-5.01	72.0	106.0
CHEST Ry ANG ACCEL (RAD/SEC2)	1.01	1512.72	-844.60	69.0	96.0
RIGHT SHOULDER (LB)	53.83	54.78	12.61	11.0	54.0
LEFT SHOULDER FORCE (LB)	41.42	42.53	6.68	7.0	230.0